IOWA STATE UNIVERSITY
Digital Repository

Retrospective Theses and Dissertations

Iowa State University Capstones, Theses and Dissertations

1973

Some aspects of deviation angle estimation for axial-flow compressors

Max Joseph Miller
Iowa State University

Follow this and additional works at: https://lib.dr.iastate.edu/rtd

 Part of the Mechanical Engineering Commons

Recommended Citation
Miller, Max Joseph, "Some aspects of deviation angle estimation for axial-flow compressors " (1973). *Retrospective Theses and Dissertations*. 4960.
https://lib.dr.iastate.edu/rtd/4960

This Dissertation is brought to you for free and open access by the Iowa State University Capstones, Theses and Dissertations at Iowa State University Digital Repository. It has been accepted for inclusion in Retrospective Theses and Dissertations by an authorized administrator of Iowa State University Digital Repository. For more information, please contact digirep@iastate.edu.

INFORMATION TO USERS

This material was produced from a microfilm copy of the original document. While the most advanced technological means to photograph and reproduce this document have been used, the quality is heavily dependent upon the quality of the original submitted.

The following explanation of techniques is provided to help you understand markings or patterns which may appear on this reproduction.

1. The sign or "target" for pages apparently lacking from the document photographed is "Missing Page(s)". If it was possible to obtain the missing page(s) or section, they are spliced into the film along with adjacent pages. This may have necessitated cutting thru an image and duplicating adjacent pages to insure you complete continuity.

2. When an image on the film is obliterated with a large round black mark, it is an indication that the photographer suspected that the copy may have moved during exposure and thus cause a blurred image. You will find a good image of the page in the adjacent frame.

3. When a map, drawing or chart, etc., was part of the material being photographed the photographer followed a definite method in "sectioning" the material. It is customary to begin photoing at the upper left hand corner of a large sheet and to continue photoing from left to right in equal sections with a small overlap. If necessary, sectioning is continued again — beginning below the first row and continuing on until complete.

4. The majority of users indicate that the textual content is of greatest value, however, a somewhat higher quality reproduction could be made from "photographs" if essential to the understanding of the dissertation. Silver prints of "photographs" may be ordered at additional charge by writing the Order Department, giving the catalog number, title, author and specific pages you wish reproduced.

5. PLEASE NOTE: Some pages may have indistinct print. Filmed as received.

Xerox University Microfilms
300 North Zeeb Road
Ann Arbor, Michigan 48106

73-25,240

MILLER, Max Joseph, 1939-
SOME ASPECTS OF DEVIATION ANGLE ESTIMATION FOR AXIAL-FLOW COMPRESSORS.

Iowa State University, Ph.D., 1973
Engineering, mechanical

University Microfilms, A XEROX Company, Ann Arbor, Michigan

THIS DISSERTATION HAS BEEN MICROFILMED EXACTLY AS RECEIVED.

Some aspects of deviation angle estimation for axial-flow compressors

by

Max Joseph Miller

A Dissertation Submitted to the

Graduate Faculty in Partial Fulfillment of

The Requirements for the Degree of

DOCTOR OF PHILOSOPHY

Majors: Mechanical Engineering
Engineering Mechanics

Approved:

Signature was redacted for privacy.

In Charge of Major Work

Signature was redacted for privacy.

For the Major Departments

Signature was redacted for privacy.

For the Graduate College

Iowa State University
Ames, Iowa

1973

TABLE OF CONTENTS

SYMBOLS AND NOTATION

b	stream tube thickness, meters
C_{p1}	pressure coefficient $(P_1^o - p_\ell)/\frac{1}{2}\rho_1 W_1^2$
C_{p2}	pressure coefficient $(p_\ell - p_1)/\frac{1}{2}\rho_1 W_1^2$
c	blade chord (fig. 3), meters
c_p	specific heat at constant pressure, J/kg ^oK
c_v	specific heat at constant volume, J/kg ^oK
D	diameter, meters
d	minimum distance of MAGNFY boundary from blade surface (fig. 5), meters
F	meridional distance from end of chord to extreme end of blade (fig. 44), meters
G	tangential distance from end of chord to extreme end of blade (fig. 44), meters
H_R	rothalpy (eq. (A3)), J/kg
H^o	stagnation enthalpy in absolute coordinate system, J/kg
h	static enthalpy, J/kg
h_m, h_{R0}	distance between grid points, meters
i	incidence angle (fig. 3), deg
M	Mach number
MSP1	meridional coordinate of point on blade suction surface (fig. 12), meters
MSP2	meridional coordinate of point on blade pressure surface (fig. 12), meters
m	meridional coordinate (fig. 4), deg

n	number of interior mesh points
P_R	pressure of rothalpy state, Newton/meter^2
p^o	stagnation pressure in absolute coordinate system, Newton/meter^2
p	static pressure, Newton/meter^2
R	radius from axis of rotation (fig. 4), meters
RI	radius of leading edge circle (fig. 45), meters
RLE	radius of fictitious leading edge circle (fig. 47), meters
RO	radius of trailing edge circle (fig. 44), meters
s	blade spacing (fig. 3), meters
T	static temperature, ^oK
T_R	temperature of rothalpy state, ^oK
T^o	stagnation temperature in absolute coordinate system, ^oK
THSP1	tangential coordinate of point on blade suction surface (fig. 12), rad
THSP2	tangential coordinate of point on blade pressure surface (fig. 12), rad
U	blade tangential speed, $R\omega$, meters/sec
u	stream function (eqs. (2) and (3))
V	fluid absolute velocity, meters/sec
W	fluid velocity relative to blade, meters/sec
w	mass flow in stream tube between two blades, kg/sec
XX	coordinate along chord (fig. 13), meters
x	distance along chord from leading edge, meters
Y	coordinate normal to chord (fig. 13), meters
YCI	perpendicular distance from center of leading edge to chord line (fig. 45), meters

YCO perpendicular distance from center of trailing edge circle to chord line (fig. 44), meters

z axial coordinate (fig. 4), meters

α angle between tangent to stream surface and the axial direction (fig. 1), deg

β angle between flow direction and axial direction (fig. 3), deg

Γ blade circulation, $s(V_{\theta,1} - V_{\theta,2})$, meters^2/sec

γ ratio of specific heats, c_p/c_v

γ^o blade setting angle (fig. 3), deg

δ deviation angle, angle between relative velocity and tangent to mean camber line at trailing edge (fig. 3), deg

ζ angle between m-axis and line connecting edge circle centers (fig. 46), deg

η_I angle between chord line and line connecting center of leading edge circle to end of chord (fig. 45), deg

η_O angle between chord line and line connecting center of trailing edge circle to end of chord (fig. 44), deg

θ angular coordinate (fig. 4), rad

κ blade angle, angle between tangent to mean camber line and axial direction (fig. 3), deg

ξ angular distance on trailing edge circle between the axial direction and the stagnation point (fig. 32), deg

ρ fluid density, kg/meter^2

σ blade solidity, c/s

ϕ^o camber angle, $\kappa_1 - \kappa_2$, deg

ω	rotational speed, rad/sec

Subscripts:

AH	along line AH in figure 5
av	average
cℓ	obtained using closure trailing edge hypothesis
c	where pressure coefficient curves close or cross
DE	along line DE in figure 5
db	downstream boundary
exp	experimental value
G	obtained using Gostelow's trailing edge hypothesis
int	where linearly extrapolated pressure coefficient curves intersect
ℓ	local value on blade surface
m	meridional component
max	maximum
min	minimum
p	pressure surface
Rθ	tangential direction
s	suction surface
TE	trailing edge
ub	upstream boundary
W	obtained using Wilkinson's trailing edge hypothesis
θ	tangential component
1	blade row entrance
2	blade row exit

Superscript:

'	relative to blade

INTRODUCTION

The estimation of the direction of flow leaving an annular cascade of blades is an important problem in axial-flow turbomachinery aerodynamics. In design, blades must be selected which turn the fluid to the desired direction in order to achieve the desired energy transfer in rotors. Turning the flow to the desired direction is also important in both rotors and stators because unexpected and unwanted losses can occur when the desired flow direction into the next blade row is not achieved. In predicting the performance of a turbomachine at operating points other than design, it is necessary to estimate the direction of flow leaving blades of specified geometry. Incorrect estimation of these flow angles will lead to faulty prediction of energy transfer in rotors and incorrect values of estimated loss in subsequent blade rows. Thus estimating leaving flow angles is a critical part of both design and analysis calculations.

Historically, for compressor applications, the direction of flow leaving a blade cascade has been predicted by estimating the difference between the average direction of the leaving flow and the direction of the blade meanline at the trailing edge. This difference is defined as deviation angle. Measurements indicate that the flow is not turned far enough to leave the blade row in the direction of the blade meanline. This is reasonable since force must be exerted on the fluid to overcome inertia and produce turning. The forces which produce turning result from the curvature of the blade passage. However, blade passages tend to be too short to perfectly guide the fluid.

No completely satisfactory methods for estimating deviation angle are

available even for the simpler case of design point operation (ref. 1). The last major improvement in deviation angle estimation methods was published in 1946 (ref. 2). In the past the search for better deviation angle prediction methods was restricted mainly to correlations of experimental data. Theoretical calculations of both potential flow and boundary layer flow were possible but not widely used. Conformal transformation calculations of potential flow, for example, were too time-consuming to be practical. Boundary layer calculations were not practical on a large scale either, if for no other reason than because they required surface pressure distributions from a potential flow solution as input. However, recent advances in size and speed of digital computers have made it practical to obtain large numbers of theoretical solutions for some two-dimensional flows. These analytical tools are increasingly being used to supplement and in some cases to supplant experimental studies.

The purpose of this dissertation is to begin development of a more satisfactory method of estimating deviation angle by applying currently available analytical tools to the problem. A flow model was chosen for the study which was simple enough to treat theoretically while still allowing useful results to be obtained. Simplifications to the real flow included the assumptions that flow was steady and two-dimensional. While viscous effects were recognized as important, they were omitted in this work, although suggestions for future inclusion are given. Deviation angles estimated for a plane cascade using an existing inviscid flow computer program were compared with experimental data. Extensive studies made to assure the numerical validity of calculated results are presented.

USE OF CASCADES IN MODELING TURBOMACHINERY FLOW

Annular Cascade Models

The real flow in a compressor is three-dimensional, unsteady, turbulent, and compressible with large viscous forces in parts of the flow region. In addition, the flow is bounded by both moving and stationary walls which are highly complicated in shape. It is not yet possible to obtain a solution of this difficult fluid mechanics problem either theoretically or experimentally without introducing simplifying assumptions. The most common flow model used assumes the flow to be represented by steady circumferentially-averaged[a] velocities, angles, and fluid properties at a discrete number of stations as indicated in figure 1. These stations are often, though not always, located in radial planes which are outside the blade rows. The flow is assumed steady relative to each blade row although in a real machine this is impossible except for the first blade row. Viscous effects are neglected locally, but the accumulated viscous effects in the form of total pressure losses along a stream surface are included. Stream surfaces are assumed to be surfaces of revolution as illustrated in the sketch of figure 2. This is an approximation since the real stream surfaces are probably skewed and warped near the blades and are even more complicated in shape near the annulus walls. Circumferentially-averaged velocities, angles, and fluid properties are

---

[a]Ideally, mass-weighted circumferential averages are used. However, in practice, several kinds of averages are substituted for a true mass-weighted circumferential average. At stations behind rotating blades, time-averaged velocities, angles, pressures, and temperatures measured with low frequency response probes at fixed circumferential locations are often used. Data from circumferential traverses or from rakes are frequently area weighted to define averages behind stationary blade rows.

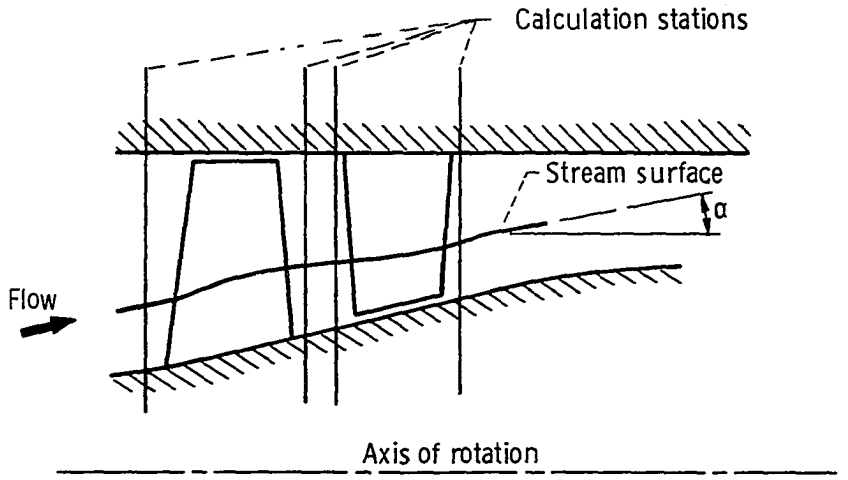

Figure 1. - Meridional plane cross section of an axial-flow compressor stage.

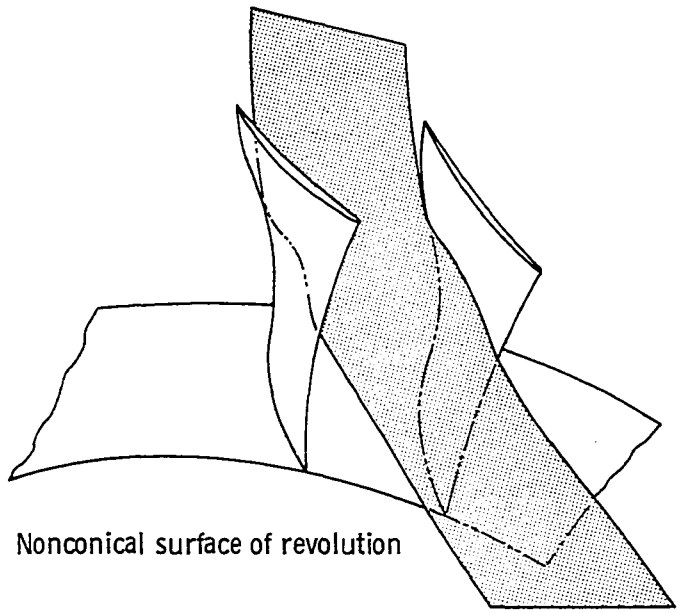

Figure 2. - Sketch of a general stream surface of revolution.

defined on these surfaces to represent the flow at a given radius and axial location.

When the stream surface of revolution is assumed to be a circular cylinder it can be developed to show the intersections of the blades as illustrated in figure 3. The circumferentially-averaged velocity at the trailing edge of the blades is represented by the vector W_2. The associated flow angle referenced to the axial direction is β_2'. Deviation angle δ is defined as the angle between the W_2 vector and the tangent to the blade mean line at the trailing edge (κ_2 in fig. 3). A more general stream surface of revolution (i.e., other than a cone) cannot be developed into an undistorted plane. In this case the exit blade angle κ_2 and the velocity W_2 are ordinarily defined on the plane tangent to the stream surface at the trailing edge. Deviation angle is then defined in the same plane.

Ultimately, the deviation angle distribution for an annular cascade, rotating or stationary, is determined (for a given fluid, inlet flow conditions, and rotational speed) by the geometric shape and arrangement of the blades and the annulus boundaries. Thus to estimate deviation angle for one stream surface in the flow model described above, it is necessary to consider not only the blade geometry on that surface, but also the blade geometry on all other stream surfaces and the annulus wall shapes. In addition fluid properties, inlet flow conditions, and rotational speed must be considered. The number of geometrical variables alone indicates the difficulty of developing a general deviation angle prediction method by correlating experimental data.

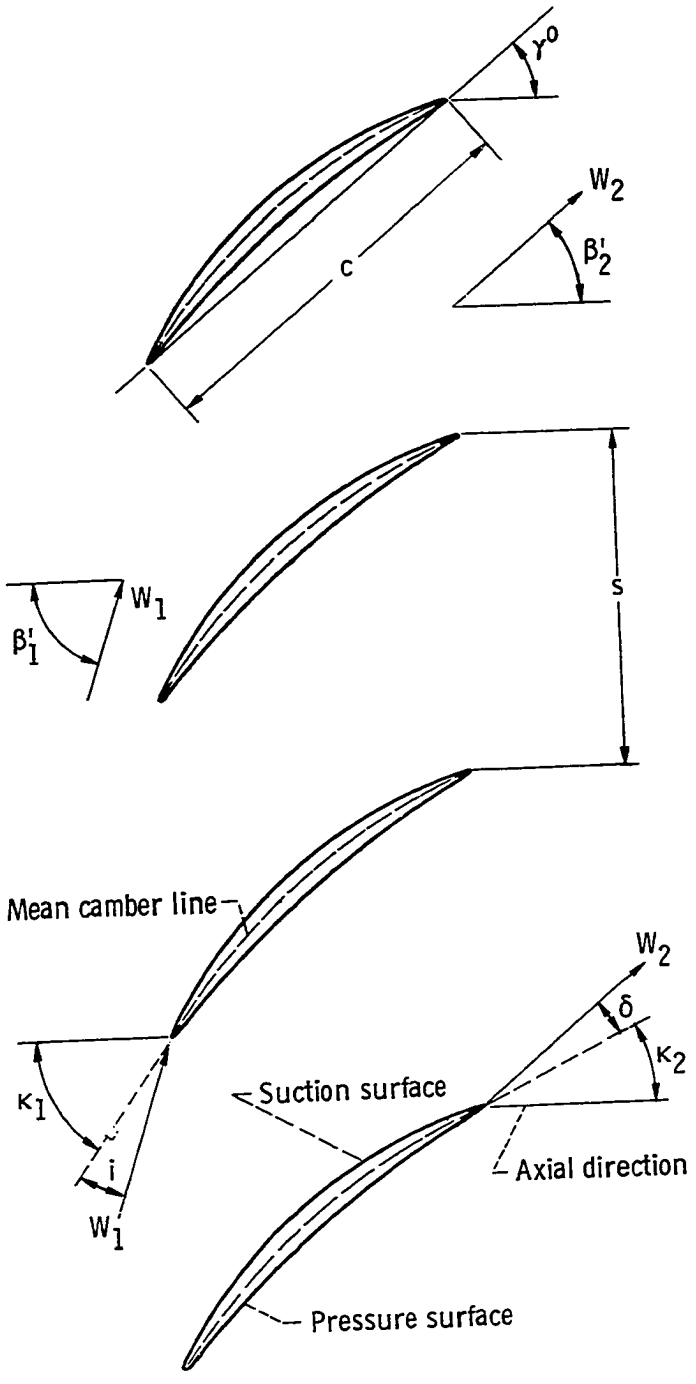

Figure 3. - Cascade view of blade sections and blade nomenclature.

A further simplification of the flow model is necessary in order to estimate deviation angles for each stream surface. The usual approach is to assume that the local blade geometry (i.e., blade geometry on the stream surface) has the dominant effect on deviation angle. The influences of the remaining flow boundaries, the inlet flow conditions, and rotational speed are accounted for by correction factors based on tests of similar blade rows or by testing and redesigning.

Plane Cascade Models

The influence of the local blade geometry on deviation angle can be studied using the untwisted blades of a plane, two-dimensional cascade. Two-dimensional flow is assured by using the same blade section along the entire blade span and by removing boundary layer fluid on the tunnel walls. Plane cascade flow is obviously simpler than flow in actual machines. For example, spanwise gradients of flow parameters are absent, as are annulus boundary layers, tip clearance flows, and centripetal forces. Although a real, viscous fluid is used, blade surface boundary layers are two-dimensional rather than three-dimensional. However, these simplifications in the flow model provide a significant advantage because tests can be made in which the blade section geometry parameters are varied systematically one at a time. This is not possible in annular cascades. Systematic testing has been reported for a few blade profile families (e.g., refs. 3, 4, 5, 6, 7, 8), but the number of variables involved make exhaustive testing impractical. Thus many combinations of geometric parameters are encountered for which extrapolation of test data is required. Extrapolation is always undesirable because of the added uncer-

tainty it introduces. Furthermore empirical correlations based on plane cascade data tend to lack generality with respect to blade profile shape (thickness distribution and meanline shape).

The problems of extrapolation and restriction to particular blade profiles associated with the use of correlated plane cascade data can be avoided by calculating the flow in the blade-to-blade plane analytically. In view of the seemingly advanced state of the art of calculations of flow about airfoils it seems that use of a theoretical model would be feasible.

THEORETICAL CASCADE MODEL

An exact theoretical calculation of plane, two-dimensional cascade flow accounting for the unsteadiness implicit in real turbulent flow and capable of describing regions of separated flow is currently impossible. Consequently simplified flow models must be used which retain enough features of real flow to yield useful results. A well developed approach is to divide the flow field into two parts with viscous boundary layer flow in a thin region near the blade surface and inviscid, irrotational flow in the remainder of the field. For flows with high Reynolds number and little or no separation, useful results can often be obtained by assuming inviscid flow throughout the cascade flow field.

A number of methods have been developed and published for calculating flow through a plane cascade using an inviscid flow model. Reviews of typical methods are given by Roudebush (ref. 9), Scholz (ref. 10), and Schilhansl (ref. 11). The inviscid flow models used have many features in common. The flow field typically contains a single row of blades with uniform flow assumed at some distance upstream and downstream from the blades. The flow is assumed steady, inviscid, and irrotational, but it is not always assumed incompressible. These assumptions together with the continuity and momentum equations can be combined to define a governing partial differential equation for the stream function or velocity potential throughout the flow field.

Boundary conditions must be given to complete the statement of the mathematical problem for subsonic flow. One condition required is that the blade profile form a streamline in the flow. Additional conditions

must be given which determine the location of the stagnation points near the leading and trailing edges. The leading edge stagnation point can be readily located by specifying the direction of the upstream uniform flow since this is usually given or known in advance. The location of the trailing edge stagnation point or equivalently the direction of the uniform downstream flow also must be given to complete the mathematical statement of the flow problem.

In real flow, viscous forces play a key role in determining the blade circulation or equivalently, the leaving flow angle, but the inviscid flow problem is indeterminate unless the leaving flow angle or the trailing edge stagnation point is specified. There are an infinite number of mathematically complete inviscid flow problems corresponding to the infinite number of locations which can be specified for the trailing edge stagnation point. Since the objective is to obtain a theoretical flow solution which approximates the real flow as closely as possible, the choice of the rear stagnation point location must be based on some knowledge of real flow patterns.

In the somewhat academic case of blades with either sharp or cusped trailing edges the Kutta condition (ref. 12) is used as the trailing edge condition. The Kutta condition requires that the velocities on the pressure and suction surface be equal at the trailing edge point. Equality of velocity implies a stagnation point if the blade surfaces form a wedge at the trailing edge, but not if they form a cusp. Imposing the Kutta condition on the problem avoids the physically implausible condition of an infinite velocity at a sharp trailing edge. Unfortunately the Kutta

condition does not apply to blades with rounded trailing edges which are normally used in turbomachines to lower material stresses. No generally accepted trailing edge hypothesis analogous to the Kutta condition exists for rounded trailing edge blades, although several proposals have been advanced. Three of these proposed trailing edge hypotheses (refs. 13, 14, and 15) are evaluated in the DEVIATION ANGLE ESTIMATION section.

Solutions of the completely specified inviscid cascade flow problem can be obtained by a number of mathematical techniques. For incompressible flow the governing equation is Laplace's equation which can be solved by conformal transformation, superposition of singularities on a uniform flow, or by a numerical finite difference technique. Conformal transformation methods remain relatively slow and are not widely used (ref. 10). Singularity techniques have been published by Schlichting (ref. 16), Martensen (ref. 17), and Giesing (ref. 18) among others. Katsanis (ref. 19) has published a computer program which uses a numerical finite difference technique to solve for the incompressible flow in cascades.

For compressible flow, the partial differential equations for stream function and velocity potential have the form of Poisson's equation. They have been solved for subsonic compressible flow by Imbach (ref. 20) using a singularity solution and by Katsanis (ref. 21) and Smith (ref. 22) using finite-difference techniques.

The computer program by Katsanis (ref. 21) was chosen for use in this study. Reasons for its choice include its capability of handling both compressible and incompressible flow and the availability of an

auxiliary program (ref. 23) which allows finer definition of flow details near the trailing edge.

INVISCID FLOW COMPUTER PROGRAMS

Only a brief description of the inviscid flow computer programs will be given here. For more details references 21 and 23 should be consulted. Both programs, TSONIC (ref. 21) and MAGNFY (ref. 23), are basically similar and the description will apply to both with the few differences noted appropriately. The programs were written in a general form which permits calculation of flow on a surface of revolution for an annular cascade either rotating or stationary as well as the simpler case of a plane cascade. The surface of revolution is assumed to be a stream surface. The calculation region for the general case is shown in figure 4. The (R,θ,z) coordinates of the surface were mapped into a (m,θ) plane by functional relations

$$\theta = \theta$$

$$m = m(R,z)$$

The resulting calculation regions are shown in the $m - \theta$ plane (fig. 5).

The flow on the assumed stream surface in figure 4 is further simplified from the real flow by the following assumptions:

1. The flow is steady relative to the blades.

2. The fluid is an ideal gas with constant c_p or is incompressible.

3. The fluid is nonviscous, and there is no heat transfer (therefore, the flow is isentropic).

4. The stagnation temperature and the velocity vector are uniform across the inlet boundary (therefore the flow is irrotational in absolute coordinates as well as isentropic).

5. The velocity is uniform across the downstream boundary.

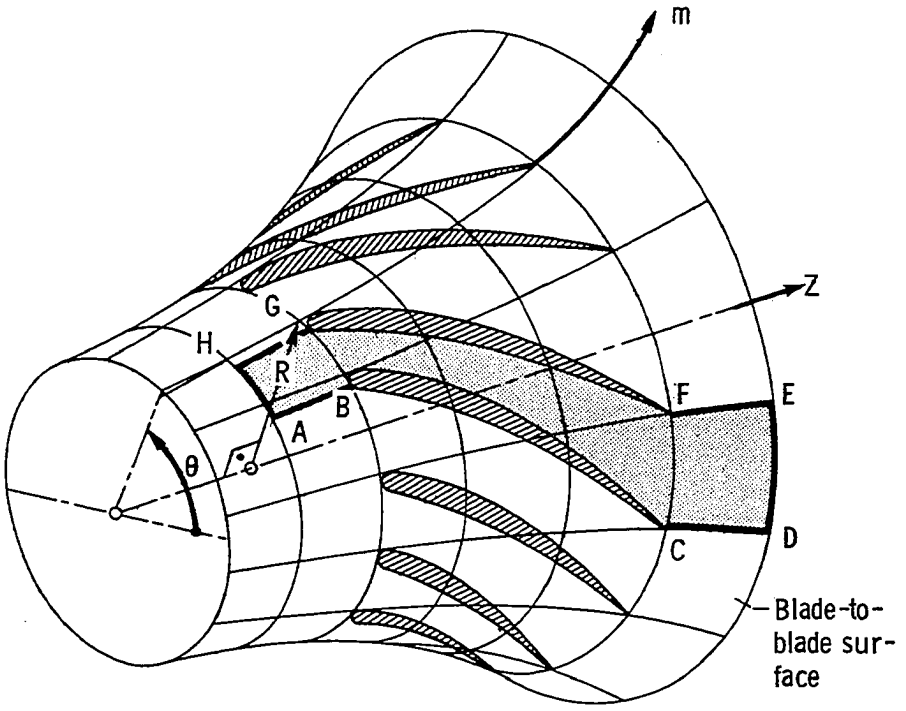

Figure 4. - Blade-to-blade surface of revolution, showing m - θ coordinates (from ref. 21).

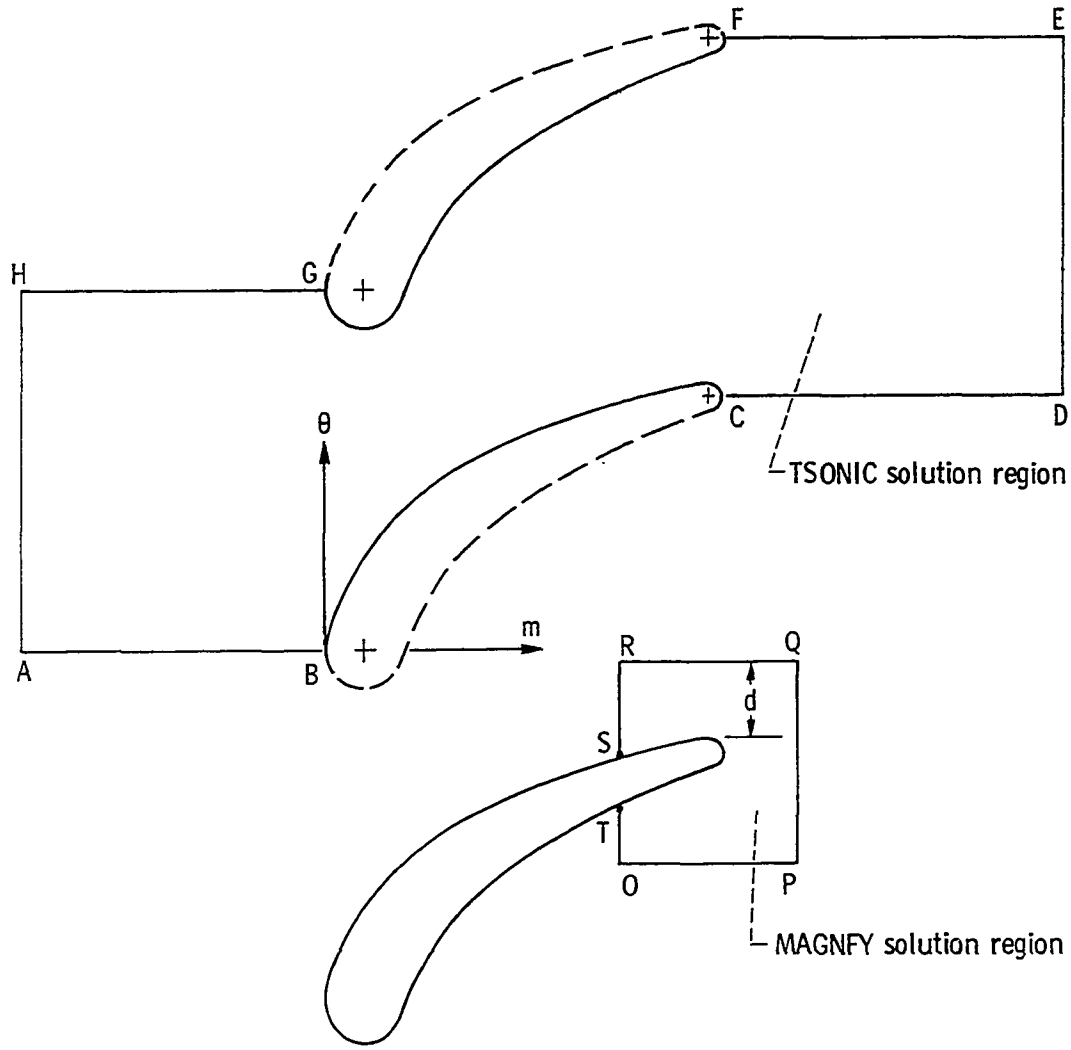

Figure 5. - Solution regions for TSONIC and MAGNFY.

6. The only forces are those due to momentum and pressure gradient.

7. The flow is subsonic except that TSONIC allows small areas of low supersonic flow.

In this study the full capabilities of the TSONIC program were not required since only low subsonic flow in plane cascades was computed. Therefore the transonic flow calculation subroutines were removed from TSONIC essentially reducing it to the subsonic TURBLE program reported in reference 24.

The assumptions listed above were incorporated into the continuity equation and the equation of motion which were then combined into a second order partial differential equation for stream function. The derivation is presented in reference 25. The equation for the stream function u used in TSONIC and MAGNFY can be obtained from equation 12(9) of reference 25 by substituting $-uw$ for the stream function of reference 25. The resulting equation is

$$\frac{1}{r^2}\frac{\partial^2 u}{\partial \theta^2} + \frac{\partial^2 u}{\partial m^2} - \frac{1}{r^2}\frac{1}{\rho}\frac{\partial \rho}{\partial \theta}\frac{\partial u}{\partial \theta} + \left[\frac{\sin \alpha}{r} - \frac{1}{b\rho}\frac{\partial (b\rho)}{\partial m}\right]\frac{\partial u}{\partial m} = \frac{2b\rho\omega}{w}\sin \alpha \qquad (1)$$

The stream function u is normalized by the mass flow per blade channel, w, so that it has a value of 0 on surface BC (fig. 5) and 1 on surface GF. The stream function is related to velocity by the equations

$$\frac{\partial u}{\partial m} = -\frac{b\rho}{w} W_\theta \qquad (2)$$

$$\frac{\partial u}{\partial \theta} = \frac{b\rho r}{w} W_m \qquad (3)$$

Equation (1) is an elliptic equation and thus boundary conditions must be specified for the solution regions of figure 5. Along BC and FG

(fig. 5) the stream function is assigned values of 0 and 1 as stated above. The assumed periodicity of the flow in the θ-direction allows the stream function on HG to be specified as the stream function value on AB for the same m-value plus 1. The same kind of periodic boundary condition is applied to lines CD and EF in figure 5. Along AH and DE $\partial u/\partial m$ is specified. Evaluation of $\partial u/\partial m$ on AH is possible since a uniform flow is assumed, thus by (2)

$$\left(\frac{\partial u}{\partial m}\right)_{AH} = \left(-\frac{b\rho}{w} W_\theta\right)_{AH} = \left(-\frac{b\rho}{w} W_m \tan \beta_1'\right)_{AH} = \left(-\frac{1}{R}\frac{\partial u}{\partial \theta} \tan \beta_1'\right)_{AH} \tag{4}$$

But the flow is uniform and periodic along AH; so

$$\left(\frac{\partial u}{\partial \theta}\right)_{AH} = \frac{u(H) - u(A)}{\theta(H) - \theta(A)} = \frac{1}{s} \tag{5}$$

Substituting (5) into (4)

$$\left(\frac{\partial u}{\partial m}\right)_{AH} = -\frac{1}{R_{AH} s} \tan \beta_1' \tag{6}$$

Similarly it can be shown that

$$\left(\frac{\partial u}{\partial m}\right)_{DE} = -\frac{1}{R_{DE} s} \tan \beta_2' \tag{7}$$

The angles β_1' and β_2' must be obtained from input information.

Boundary conditions for MAGNFY are set by specifying the value of stream function on all segments of the boundary (fig. 5). Stream function values from TSONIC output are specified at discrete points on OPQRST. The stream function is set to zero on the blade surface ST.

Solution of equation (1) subject to the stated boundary conditions was accomplished by approximating the derivatives in (1) by finite difference expressions. The resulting finite difference equation was applied

at interior mesh points of a uniform grid covering the solution region (see fig. 6). A nonlinear algebraic equation for the stream function at each interior mesh point in terms of the stream function and density values at a few surrounding points was obtained. Thus a system of n nonlinear algebraic equations in n unknowns (stream function values at n interior mesh points) was evolved. This system of equations is solved in two levels of iteration. First the system is linearized by assuming a value for density at each interior mesh point. The system of linear equations is then solved to obtain a value for stream function at each interior mesh point by the iterative process of successive over-relaxation described on page 77 of reference 26. Velocity derivatives are obtained by numerically differentiating the stream function solution and then equations (2) and (3) are used to calculate an improved estimate of density at each mesh point. A new system of linear equations is developed using the improved estimate for density. The linear system is solved for stream function and the process is continued until the outer iteration for density and the inner iteration for stream function have both converged.

The converged value of stream function at each mesh point is printed as output. Velocity magnitude and direction are printed for each mesh point and for the points where the mesh lines intersect the blade surfaces.

For this study both TSONIC and MAGNFY were modified to provide blade surface pressure coefficients at the intersections of the mesh lines and blade surfaces as additional output. The points of intersec-

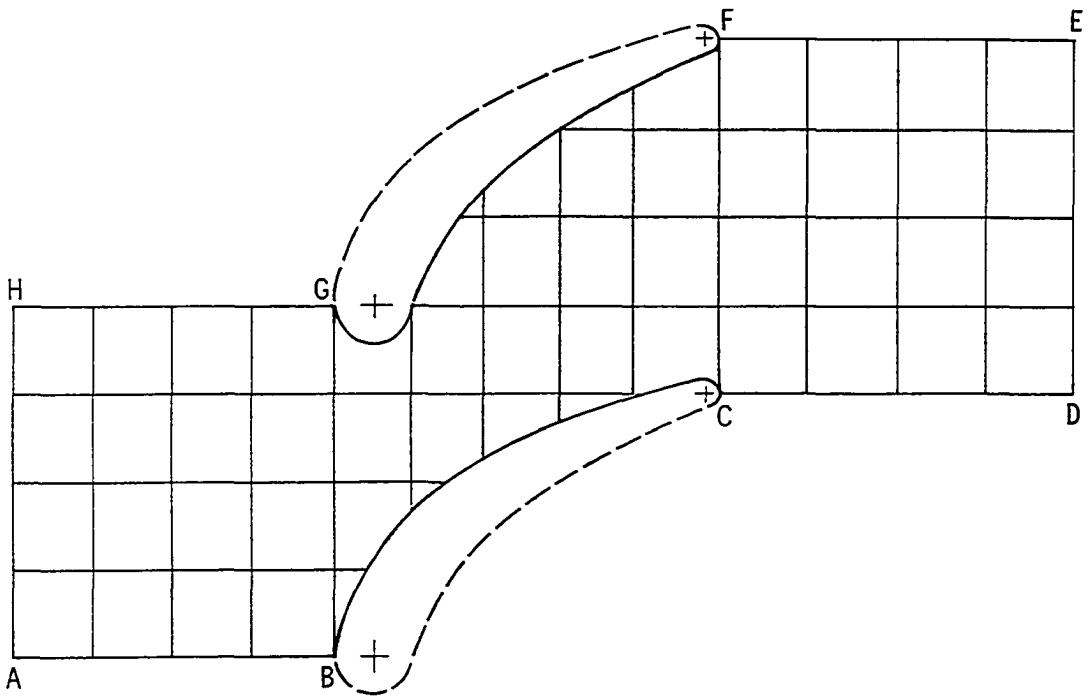

Figure 6. - Type of mesh used in TSONIC solution.

tion were assigned a fraction of chord value by projecting a line from the leading edge to the intersection point onto the chord line and dividing the length of the projection by the length of the chord line. The coding changes and additions necessary to generate this additional output are given in APPENDIX A. A number of other coding changes made for various reasons are also given in APPENDIX A.

The programs were run on an IBM 7094-2/7044 direct coupled system.

PROBLEMS IN UTILIZATION OF THE INVISCID FLOW PROGRAMS

In the first attempts to use the two computer programs (ref. 21 and 23) described in the INVISCID FLOW PROGRAMS section, a user is confronted with a number of problems concerning input data. Several of these problems were investigated in some detail to assure the numerical validity of the calculated results presented in the DEVIATION ANGLE ESTIMATION section. Complete generality cannot be claimed for the conclusions reached which are presented in this section, but they should offer helpful guidelines for subsequent first time users of these programs.

Selection of TSONIC Boundary Locations

The locations of the upstream and downstream boundaries for the TSONIC solution region (lines AH and DE, fig. 5) are specified through the input data cards. The selection of the distance between the blade edges and the boundaries is based on a compromise between two conflicting requirements. From physical considerations the boundaries should be placed far enough from the blades so that the assumed uniform flow at the boundaries is indeed realized in the solution. However, to minimize the number of interior mesh points, and thus the storage requirements and computing costs, it is desirable to keep the boundaries close to the blades.

To establish guidelines for making this compromise, example calculations were run for two cascade geometries. In the examples, the location of the upstream and downstream boundaries were changed systematically while all other input variables were fixed. The effects of the boundary locations on the solution were examined by comparing the nonuniformity in

velocity magnitude and direction at the upstream and downstream boundaries and by comparing velocity magnitudes at representative locations on the blade surface. The cascade geometry used in these examples was a 10C4/30C50 profile (see ref. 27 for nomenclature) with a solidity σ of 1. A comparison of the nonuniformity of velocity on the upstream and downstream boundaries for two different inlet flow angles is shown in figures 7 and 8. The velocity nonuniformity is represented by the difference between the maximum and minimum velocities at boundary grid points divided by the average value of the velocity at the boundary. The angle nonuniformity is simply presented as maximum difference in the angles calculated on the boundary. The distance of the boundaries from the blade edges is normalized by the chord in figures 7 and 8. This nondimensional distance parameter lacks generality as can be appreciated by considering the limiting case where the chord length approaches zero. Because of this lack of generality and the meager data presented, conclusions drawn from figures 7 and 8 should be used as guidelines and not applied indiscriminately without verification.

The curves in figures 7 and 8 indicate that velocity and angle nonuniformities can be reduced to approximately one percent and one half degree, respectively, by locating the boundaries at least 0.72 chord length upstream and 0.47 chord length downstream from the blade edges. As a practical matter, however, this degree of uniformity is not needed for most purposes since a small amount of nonuniformity on the up- and downstream boundaries does not have a large effect on the flow solution near the blades. To illustrate this point representative blade surface

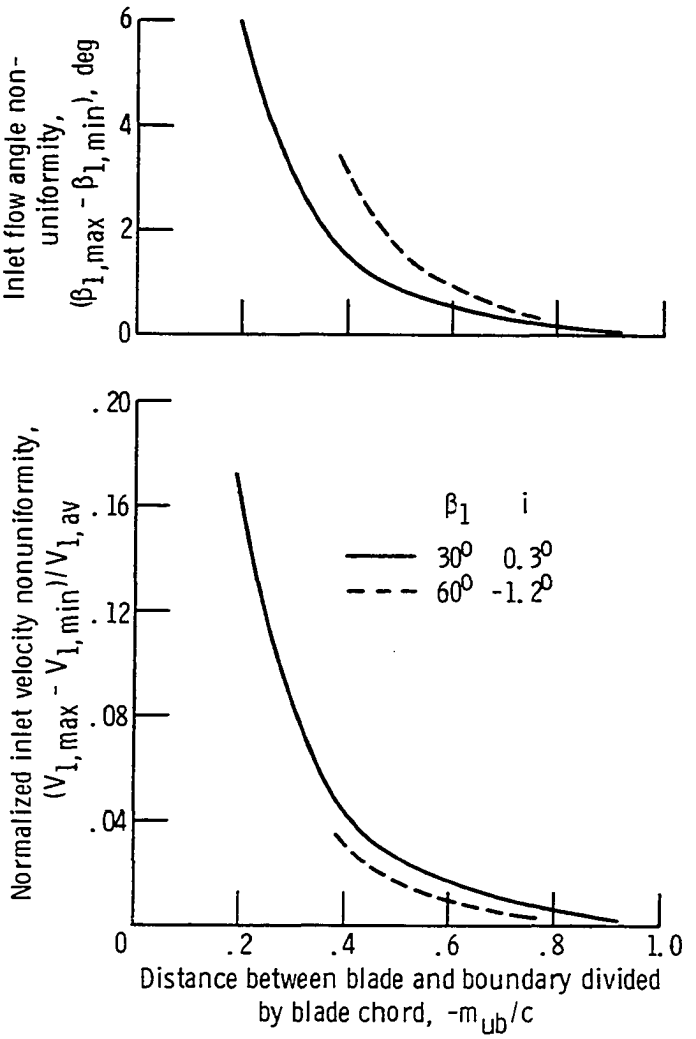

Figure 7. - Effect of the location of the upstream boundary on the uniformity of flow at that boundary in the TSONIC solution.

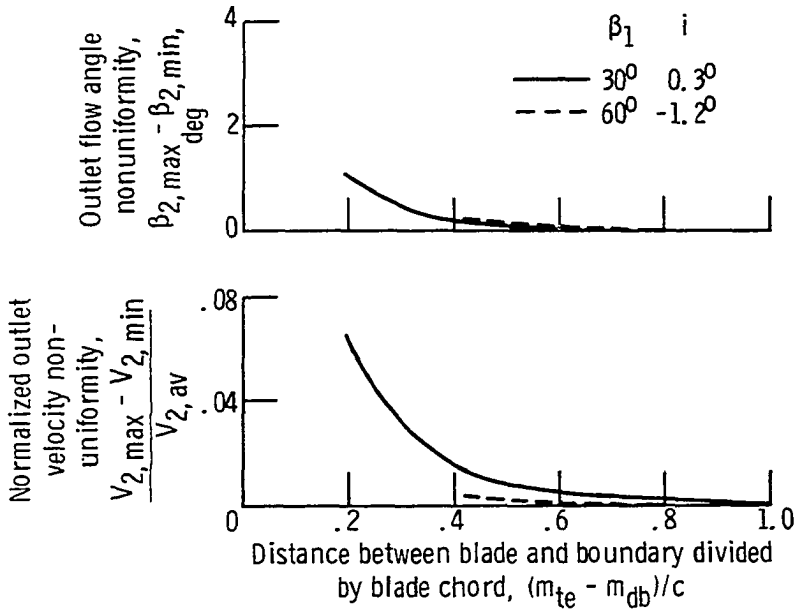

Figure 8. - Effect of the location of the downstream boundary on the uniformity of flow at that boundary in the TSONIC solution.

velocities are shown in figures 9 and 10 as a function of boundary location.

In all example cases the upstream and downstream boundaries were located the same distance from the blade edges. However, additional examples which are not presented indicated that practically the same quantitative results are obtained if one boundary location is fixed and the other one varied. Also the above conclusions were not found to be significantly affected by the mesh size used.

Based on the results presented in figures 7 to 10, the boundaries in this study were located from 0.75 to 0.84 chord lengths from the leading and trailing edges. This choice assured valid numerical results without increasing computing time unduly.

Selection of TSONIC Mesh Size

Numerical solutions of a differential equation obtained using finite-difference techniques are assumed to approximate the true solution more and more closely as the finite-difference mesh size is decreased. For engineering work there is no advantage in reducing the mesh size below a value judged to allow calculation of a solution approximating the true solution within a reasonable tolerance. In solving the boundary value problem described in INVISCID FLOW COMPUTER PROGRAMS it is difficult if not impossible to determine with certainty how small a mesh is required. However, a reasonable estimate of the mesh size required to give a good approximation to the true solution was obtained by comparing approximate solutions obtained using several different mesh sizes.

The approximate solutions were represented by velocities calculated

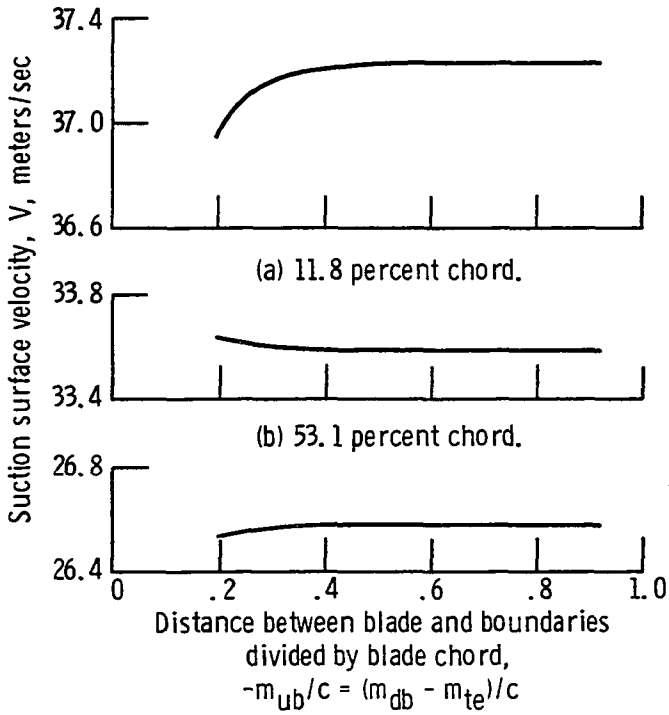

Figure 9. - Effect of the upstream and downstream boundary locations on representative suction surface velocities for $\beta_1 = 30^0$, $i = 0.3^0$.

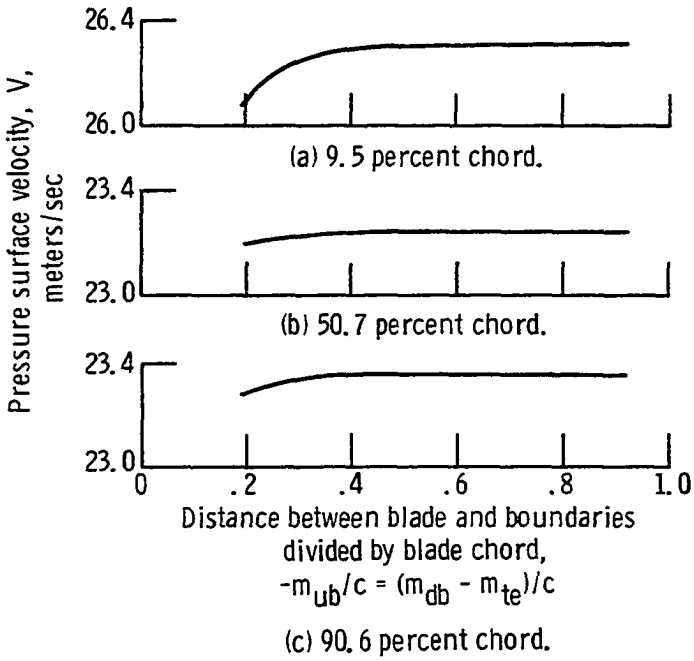

Figure 10. - Effect of the upstream and downstream boundary locations on representative pressure surface velocities for $\beta_1 = 30^0$, $i = 0.3^0$.

at three points on the blade suction surface. The mesh was chosen to be approximately square in $m - R\theta$ coordinates. The mesh length in the θ-direction enters the difference equation as $h_{R\theta} = (R)(\Delta\theta)$ (APPENDIX A, ref. 24) even though the solution region is the $m - \theta$ plane. The variations in representative blade suction surface velocities with decreasing grid size are shown in figure 11. Calculated points are connected with straight lines to emphasize the discrete nature of the data. The velocity magnitudes in figure 11 change only slightly as $(h_m + h_{R\theta})/2c$ is reduced below 0.035 (note the expanded scale for velocity). On the basis of the example calculations presented in figure 11 a mesh size parameter $(h_m + h_{R\theta})/2c$ value less than 0.035 was used for all calculations presented in the DEVIATION ANGLE ESTIMATION section.

Determination of Blade Geometry Input Data

For both the TSONIC and MAGNFY programs blade geometry information is required which can be quite time consuming to determine. Quantities required are illustrated in figure 12 taken from reference 21. As indicated in figure 12, $m - \theta$ coordinates along the blade surface with respect to the particular coordinate system shown are required. In the case of a plane cascade, an artificial radius is chosen for the stream surface in order to determine θ-coordinates for input. An artificial number of blades must also be specified to maintain the desired spacing between blades. Since blade coordinates are often known with respect to the chord line a somewhat laborious transformation of coordinates may be necessary to prepare input data each time calculations are made for a different blade setting angle. Also the true tangent angle (not in the

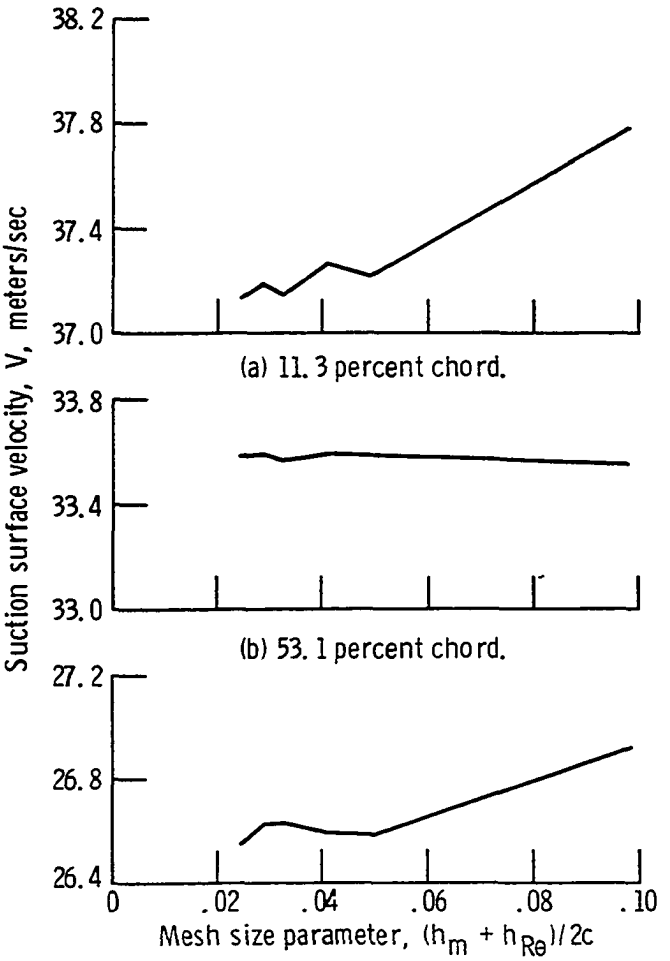

Figure 11. - Effect of mesh size on suction surface velocities for a 10C4/30C50 cascade. $\beta_1 = 30^0$, $i = 0.3^0$

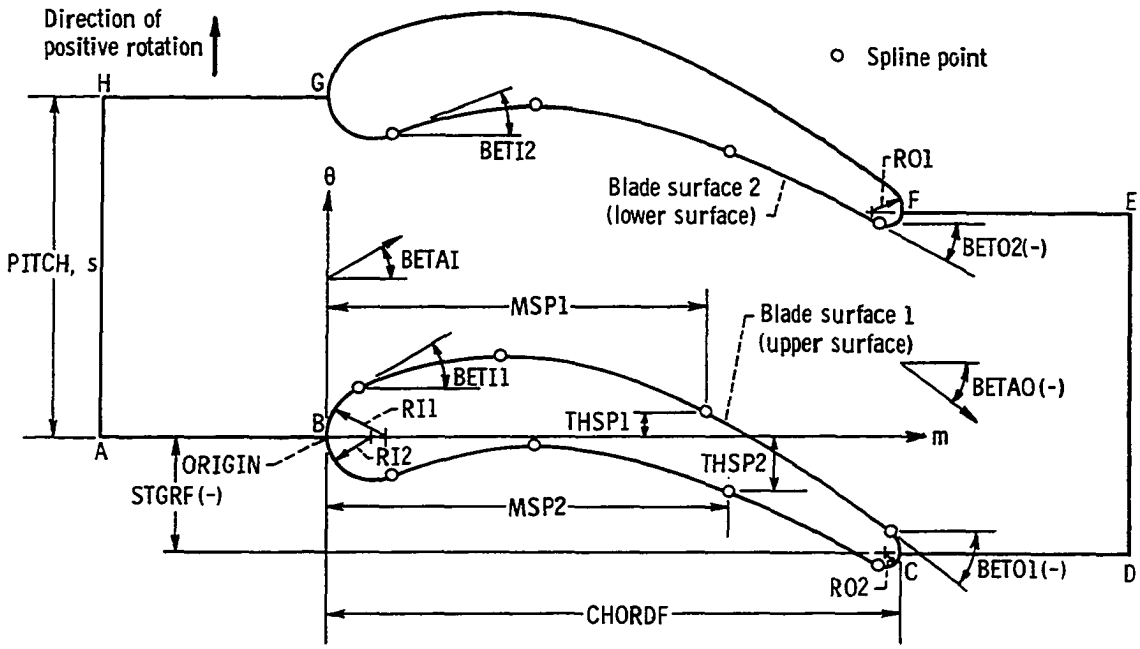

Figure 12. - Geometric input variables on blade-to-blade stream surface. Angles BETAI, BETAO, BETI1, BETI2, BETO1, and BETO2 must be given as true angle β in degrees, not the angle as measured in m-θ plane. Either use $\tan\beta = r\, d\theta/dm$ to obtain β, or measure the true angle (from ref. 21).

m - 0 plane) at the four points where the blade surfaces meet the edge circles must be supplied as input. For a general profile which is not analytically describable it may be necessary to resort to graphical methods to determine these points and the corresponding surface angles. Also coordinates of the extreme downstream point on the trailing edge must be calculated. When the blade section is a double-circular-arc profile lying on a cylindrical surface all the geometrical input described can be conveniently obtained using the computer program described in reference 28. For all other sections considerable effort and time is required unless a similar program is available.

Since a 10C4/30C50 profile in plane cascade was selected for this study a computer program was written to expedite determination of the necessary geometrical quantities. This program called ARBBP is described in APPENDIX B. It requires blade coordinates in one of three coordinate systems shown in figure 13 as input. In addition radii of the edge circles must be given and the location of the edge circle centers must be given when coordinate system 3 is used. All of the geometric quantities shown in figure 12 which are needed for TSONIC input data are calculated in ARBBP and printed as output. The ARBBP output includes blade coordinates in the coordinate system of figure 12. These blade coordinates are obtained by mapping both the original input coordinate points and interpolated points from a coordinate system of figure 13 to the coordinate system shown in figure 12.

Choosing a suitable subset of coordinate points (MSP1, THSP1) and (MSP2, THSP2) (see fig. 12) from the ARBBP output to use for TSONIC and

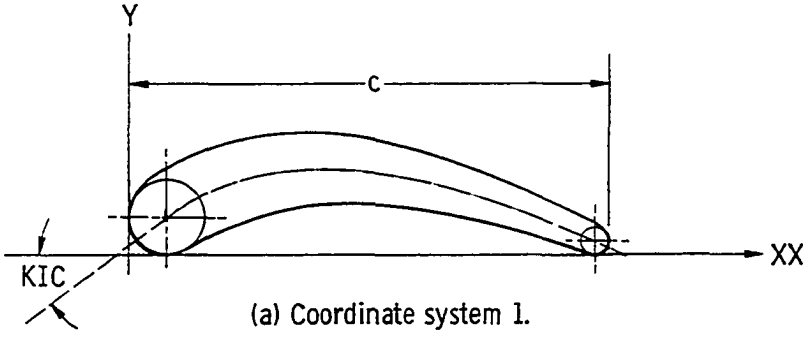

(a) Coordinate system 1.

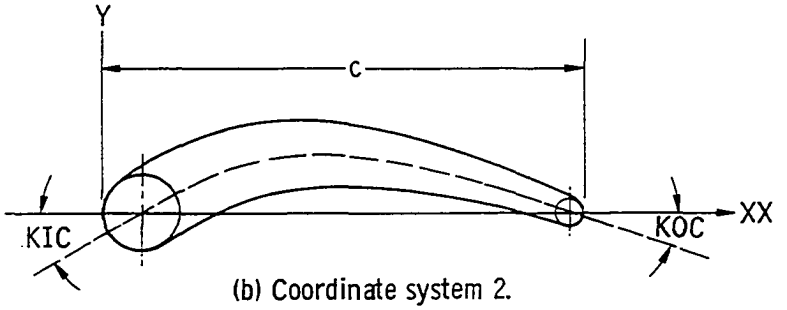

(b) Coordinate system 2.

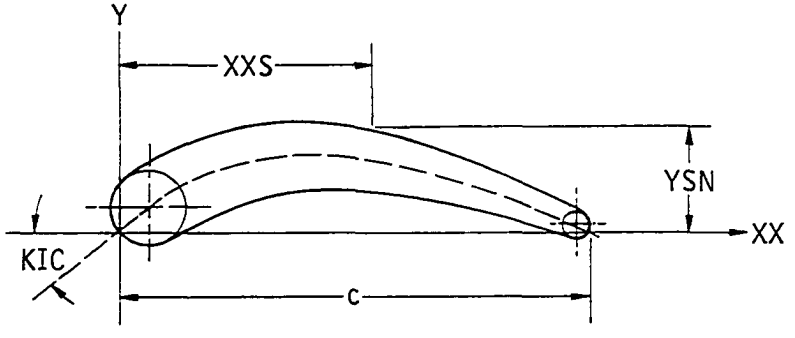

(c) Coordinate system 3.

Figure 13. - Optional coordinate systems for ARBBP input data.

MAGNFY input was the most time-consuming difficulty encountered in using these programs. Piecewise cubic spline curves (ref. 29) are fitted through the points in TSONIC and MAGNFY to represent the blade surfaces in the numerical solution procedure. The proper number of blade coordinates must be selected and located at appropriate positions on the profile to obtain spline curves with smoothly varying curvatures which accurately describe the blade.

Examples showing an unsuitable and a suitable set of coordinate points for the same blade profile are illustrated in figures 14 and 15, The set of coordinate points shown in figure 14 do not describe the blade adequately especially near the leading edge where the surface curvature varies rapidly. By adding coordinates judiciously as illustrated in figure 15 it was possible to describe the blade quite satisfactorily. That the choice of coordinates has a significant effect on the calculated solution can be seen by comparing the blade surface velocities shown in figures 14 and 15.

The cubic spline representation enters the calculated solution in two ways. One way is through the boundary conditions at intersections of the grid lines with the blade surfaces (fig. 6). The locations of the intersections are found by interpolating the cubic spline curves. Also, in obtaining surface velocities from the stream function solution at the grid line intersections, it is necessary to differentiate the cubic spline curves to determine the slope of the blade surface.

No direct method of choosing a suitable set of profile coordinates was found, so a trial and error procedure was used in this work. The

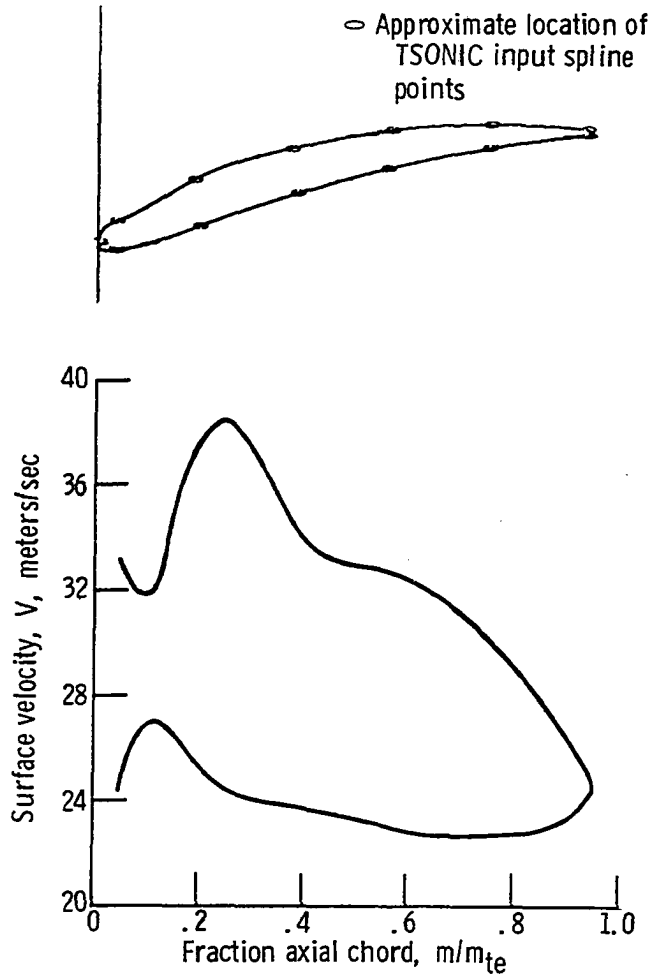

Figure 14. - Example of spline fit and blade surface velocities calculated for a 10C4/30C50 blade using an unsuitable set of profile coordinates. $\beta_1 = 30^0$, $i = 0.3^0$, $\delta = 8.7^0$, $\sigma = 1.0$.

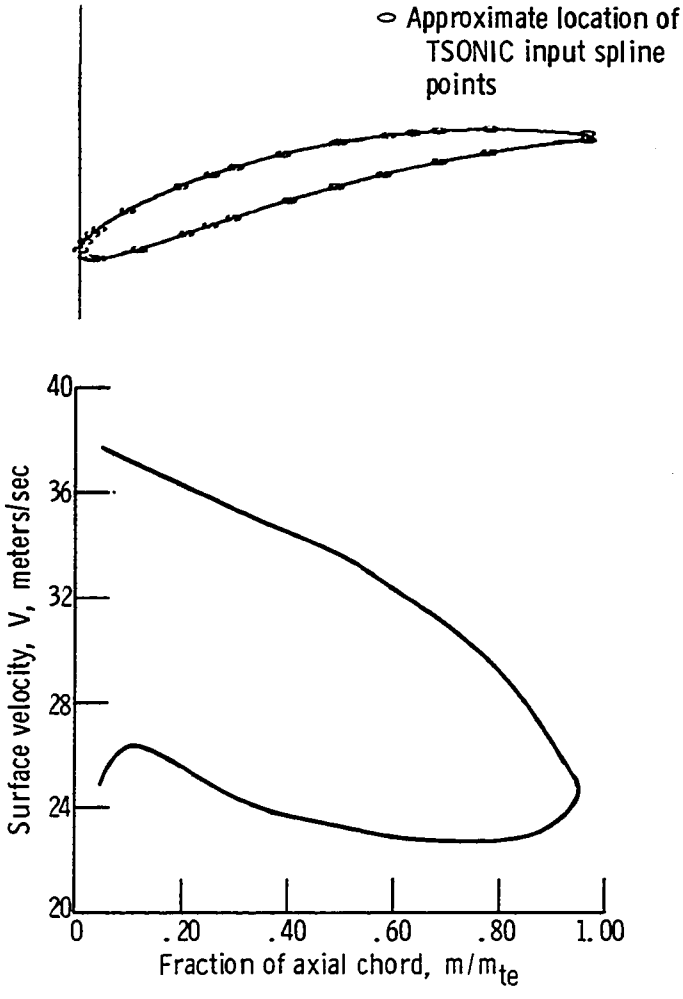

Figure 15. - Example of spline fit and blade surface velocities calculated for a 10C4/30C50 blade using a suitable set of profile coordinates. $\beta_1 = 30^0$, $i = 0.3^0$, $\delta = 8.7^0$, $\sigma = 1.0$.

procedure used was to select a set of coordinates and then examine the variation of curvature along the surface calculated using a cubic spline curve fitted to the coordinate points. This can be done by preparing TSONIC input cards and running the program for a limited time (less than 30 seconds in this investigation). The resulting output contains curvature values computed at the intersections of the vertical grid lines with the blade surfaces. If the curvature varies smoothly along the blade surface the input coordinates used for the calculation are usually considered satisfactory. To illustrate this point the curvatures calculated for the examples of figures 14 and 15 are shown in tables 1 and 2. Notice especially that curvatures for surface 1 (suction surface) change sign in table 1 and do not vary smoothly along the surface. In contrast the curvatures shown in table 2 vary smoothly on both surfaces. The change of sign on curvature on surface 2 (pressure surface) is representative of the actual blade shape.

If the selected set of coordinates does not result in smoothly varying curvatures then it may be necessary to add points, omit points, or replace points to obtain a suitable set. In general coordinates must be spaced close together where the curvature is large and farther apart where it is small. In case the original coordinates were obtained graphically or by some other inexact method it may be necessary to change the last few digits of some coordinates to obtain a smooth fit. In doing this care must be exercised to preserve the correct shape of the blade section.

It is somewhat easier to judge what changes are needed to obtain a

Table 1. Curvatures calculated in TSONIC using input coordinates shown in figure 14.

Meridional coordinate	Suction surface		Pressure surface	
	dθ/dm	Curvature	dθ/dm	Curvature
0	0.10E+11	0	-0.10E+11	0
0.615E-02	.72	34.0	0.24	30.4
.123E-01	1.04	11.8	.51	17.5
.184E-01	1.11	-2.8	.65	7.0
.246E-01	.94	-17.7	.69	-1.9
.307E-01	.70	-15.8	.65	-2.9
.369E-01	.52	-11.8	.61	-2.6
.430E-01	.42	-6.3	.58	-2.3
.492E-01	.38	-0.9	.55	-1.9
.553E-01	.37	-2.2	.53	-2.1
.615E-01	.33	-3.5	.50	-2.4
.676E-01	.29	-4.9	.47	-2.7
.738E-01	.23	-6.3	.44	-3.0
.799E-01	.16	-6.1	.41	-3.0
.861E-01	.10	-5.6	.37	-2.9
.922E-01	.52E-01	-5.2	.34	-2.9
.984E-01	.19E-02	-4.7	.31	-2.9
.104	-0.44E-01	-4.4	.28	-3.4
.110	-0.89E-01	-4.2	.24	-3.9
.116	-0.13	-3.9	.19	-4.4
.123	-0.10E+11	0	.10E+11	0

suitable set of coordinates if curvatures at the input coordinate points themselves are available. A computer program INCHK was developed to calculate curvatures at the input coordinate points as well as to provide addition capabilities described later in this section. A number of TSONIC subroutines were used in INCHK so that the TSONIC input cards comprise the bulk of the INCHK input data. One extra input card which is described in APPENDIX C is required in addition to the TSONIC input cards. The listing for INCHK together with a description of input and output is also given in

Table 2. Blade surface curvatures calculated in TSONIC using input coordinates shown in figure 15

	Suction surface		Pressure surface	
Meridional coordinate	dθ/dm	Curvature	dθ/dm	Curvature
0	0.10E+11	0	-0.10E+11	0
0.615E-02	1.29	-21.2	0.32	28.7
.123E-01	1.00	-10.6	.53	10.9
.184E-01	.85	-9.1	.61	3.7
.246E-01	.74	-7.0	.63	.3
.307E-01	.64	-7.1	.64	.4
.369E-01	.57	-5.0	.62	-2.6
.430E-01	.51	-5.2	.59	-2.5
.492E-01	.44	-5.5	.56	-2.4
.553E-01	.38	-5.5	.53	-2.4
.615E-01	.32	-5.4	.50	-2.4
.676E-01	.26	-5.2	.47	-2.6
.738E-01	.21	-5.1	.44	-2.8
.799E-01	.16	-5.0	.41	-3.0
.861E-01	.11	-5.0	.37	-3.1
.922E-01	.59E-01	-5.1	.34	-3.0
.984E-01	.70E-02	-5.2	.31	-2.8
.104	-0.44E-01	-4.8	.28	-3.3
.110	-0.90E-01	-4.3	.24	-3.9
.116	-0.13	-3.8	.19	-4.4
.123	-0.10E+11	0	.10E+11	0

APPENDIX C.

A further complication arises in selecting a suitable set of coordinates because the cubic spline curves are not invariant with respect to rotation. Thus if the same physical set of points is used as input coordinates to describe a blade in two different orientations (blade setting angles), two physically different shapes are obtained using cubic spline fits. Because of this, a slightly different set of input coordinate points for TSONIC is usually required each time a different blade setting angle is used for a given blade section.

Because the spline fits used in TSONIC are not invariant with respect to rotation, some means of checking the resulting blade shapes is required when a series of calculations are made for the same profile at different setting angles. The results presented in the DEVIATION ANGLE ESTIMATION section were calculated for a single profile at different setting angles. To check that the spline curves defining the blade shape at different setting angles were reasonably consistent, blade surface angles were compared against surface angles calculated for a reference baseline cascade with a blade setting angle of -0.26°.

The comparison of surface angles was accomplished using results from the INCHK program. A subprogram in INCHK rotates the coordinates and angles associated with the spline curves at a given blade setting angle into corresponding coordinates and angles in the reference position. Figure 16 illustrates the reference position. By mapping the surface angles calculated for different blade setting angles into a common reference position it is possible to compare them using plots of surface angle versus meridional distance m (fig. 17). The largest inconsistencies in the spline fits occurred on the suction surface near the leading edge of the blades. Over the last 90 percent of the blade surface the surface angles differed by less than 1/2 degree for blade setting angles ranging from -0.26 to 46.2 degrees.

Selection of MAGNFY Boundary Locations

In this study the MAGNFY program was used to obtain a more detailed solution near the trailing edge to allow a better definition of the stagnation point location. The shape of the calculation region is illus-

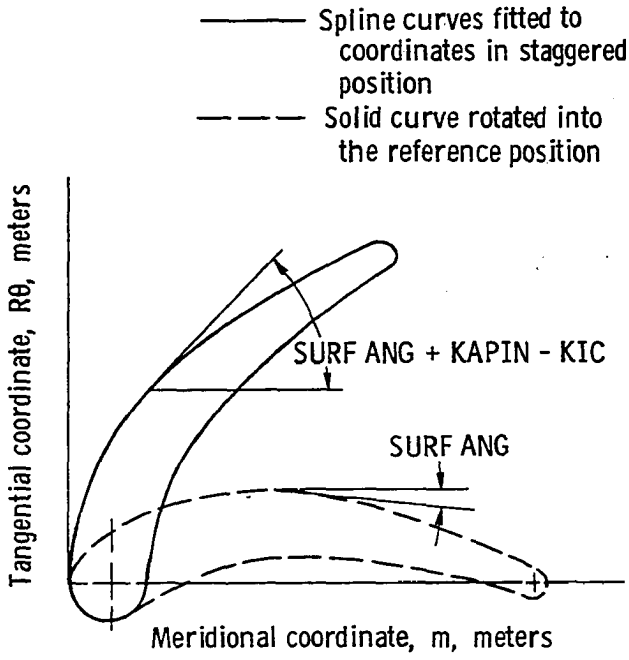

Figure 16. - Reference blade position used in the INCHK program

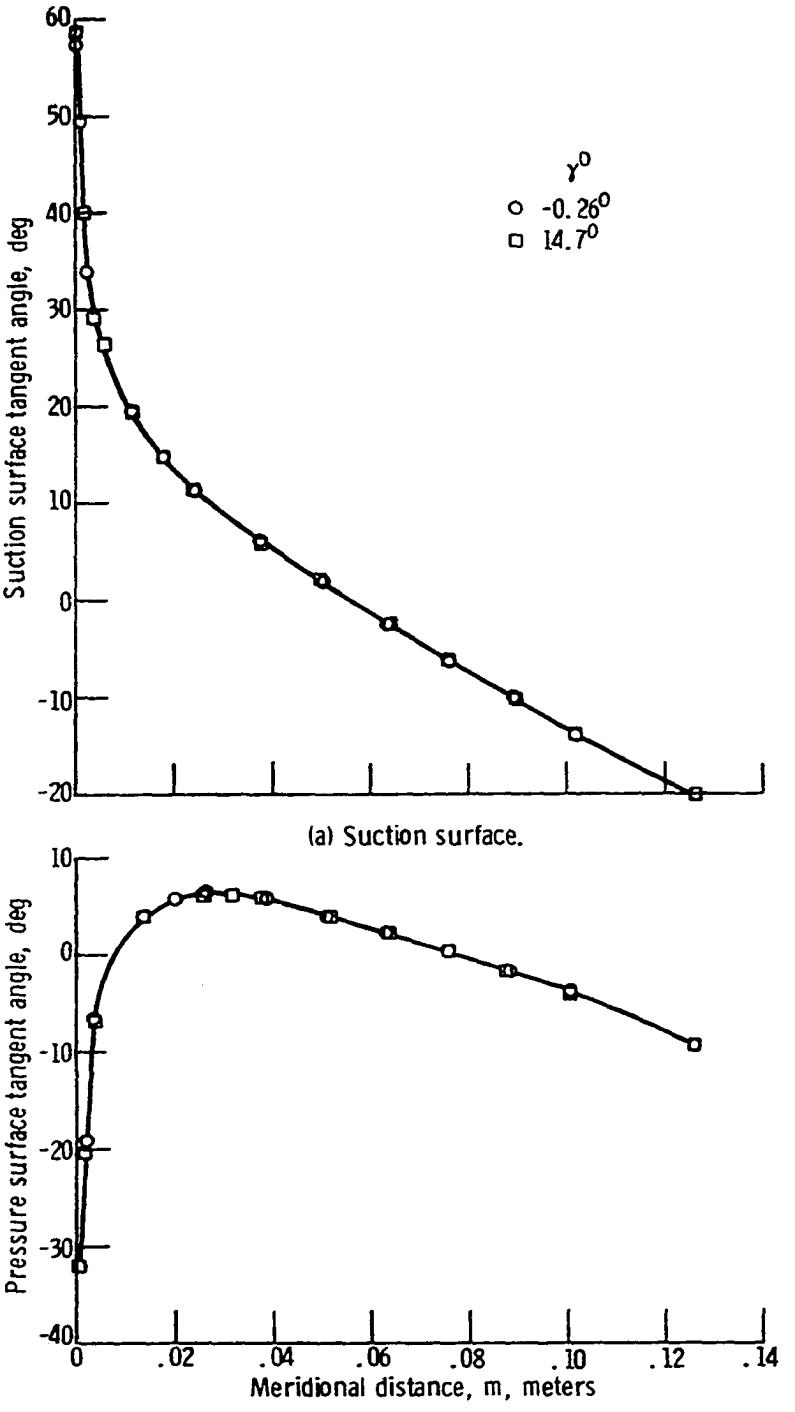

(a) Suction surface.

(b) Pressure surface.

Figure 17. - Comparison of blade surface angles for cubic spline representation of 10C4/30C50 profile at $\gamma^0 = 14.7^0$ with the reference blade surface angles at $\gamma^0 = -0.26^0$.

trated in figure 5. The size of the calculation region must be large enough to allow valid boundary conditions to be specified and small enough to allow a fine grid to be used without exceeding computer storage capacity. Boundary conditions are given by specifying the value of stream function on every segment of the boundary. Values of stream function along TO, OP, PQ, QR, and RS (fig. 5) are obtained from a TSONIC solution. Thus the MAGNFY boundaries must be set far enough from the trailing edge so that the stream function solution is not significantly influenced by the fine details of the trailing edge shape. That is, the boundaries should be located so that the same stream function values would be calculated there with TSONIC using either the normal coarse grid or a very fine grid throughout the TSONIC solution region.

Guidelines for the selection of MAGNFY boundary locations were developed from example calculations in which the boundaries were moved progressively closer to the trailing edge. The calculated stream function values along the vertical grid line at the trailing edge were chosen to represent the example solutions and are shown in figure 18. No significant differences were noted for solutions where the boundaries were located more than 5.4 trailing edge diameters from the trailing edge (fig. 18). Even when the nearest boundary was 2.7 diameters from the trailing edge, a change of less than 1% occurred in the stream function plotted in figure 18. This change was interpreted to mean that the TSONIC solution would change significantly only in the region less than 3 diameters from the trailing edge if a fine grid were used. Thus TSONIC stream function values at points more than 3 diameters from the trailing

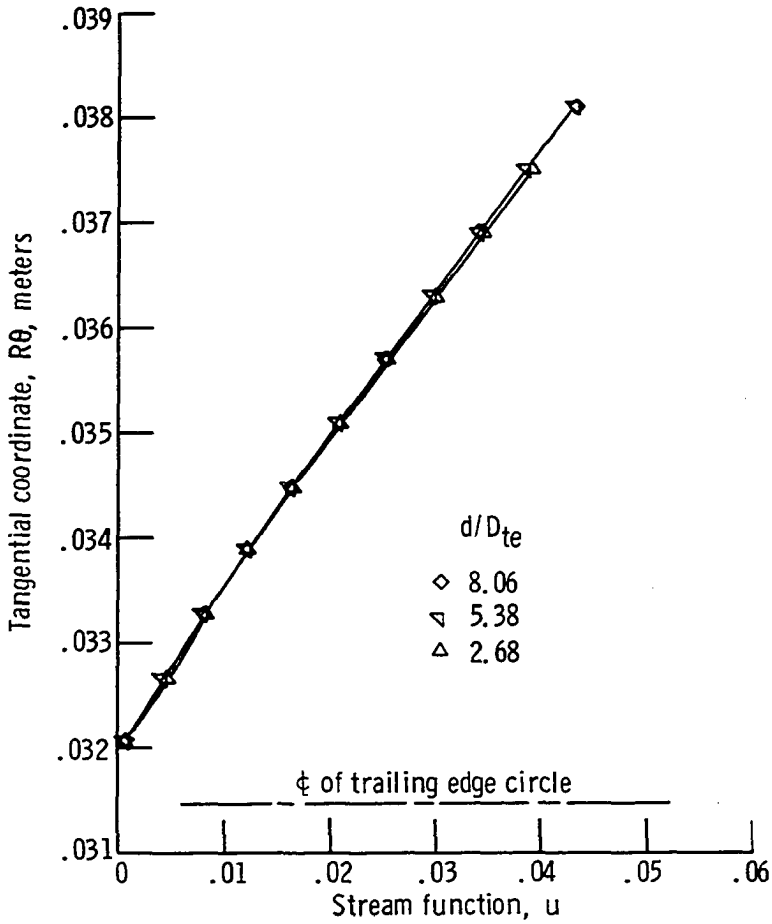

Figure 18. - Effect of MAGNFY region size on stream function near trailing edge. m = 0.12304 meters (~100 percent chord)

edge would be valid boundary values for a MAGNFY solution. This result is consistent with the recommendation given in reference 30 in connection with a similar problem. To be conservative the MAGNFY boundaries were set a distance of not less than 5.4 diameters from the trailing edge for the calculations presented in the DEVIATION ANGLE ESTIMATION section. The resulting calculation regions were small enough to allow a suitably fine grid to be used without requiring excessive storage.

Selection of MAGNFY Mesh Size

An investigation was conducted to determine how small the MAGNFY grid size should be to adequately define the boundary shape at the trailing edge. A series of MAGNFY solutions were calculated using different grid sizes. The stream function values which were calculated along the vertical grid line at the trailing edge are shown in figure 19 to indicate the effect of mesh size on the solution. No significant differences were found in the stream function values calculated near the trailing edge for the mesh sizes given in figure 19. It was concluded that the shape of the trailing edge was reflected in the numerical solution for all mesh sizes in figure 19. Therefore a mesh size of about 0.0033 was used to obtain the results of the DEVIATION ANGLE ESTIMATION section.

Determination of the Rear Stagnation Point

One aspect of the study required that the point be determined at which the stagnation or dividing streamline leaves the trailing edge of the blade. The MAGNFY program was modified (APPENDIX A) to compute the location of the stagnation streamline at each vertical grid line downstream of the blade. It was then necessary to extrapolate a curve through

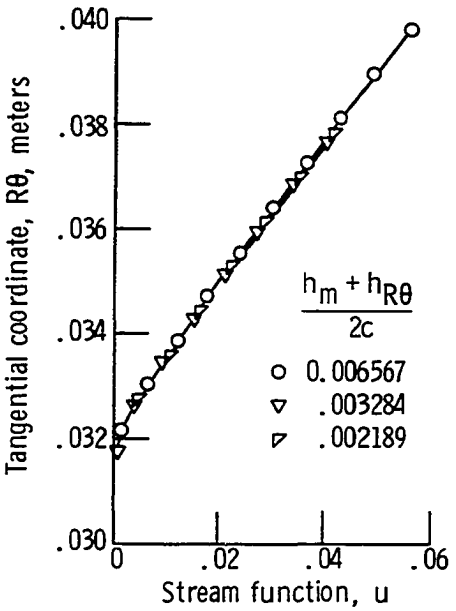

Figure 19. - Effect of mesh size on stream function near trailing edge - MAGNFY results. m = 0.12304 meters (~100 percent chord)

these points to determine the intersection of the stagnation streamline and the blade. Graphical extrapolation was tried, but proved to be quite inconsistent and unsatisfactory. An analytical method was developed which proved to be consistent and fast. The method consisted of fitting a parabola, in the least squares sense, to six points on the stagnation streamline determined by the MAGNFY program. The six points were spaced on alternate vertical grid lines beginning with the first grid line downstream of the blade trailing edge. The intersection of the least-square parabola and the trailing edge circle was then obtained by iteration. This method was incorporated into a computer program STGPLS which is described in APPENDIX D. The intersection point is taken as an approximation to the location of the stagnation point. The uncertainty arises because the stagnation streamline must be extrapolated between the edge circle and the first vertical grid line downstream. The extrapolation distance was minimized by using the smallest grid size possible without exceeding 2000 grid points in the MAGNFY solution region.

Selection of Program Tolerances

As described in the INVISCID FLOW COMPUTER PROGRAMS section the numerical solution used in TSONIC and MAGNFY involves an iteration on both density and stream function. These iterations are considered to converge whenever the densities and stream functions calculated in two successive solutions differ by less than a specified tolerance. To determine suitable tolerances to use in this study a few example TSONIC solutions were obtained using different tolerances. The effect of stream function tolerance on the velocities at three points on the blade suction surface is

shown in figure 20. On the basis of results in figure 20 it was concluded that the tolerance of 0.000001 built into the program is quite satisfactory. Similar curves of suction surface velocity as a function of density tolerance show no significant change for a range of density tolerance from 0.1 to 0.0001. This result may be misleading since the inlet Mach numbers in the calculations were quite low (about 0.08) so that density gradients were small.

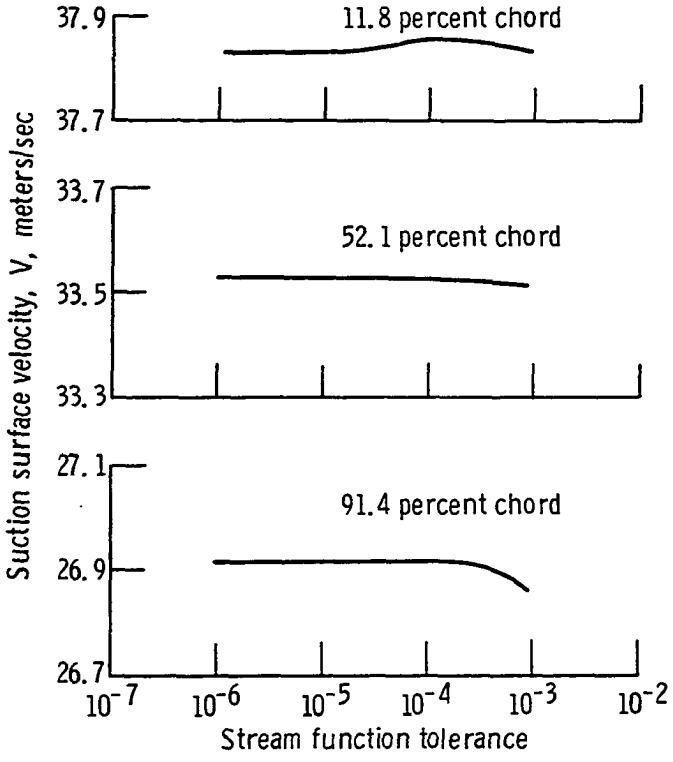

Figure 20.- Effect of stream function iteration tolerance on the suction surface velocities calculated with TSONIC for a 10C4/30C50 profile. $\beta_1 = 30^0$, $i = 0.3^0$, $\delta = 8.7^0$, $\sigma = 1.0$

DEVIATION ANGLE ESTIMATION

Deviation angles and blade surface pressure distributions calculated for a zero-thickness flat plate cascade and a thick cambered cascade are presented in this section. As noted in the THEORETICAL CASCADE MODEL section, estimating deviation angle using an inviscid flow calculation requires some assumption regarding the flow around the trailing edge. The Kutta condition was used in the flat plate calculations and the results were compared with the conformal mapping theory of Weinig (ref. 31). Results for the cambered cascade were calculated using three different trailing edge hypotheses and are compared with experimental data.

Flat Plate Calculation

A numerical solution for the flow through a flat plate cascade satisfying the Kutta condition was calculated using the TSONIC program. Calculations were made for a cascade with a 20 degree blade setting angle, a solidity of 1.0, and an inlet flow angle of 30 degrees. Pressure distributions and stagnation streamlines are shown in figures 21 to 23 which correspond to zero circulation (for reference) and to the circulation fixed by the Kutta condition. The deviation angle for which the dividing streamline leaves the blade at the trailing edge point (Kutta condition) was found to be 0.48 degree (fig. 23). A deviation angle of 0.48 degree was also calculated for the same cascade using the conformal mapping results of Weinig (ref. 31). The excellent agreement between the two methods is a basis for confidence in the numerical techniques used in the TSONIC and MAGNFY programs and in the stagnation streamline extrapolation used in the STGPLS program to locate the rear stagnation point.

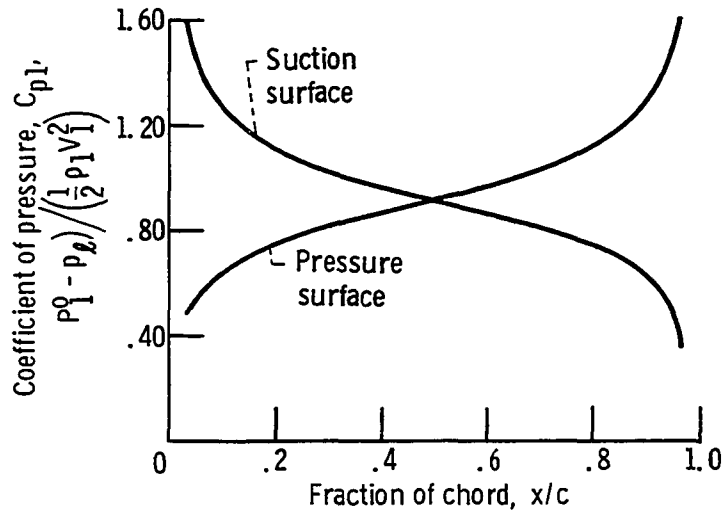

Figure 21. - Pressure distribution for a zero-thickness flat plate cascade having zero turning calculated with TSONIC. $\beta_1 = 30^0$, $i = 10^0$, $\delta = 10^0$

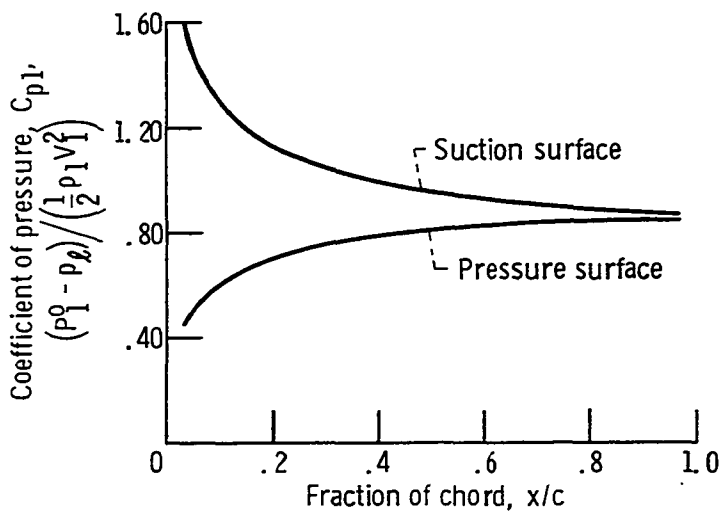

Figure 22. - Pressure distribution calculated with TSONIC for a zero-thickness flat plate cascade with the Kutta condition satisfied. $\beta_1 = 30^0$, $i = 10^0$, $\delta = 0.48^0$

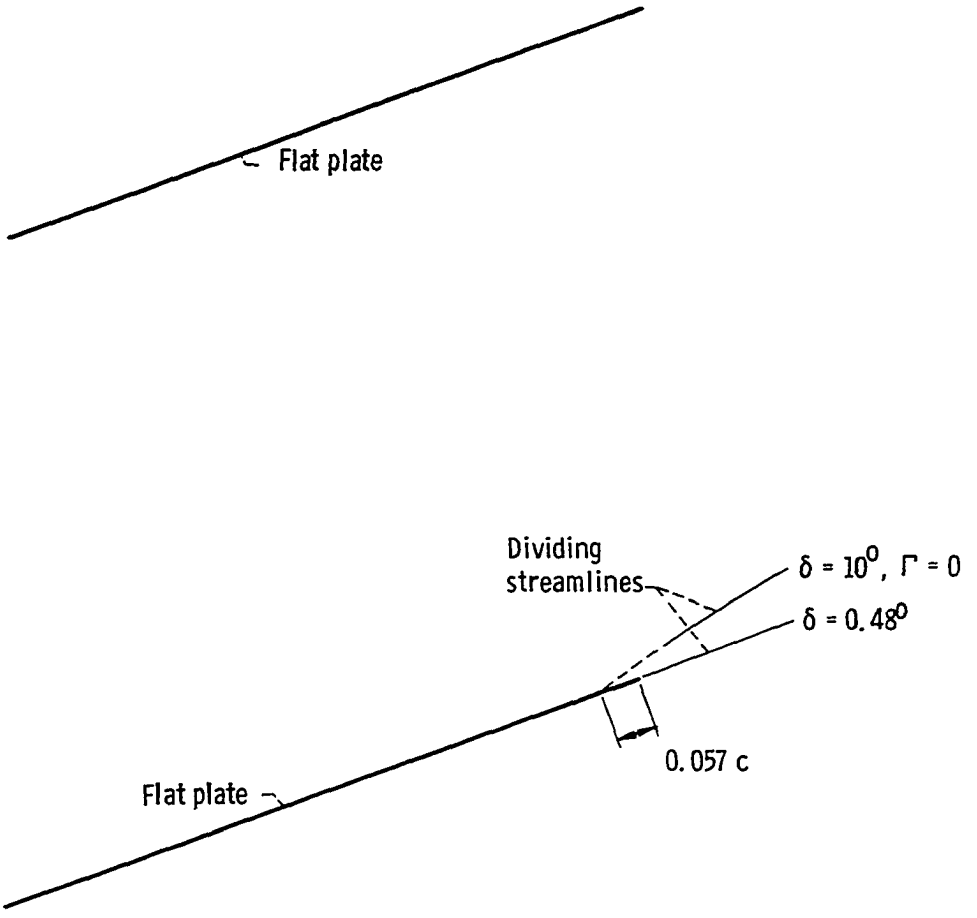

Figure 23. - Dividing streamlines for a zero-thickness flat plate cascade calculated using the TSONIC, MAGNFY, and STGPLS programs. $\beta_1 = 30^0$, $i = 10^0$, $\sigma = 1.0$, $c = 0.127$ meters, $M_1 = 0.08$

Selection of Cambered Airfoil Cascade

Several features were required in the cambered airfoil section chosen to evaluate deviation angle estimation using the inviscid flow computer programs. The first requirement was availability of reliable plane cascade air data with a systematic variation of incidence angle and inlet flow angle. Plane cascade flow was the most logical choice to compare with the calculated flow because it is the real flow most closely approximated by the mathematical model used. The section was required to have a well defined rounded trailing edge. This requirement eliminated the NACA 65-series profile. Also a section with a camber angle low enough to avoid extensive regions of flow separation except at high incidence angles was desired. All these requirements were satisfied by the 10C4/30C50 blade section. A systematic set of plane cascade measurements for this blade are given in reference 32. An additional advantage of these data was that the tests were carefully conducted to produce two-dimensional flow conditions. Coordinates describing the 10C4/30C50 section given in reference 32 were used to generate geometrical input for the inviscid flow solutions presented in the remainder of this section. A summary of the flow and blade angles for which deviation angles were estimated is given in table 3.

Calculations Using Experimental Deviation Angles

It is of considerable interest to compare the inviscid flow solutions calculated using the experimentally determined deviation angles for a decelerating cascade with measurements of the real flow. The features of most interest in the inviscid solutions are the blade surface

Table 3. Cascade conditions for which deviation angles were estimated (10C4/30C50 profile, $\sigma = 1.0$, $M_1 = 0.08$)

Inlet flow angle, β_1, deg	Incidence angle, i, deg	Experimental deviation angle, δ_{exp}, deg	Blade setting angle, γ^o, deg
30	-7.7	8.8	22.7
30	0.3	8.7	14.7
30	11.3	12.15	3.7
60	-9.0	10.45	54.0
60	-1.2	11.3	46.2
60	6.6	14.4	38.4

pressure distributions because of their strong influence on boundary layer development and the resulting losses, and the stagnation streamlines because of the dependence of deviation angle on the location of the rear stagnation point. Comparisons of calculated and measured pressure distributions for the 10C4/30C50 profile in cascade are shown in figures 24 and 25. The comparisons in figures 24 and 25 are generally good with the largest discrepancies occurring near the leading edge. Pressure measurements over the last 30 percent of chord were not given in reference 32 for most operating points and thus are not shown except in figure 24(b).

A typical stagnation streamline calculated using the experimental deviation angle is shown in figure 26 for a 10C4/30C50 cascade with inlet flow angle of 30 degrees. The stagnation streamline for zero circulation is shown for reference.

Calculations Using Three Trailing Edge Hypotheses

Wilkinson's hypothesis. - Wilkinson (ref. 14) suggests that the

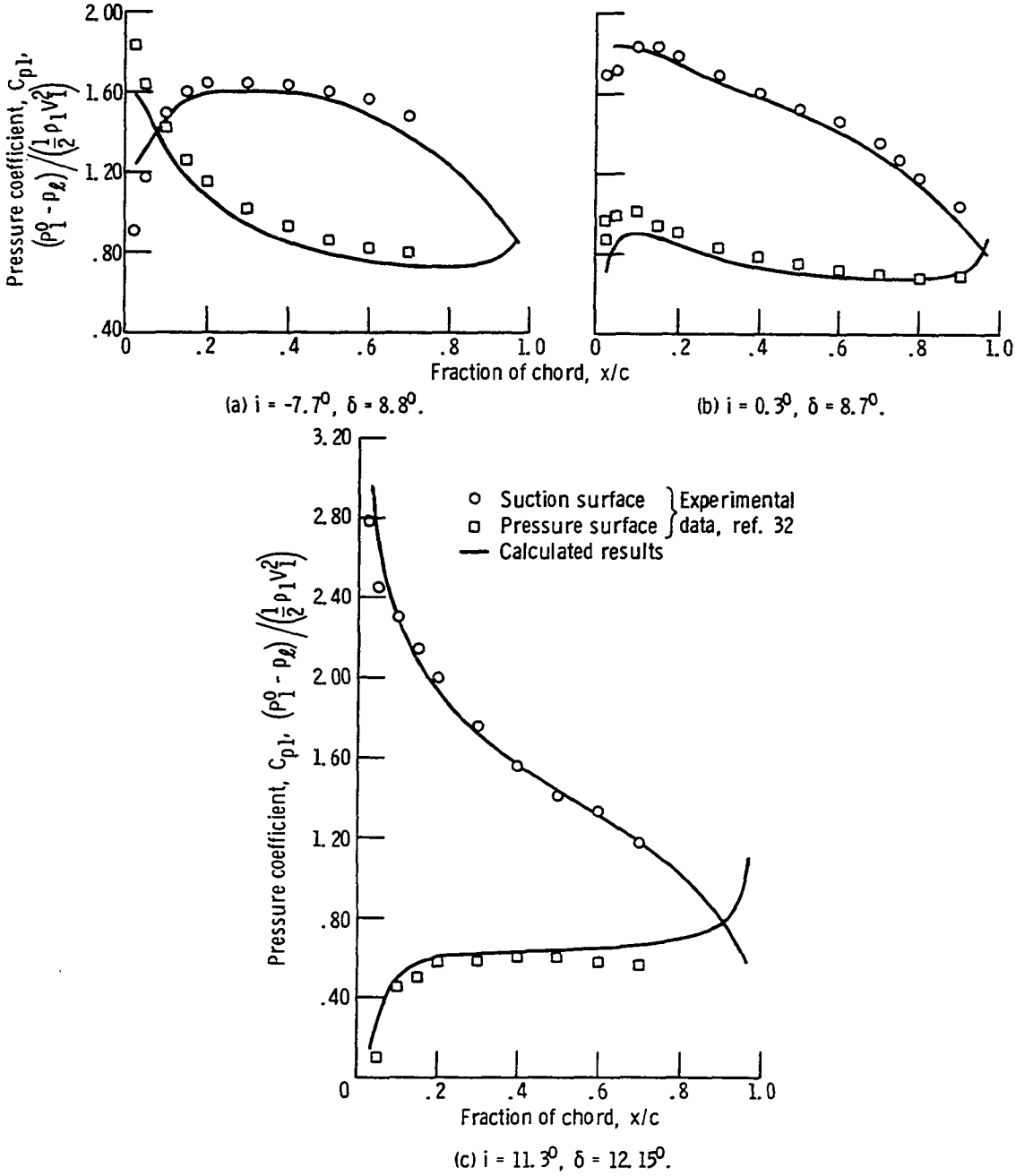

Figure 24. - Comparison of blade surface pressure distributions calculated for a 10C4/30C50 cascade using experimental deviation angles with measurements from reference 32. $\beta_1 = 30^0$, $\sigma = 1.0$

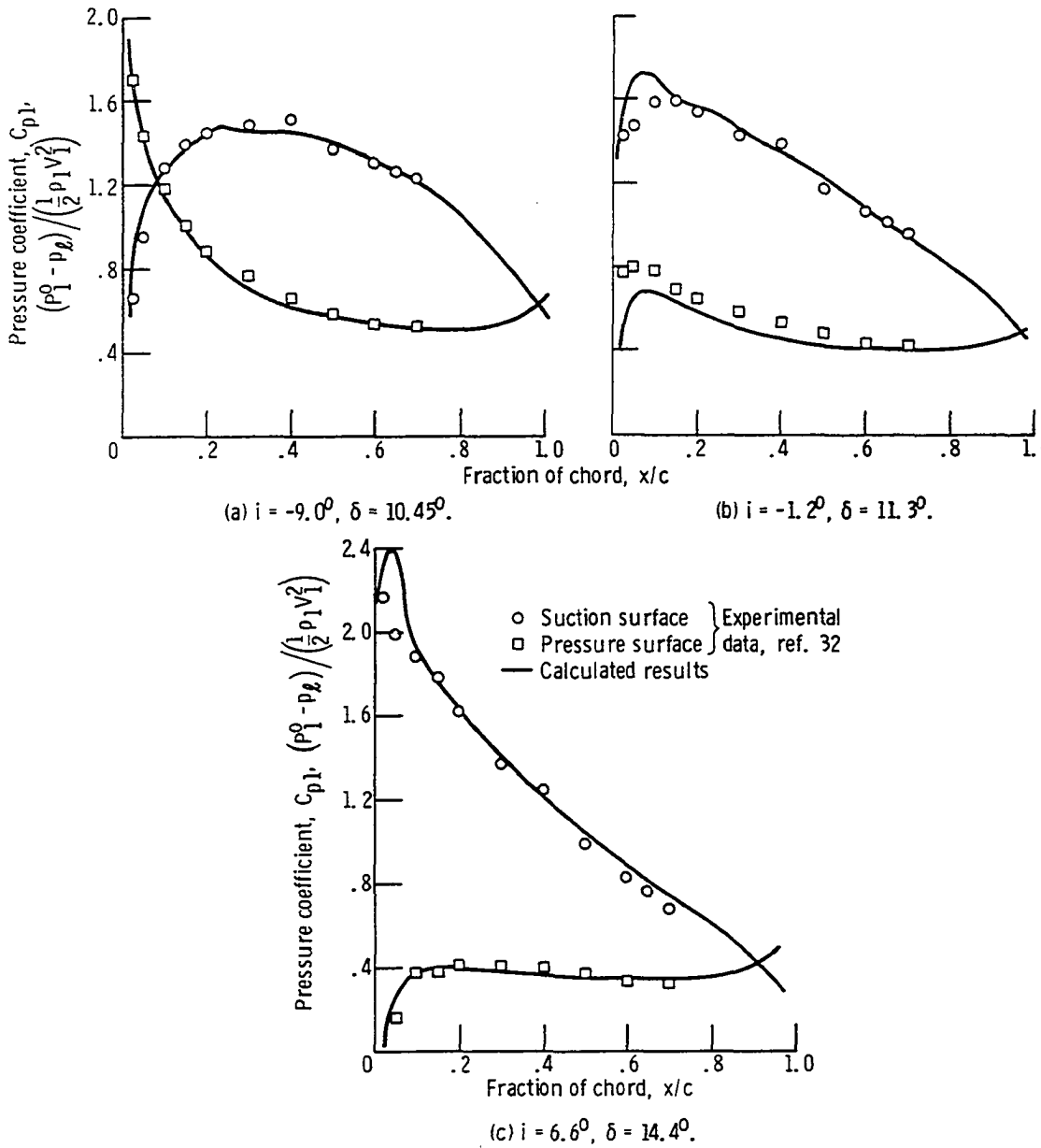

Figure 25. - Comparison of blade surface pressure distributions calculated for a 10C4/30C50 cascade using experimental deviation angles with measurements from reference 32. $\beta_1 = 60^0$, $\sigma = 1.0$

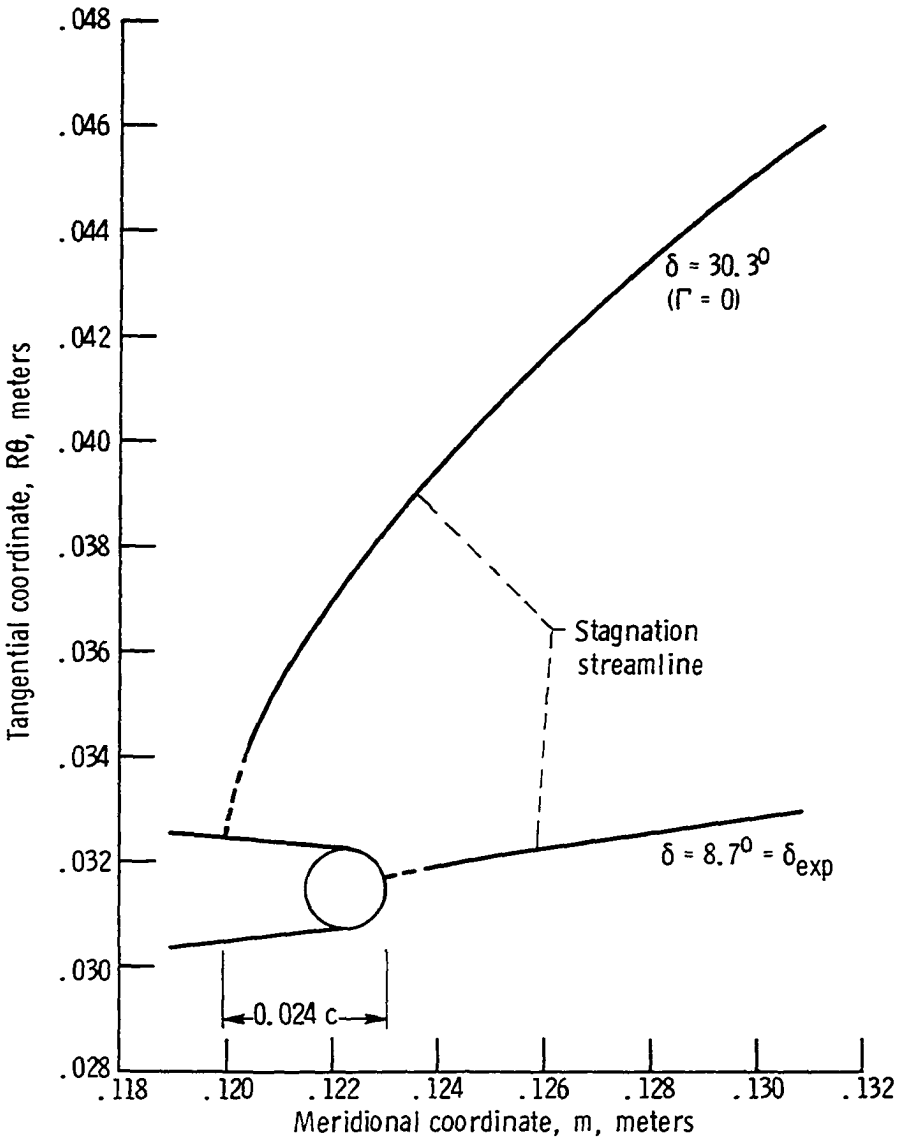

Figure 26. - Stagnation streamlines calculated for a 10C4/30C50 cascade using experimental deviation angle and using zero turning. $\beta_1 = 30^0$, $i = 0.3^0$, $\sigma = 1.0$

simplest form of trailing edge hypothesis is to locate the rear stagnation point at the point of maximum curvature or at the end of the mean camber line. The circular trailing edge of a 10C4/30C50 has no single point of maximum curvature so the stagnation point was located at the end of the mean camber line for this study. A series of calculations were required to determine the outlet flow angle (used as a boundary condition in TSONIC) for which the rear stagnation point coincided with the end of the mean camber line. Pressure distributions (fig. 27) and stagnation stream lines were obtained for several values of deviation angle (fig. 28). The resulting relationship between deviation angle and stagnation point location (fig. 29) was interpolated to obtain the deviation angle for which the stagnation point fell on the end of the mean camber line. A comparison of the deviation angles so obtained with measured values is shown in figure 30(a). The estimated deviation angles shown in figure 30(a) are from 2.6 to 6.4 degrees lower than the measured angles.

Closure hypothesis. - Another trailing edge hypothesis commonly used (ref. 15) is to set the leaving angle so that the curves of pressure or velocity for the two surfaces cross at the trailing edge (x/c = 1.0). This necessarily requires an extrapolation of the calculated curves (fig. 31) since the inviscid flow velocities on one or both surfaces often exhibit rapid accelerations near the trailing edge before rapidly decelerating to reach the stagnation point. The changes in surface pressure at the trailing edge probably do not occur as rapidly in real flow because of the presence of the surface boundary layers and the wake. Thus the

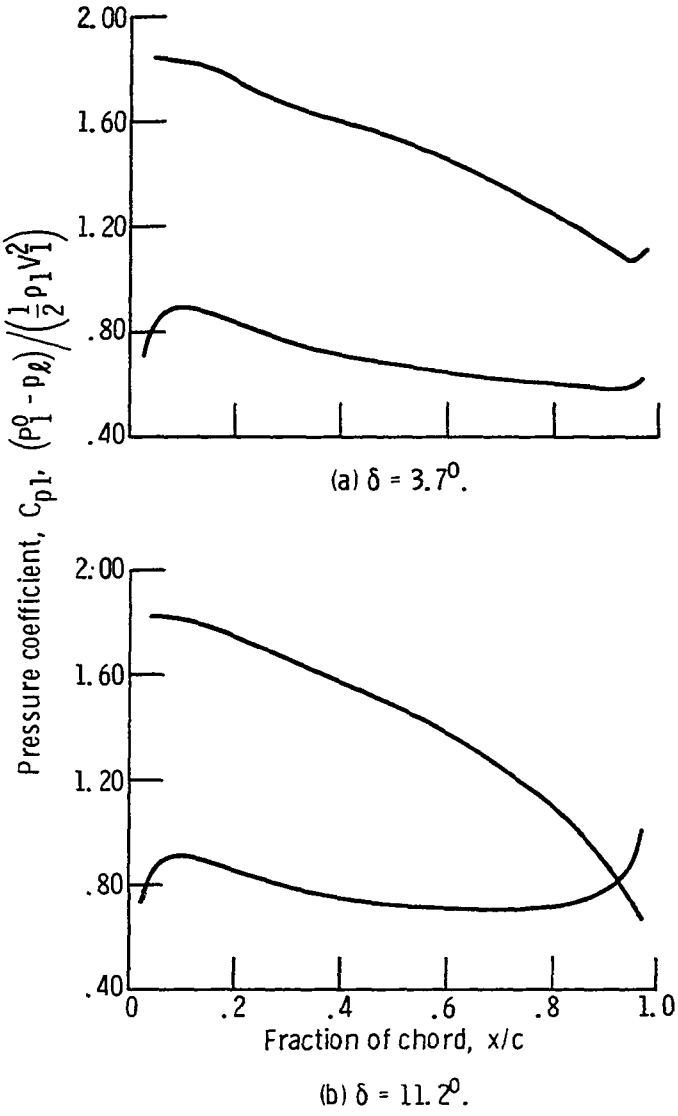

Figure 27. - Pressure distributions calculated for a 10C4/30C50 cascade using two values of deviation angle. $\beta_1 = 30^0$, $i = 0.3$, $\sigma = 1.0$

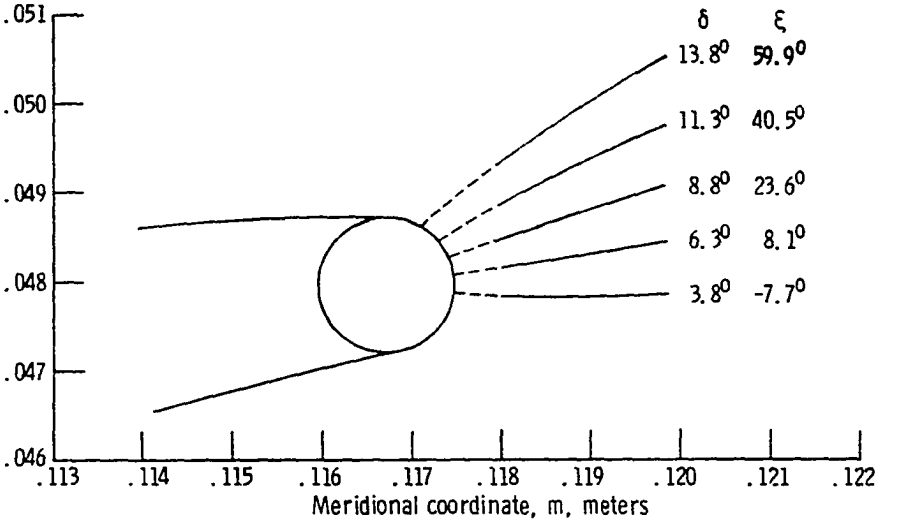

(a) $i = -7.7^0$.

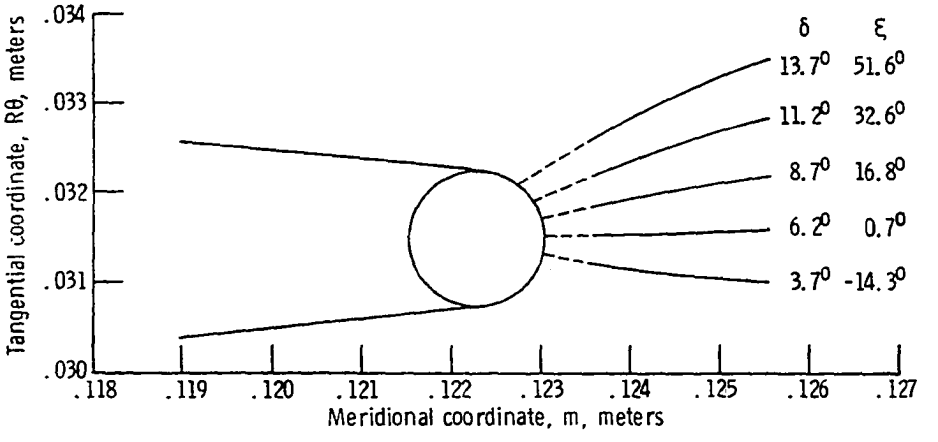

(b) $i = 0.3^0$.

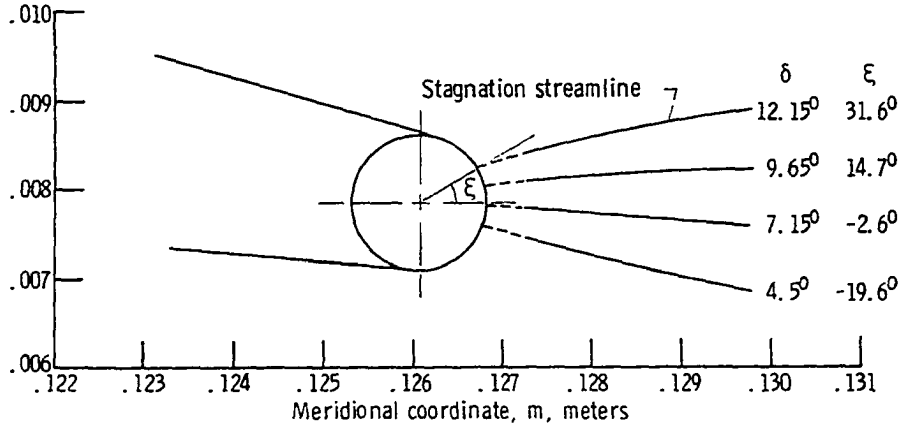

(c) $i = 11.3^0$.

Figure 28. - Stagnation streamline locations for inviscid solution at several values of outlet flow angle. $\beta_1 = 30^0$, $\sigma = 1$

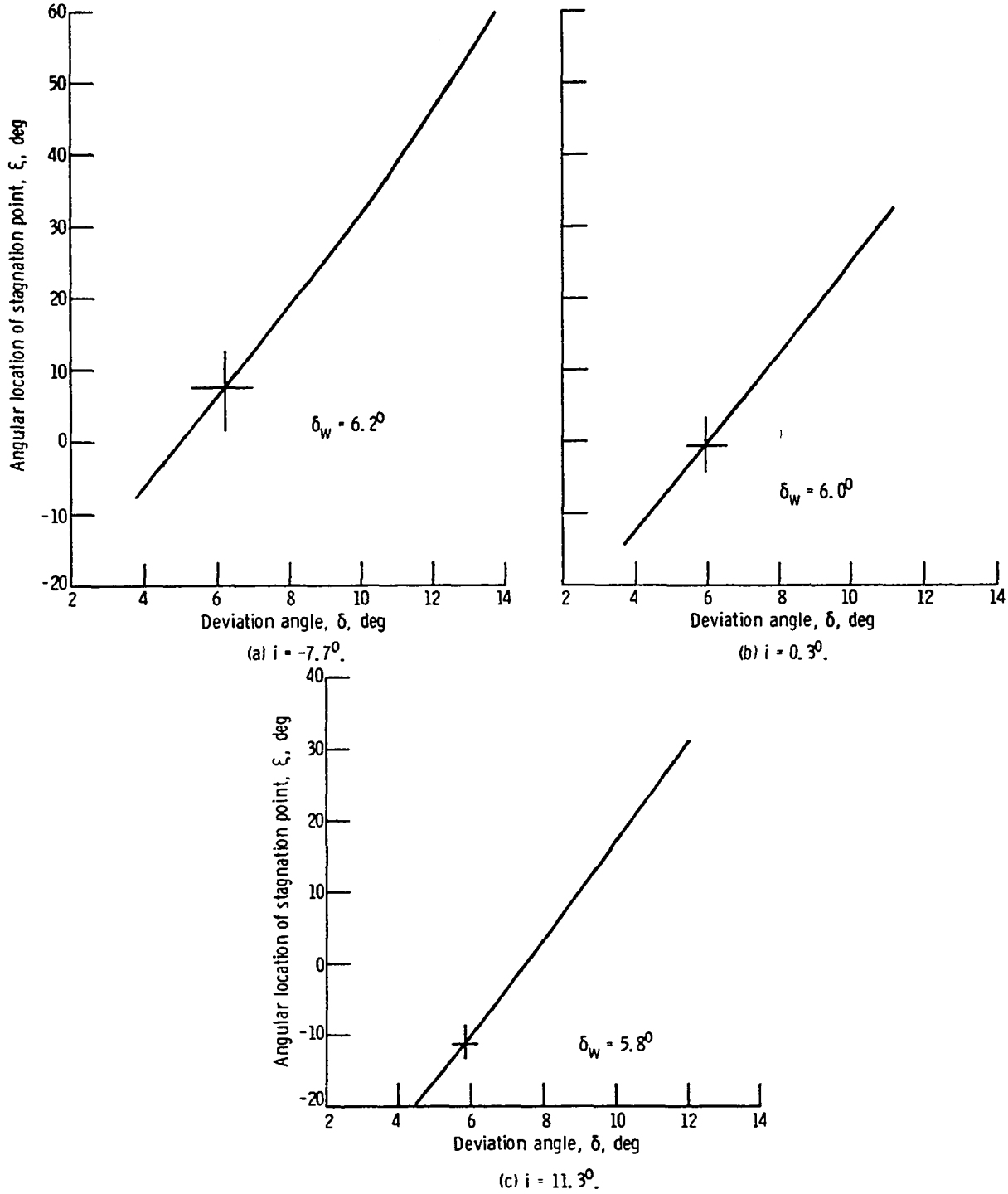

Figure 29. - Deviation angle as a function of stagnation point location for a 10C4/30C50 cascade. β_1 = 30°, σ = 1.0

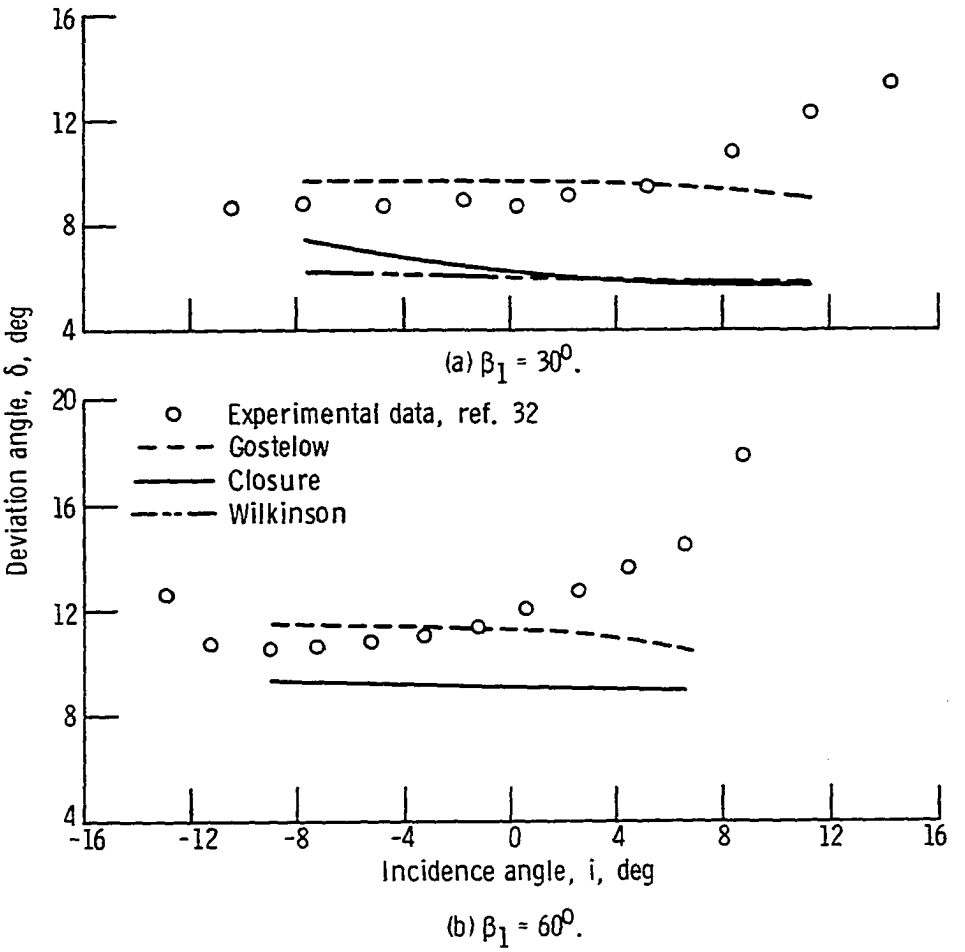

Figure 30. - Comparison of measured and calculated deviation angle for a 10C4/30C50 cascade with solidity of 1.0.

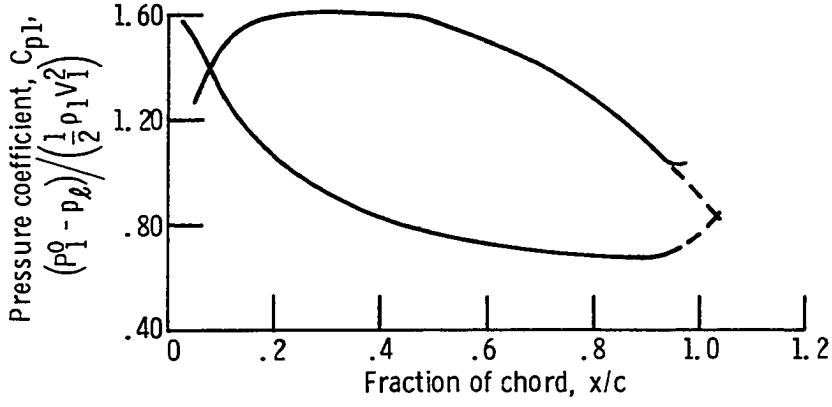

Figure 31. - Example of extrapolation required in application of the closure trailing edge hypothesis. $\beta_1 = 30^0$, $i = -7.7^0$, $\delta = 6.3^0$, $\sigma = 1.0$

local acceleration on the suction surface in figure 31 beginning at $x/c = 0.95$ was ignored in applying the closure hypothesis. Justification for applying this trailing edge hypothesis is the supposition that in real flow the surface pressures approach a common value which exists in the wake in the immediate vicinity of the trailing edge circle. Furthermore the surface pressure distribution near and on the trailing edge from the inviscid solution is not likely to bear much resemblance to the real pressure distribution as explained above. Thus extrapolating the surface pressure curves from a point away from the trailing edge is an effort to obtain a better approximation to the pressure distribution of real flow than that obtainable from inviscid flow calculations. The assumption is that a continuation of the inviscid pressure curves toward the trailing edge is a good approximation of the real pressure distribution. There are difficulties inherent in the method including determination of the point where the extrapolation should begin and the shapes of the extrapolated curves. In this study graphical extrapolations of the suction and pressure surface pressure distributions were started at an x/c of 0.94 and 0.97, respectively. The shapes of the extrapolated curves were selected to be a continuation of the shape of the calculated curves at those points.

Estimation of deviation angle using this hypothesis is a trial and error process. Pressure distributions calculated for several values of deviation angle are extrapolated until the curves for the two surfaces cross or close. The x/c value where the curves cross is plotted as a function of δ and the resulting curve is interpolated at $x/c = 1.0$.

to obtain the estimated deviation angle δ_c. The curves of δvs$(x/c)_{c\ell}$ for the C4 cascade at inlet flow angles of 30 and 60 degrees are shown in figures 32 and 33. Notice that for every 1 percent change in $(x/c)_{c\ell}$ the corresponding deviation angle change is 0.5 to 0.7 degree. The estimated deviation angles δ_c are compared with the measured value in figure 30. In general the deviation angles estimated using this hypothesis are significantly lower than the measured angles.

The pressure distributions calculated using the estimated deviation angles are shown in figures 34 and 35. Measured pressures are shown for comparison. The discrepancies between measured and calculated pressure coefficients in figures 34 and 35 are generally larger than those which resulted when experimental deviation angles were used in the calculation (figs. 25 and 26).

Gostelow's hypothesis. - Gostelow et al. (ref. 13) suggests that an appropriate approach is to linearly extrapolate the surface pressure curves from $x/c = 0.85$ until they cross. The correct deviation angle is assumed to be the value for which the extrapolated curves cross at $x/c = 1.0$. An example pressure distribution showing how the curves are extrapolated is shown in figure 36. To estimate deviation angle using this hypothesis, a series of calculations are made for different deviation angles and plots similar to figure 36 are constructed. Then a plot of δ versus $(x/c)_{int}$ is extrapolated to obtain the δ which corresponds to $(x/c)_{int} = 1.0$.

Deviation angles were estimated for the 10C4/30C50 cascade over a range of incidence at inlet flow angles of 30 and 60 degrees. The curves

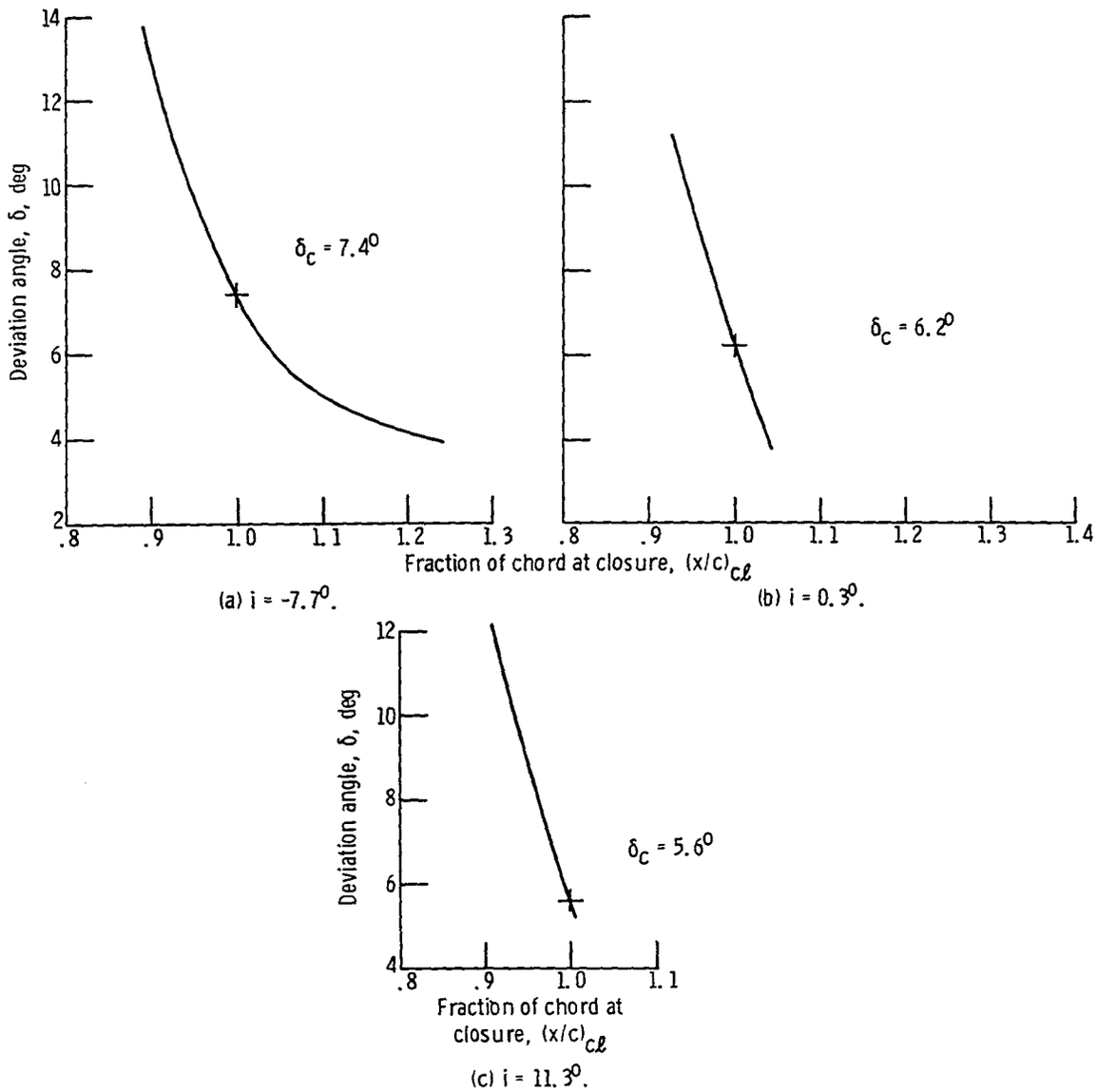

Figure 32. - Relationship between the closure point of the pressure distribution and the deviation angle for a 10C4/30C50 cascade. $\beta_1 = 30^0$, $\sigma = 1.0$

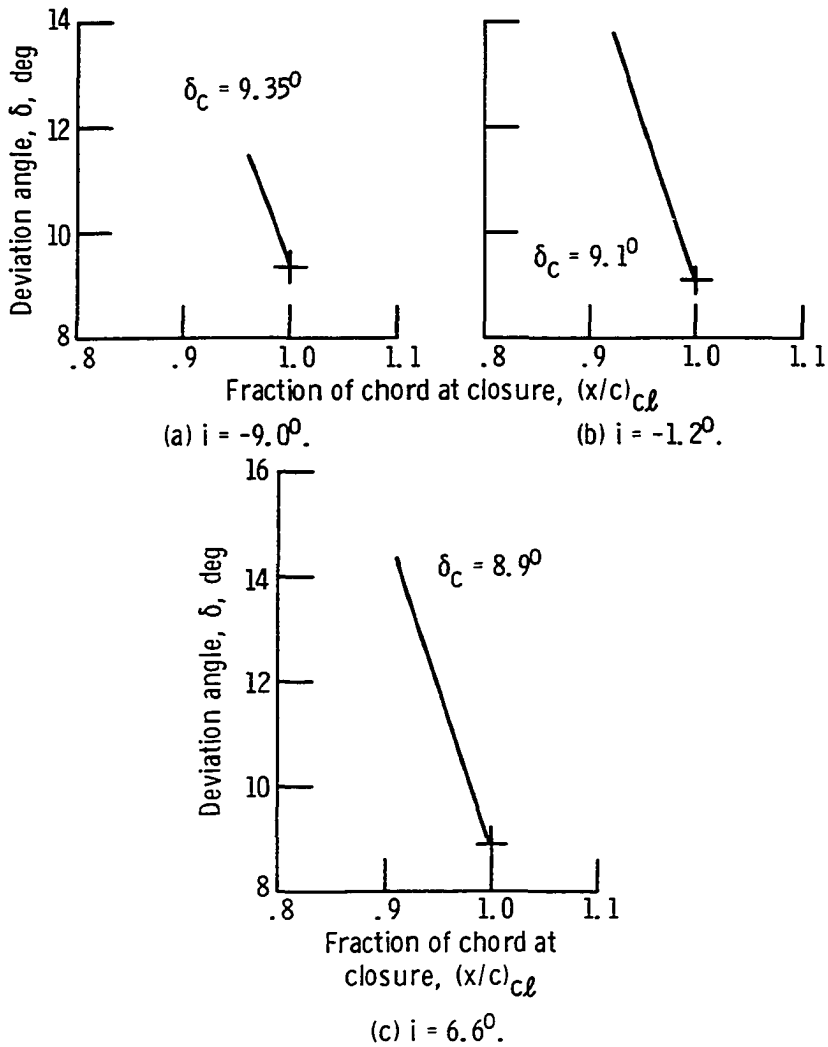

Figure 33. - Relationship between the closure point of the pressure distribution and the deviation angle for a 10C4/30C50 cascade. $\beta_1 = 60^\circ$, $\sigma = 1.0$

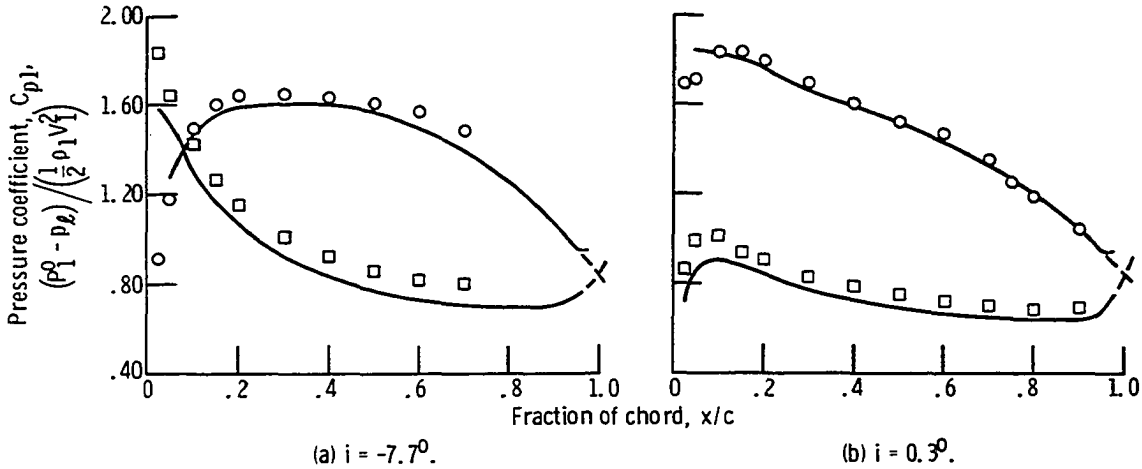

(a) $i = -7.7^0$.

(b) $i = 0.3^0$.

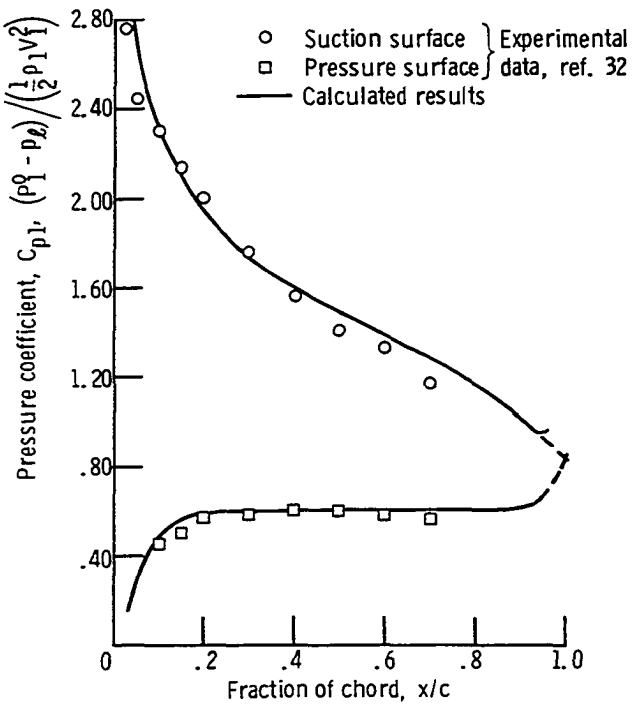

(c) $i = 11.3^0$.

Figure 34. - Comparison of pressure distributions calculated using the closure hypothesis with experimental data for a 10C4/30C50 cascade. $\beta_1 = 30^0$, $\sigma = 1.0$

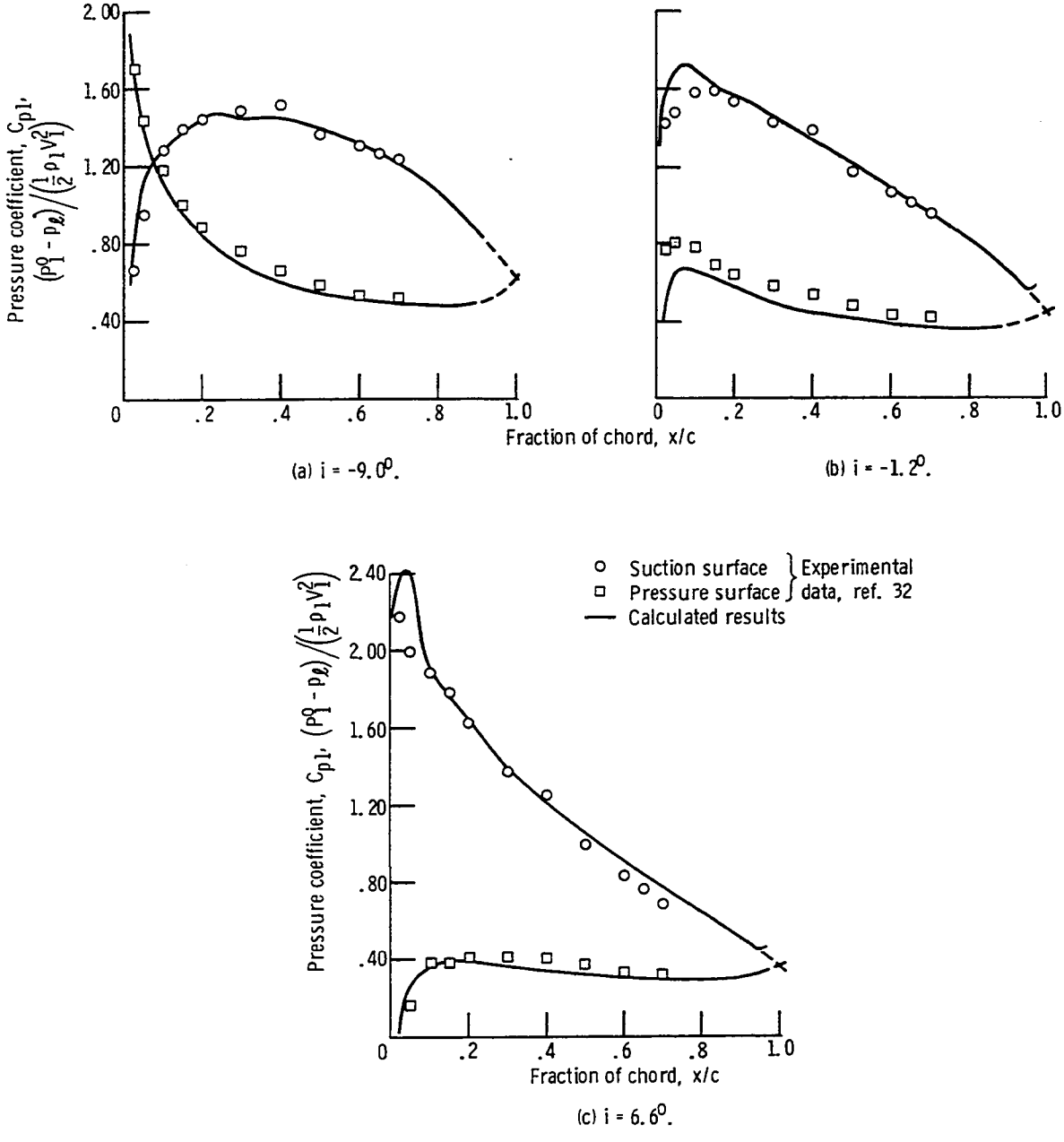

Figure 35. - Comparison of pressure distributions calculated using the closure hypothesis with experimental data for a 10C4/30C50 cascade. $\beta_1 = 60^0$, $\sigma = 1.0$

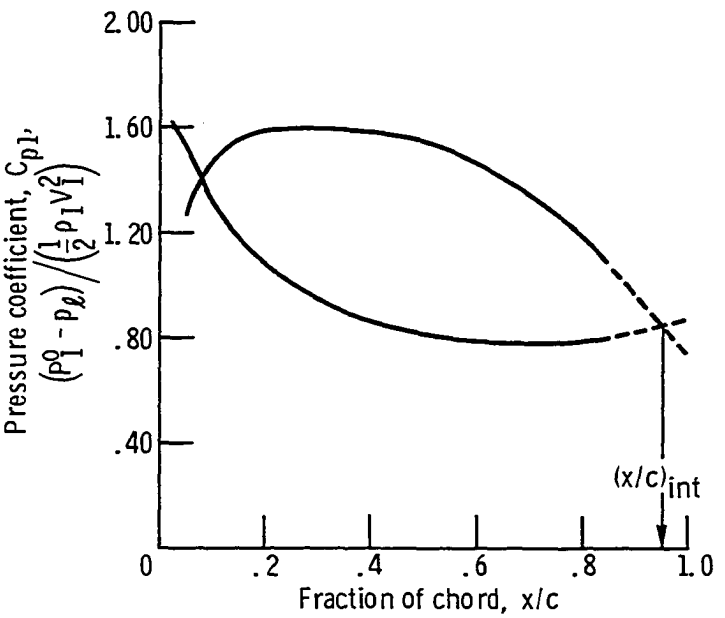

Figure 36. - Linear extrapolation of a calculated pressure distribution for a 10C4/30C50 cascade. $\beta_1 = 30^0$, $\delta = 11.3^0$, $\sigma = 1.0$

of δ versus $(x/c)_G$ are shown in figures 37 and 38. The estimated deviation angle δ_G are compared with measured values in figure 30. The calculated deviation angles are reasonably close to the measured angles except at high incidence angles where increased drag coefficients (ref. 32) indicate thickened and possibly separated suction surface boundary layers. Comparisons of calculated and measured pressure distributions are shown in figures 39 and 40. Discrepancies between the calculations and measurements shown in figures 39 and 40 are slightly greater than those in figures 25 and 26.

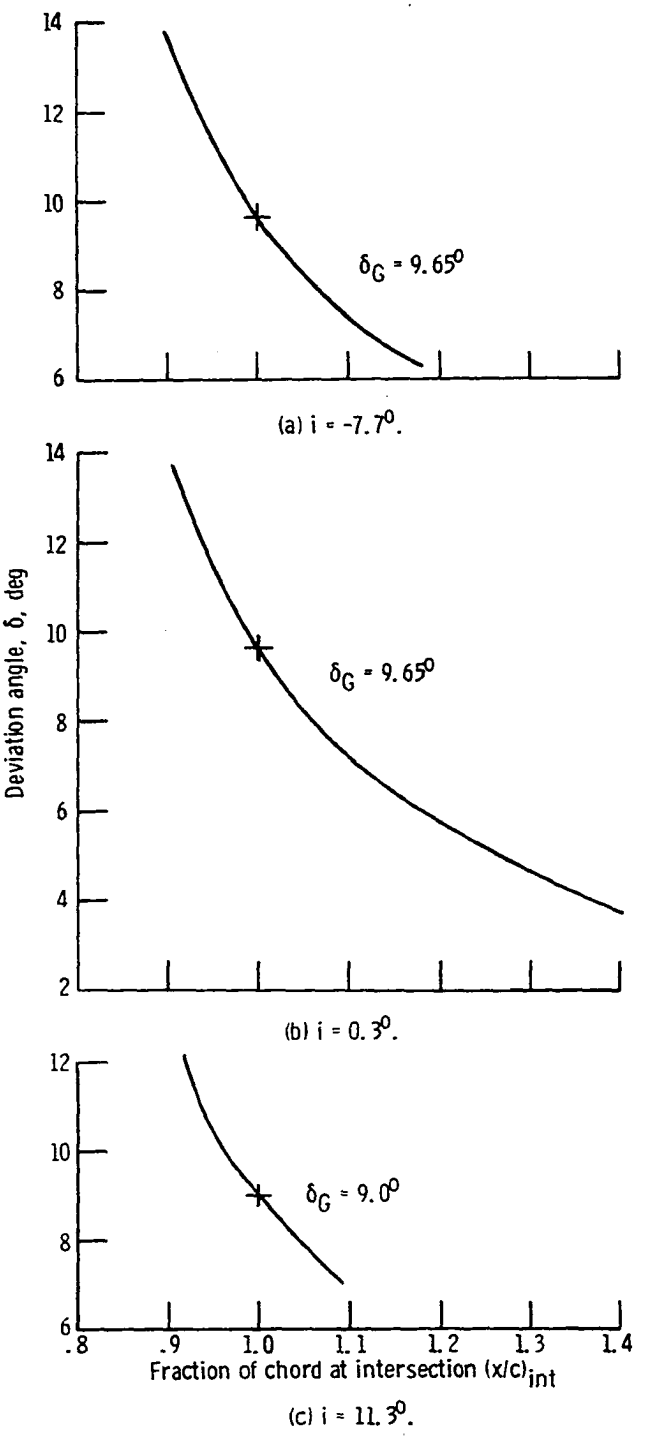

Figure 37. - Relationship between deviation angle and the point of intersection of linearly extrapolated pressure distributions for a 10C4/30C50 cascade. $\beta_1 = 30^\circ$, $\sigma = 1.0$

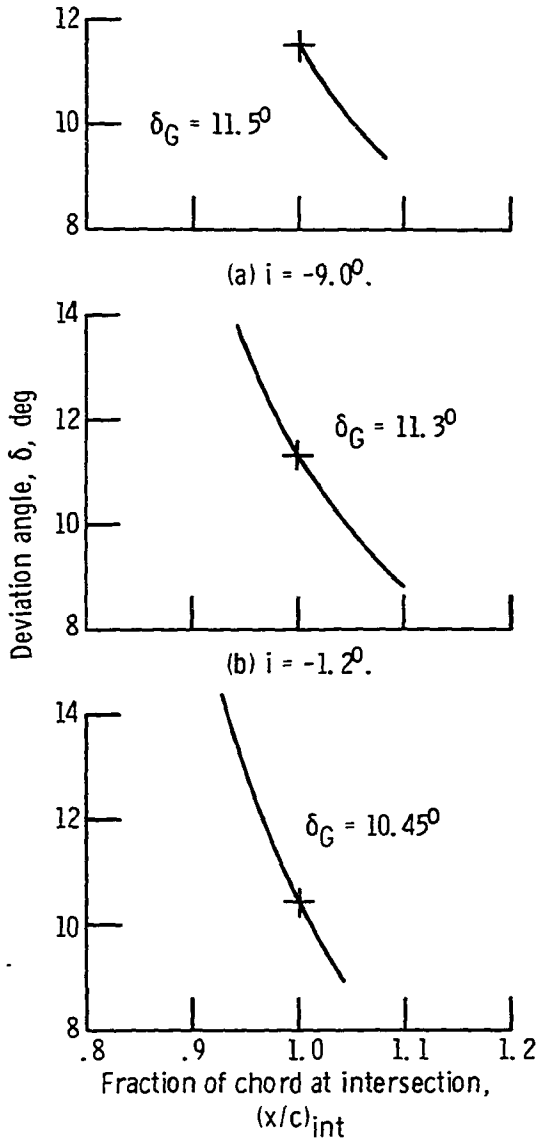

Figure 38. - Relationship between deviation angle and the point of intersection of linearly extrapolated pressure distributions for a 10C4/30C50 cascade. $\beta_1 = 60^\circ$, $\sigma = 1.0$

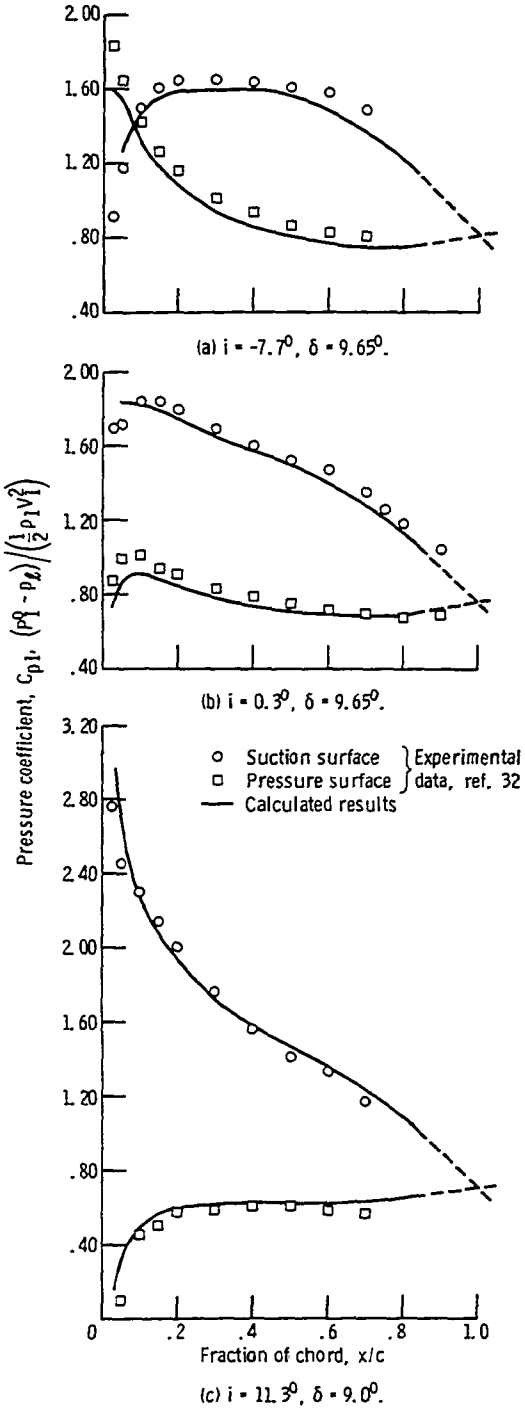

Figure 39. - Comparisons of pressure distributions calculated for a 10C4/30C50 cascade using Gostelow's hypothesis with experimental data. $\beta_1 = 30^0$, $\sigma = 1.0$

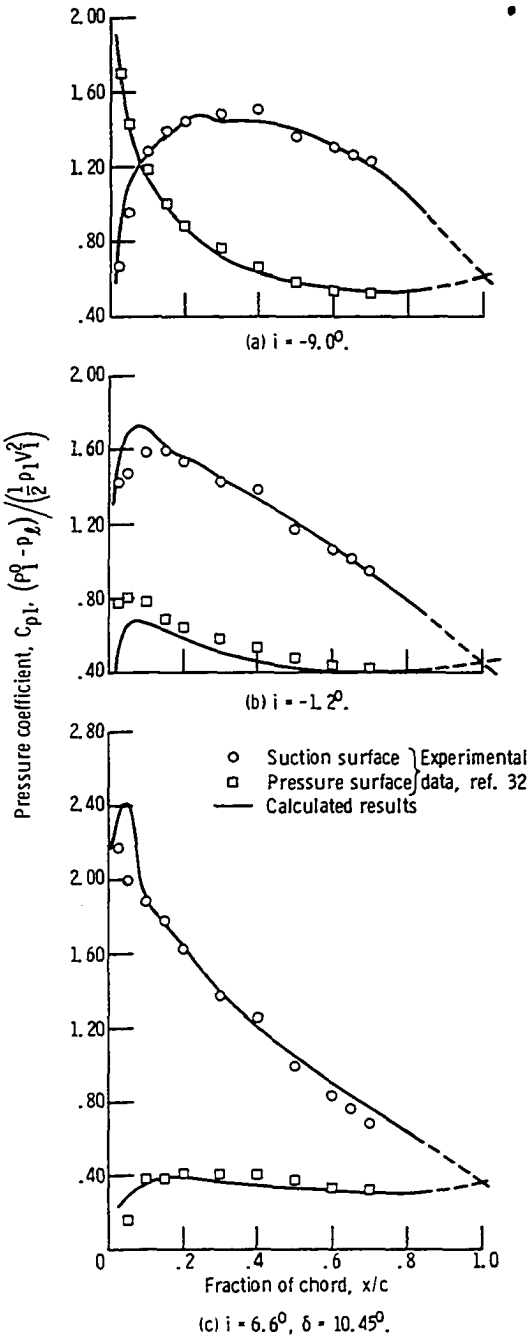

Figure 40. - Comparison of pressure distributions calculated for a 10C4/30C50 cascade using Gostelow's trailing edge hypothesis with experimental data. $\beta_1 = 60^\circ$, $\sigma = 1.0$

DISCUSSION OF RESULTS

Of the three trailing edge hypotheses used to estimate deviation angle, Gostelow's was most successful (fig. 30). It resulted in rather close estimation of deviation angle over a substantial range of incidence and blade setting angle. However at high incidence angles, where reference 32 indicates the coefficient of drag was approximately twice the minimum value, the deviation angles estimated using Gostelow's method are significantly lower than the measurements. This indicates that the method cannot be expected to work well for highly loaded blades with significant areas of separated flow.

Wilkinson's hypothesis also underestimated deviation angles by a significant fraction of the total turning. Such an arbitrary location for the rear stagnation point would give good results only if a small change in deviation angle corresponded to a rather large shift in stagnation point location. However, as indicated in figures 26 and 28, the opposite is true so that the stagnation point must be located quite exactly to estimate deviation angle accurately.

The closure hypothesis resulted in significant underestimation of deviation angles over the entire operating range (fig. 30). In fact the pressure distribution curves calculated using experimental deviation angles all crossed at $x/c < 1.0$ (figs. 24 and 25). Furthermore the percent chord location at which the curves crossed decreased as incidence angle increased at a given inlet flow angle.

A new trailing edge hypothesis was developed on the basis of the above observations and the following reasoning. As incidence angle

varies, the change in measured deviation angle, and thus the change in the location at which the corresponding inviscid flow pressure distribution crosses, is probably closely related to the thickness of the boundary layer on the suction surface. The boundary layer thickness is in turn dependent on the velocity deceleration which takes place on the suction surface. Thus the pressure distribution crossing location calculated using the experimental deviation angle should be related to the decrease in pressure coefficient on the suction surface. In figure 41 the chordwise location where the inviscid pressure distributions calculated in this study with experimental deviation angles crossed is shown as a function of the pressure coefficient change on the suction surface. The pressure coefficient change used was the difference between the maximum pressure coefficient between $0.05 \leq x/c \leq (x/c)_{c\ell}$ and the pressure coefficient at $(x/c)_{c\ell}$. The calculated curves in figures 24 and 25 were used to obtain the points plotted in figure 41. No claims can be made for the generality of the relationship shown in figure 41 except that it holds over a fairly wide range of incidence angle and blade setting angle for the 10C4/30C50 section. Nevertheless it should prove to be a better trailing edge hypothesis for blades in general than the closure hypothesis.

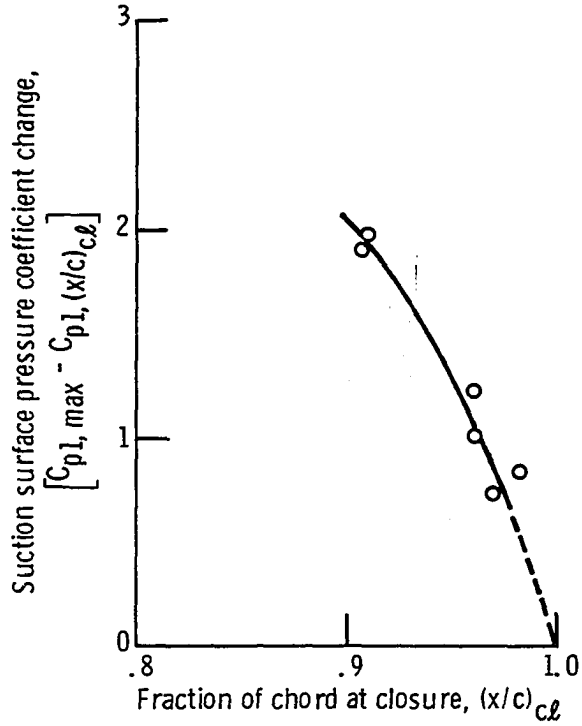

Figure 41. - Relationship between the pressure distribution closure location and the suction surface diffusion for a 10C4/30C50 cascade calculated using experimental deviation angles. $\sigma = 1.0$

CONCLUSIONS

Development of a more satisfactory procedure of estimating deviation angles over a range of incidence angle was begun using inviscid flow calculations. Since the outlet flow angle is required to solve the inviscid flow equations, a trial and error procedure involving a trailing edge hypothesis was required to estimate deviation angle. The trailing edge hypothesis suggested by Gostelow et al. (ref. 13) was found to give satisfactory results except at high incidence angles. Locating the rear stagnation point at the end of the mean camber line was found to be unsatisfactory as a trailing edge hypothesis. Requiring a curved extrapolation of the pressure distributions to close at the trailing edge also proved to be an unsatisfactory procedure. A new trailing edge hypothesis applicable to the 10C4/30C50 blade section over a wide range of incidence and blade setting angle is presented.

SUGGESTIONS FOR FURTHER WORK

The general lack of agreement between estimated and measured deviation angles at high incidence angles (fig. 30) suggests that viscous effects must be included in any general deviation angle estimation procedure. One simplified approach is to use the proposed trailing edge hypothesis based on figure 41 in conjunction with an inviscid flow calculation. This hypothesis should be evaluated for a range of profile shapes, camber angles, solidities, inlet Mach numbers, and axial velocity ratios.

A better general approach would incorporate viscous flow calculations directly into the deviation angle estimation method. This could be done in principle by calculating the inviscid and boundary layer flow and applying Preston's theorem (ref. 33) to the combined flow solution. Preston's theorem, for the case of an airfoil with steady, irrotational approaching flow, asserts that the net vorticity shed from the blade surface boundary layers into the wake must be zero. This idea has been applied to isolated airfoils (ref. 33) but so far has not been fully evaluated for cascade flow (ref. 13). Several difficulties would be encountered in calculating the required boundary layers for cascades. These include accurate prediction of transition, calculation of turbulent boundary layers in large adverse pressure gradients, prediction and description of the separated flow, and inclusion of wake properties. However, the fundamental nature of this approach warrants a careful evaluation to assess whether viscous flow theory is mature enough to be incorporated into a deviation angle estimation method.

ACKNOWLEDGMENTS

Thanks are expressed to Professors Robert C. Fellinger, Robert J. Lambert, Gundo A. Nariboli, Theodore H. Okiishi, George K. Serovy, and Donald F. Young for serving as the author's graduate study committee.

The author is indebted to Professor George K. Serovy for encouragement, advice, and support received in both the development of this dissertation and in the preceding graduate study program. This help is sincerely appreciated.

This work has been financially supported by the National Aeronautics and Space Administration under Grant NGR 16-002-036 as part of the Lewis Graduate Research Program in Aeronautics. This financial support and the use of the NASA computer and other facilities is gratefully acknowledged.

APPENDIX A. ADDITIONS AND MODIFICATIONS TO INVISCID FLOW PROGRAMS

Additions to the TSONIC and MAGNFY programs were made in order to calculate additional information. Subprograms were added to both TSONIC and MAGNFY which calculate blade surface pressure coefficients and the fraction of true chord at which the mesh lines intersect the blade surfaces. Coding was added to MAGNFY to obtain the θ-coordinate at which the stagnation streamline crosses the vertical grid lines downstream of the blade trailing edge. Also some miscellaneous changes were made to avoid undefined variables and improperly defined array subscripts. Documentation of these additions and modifications are given below.

Pressure Coefficient Calculations

The subprograms for calculating pressure coefficient and fraction of chord which were added to TSONIC and MAGNFY are identical except for a few details. The pressure coefficient subprograms are valid for both stationary and rotating blade rows and for stream surfaces with changing radius with one exception which will be noted below.

Pressure coefficient is defined in two ways,

$$C_{p1} = (P_1^o - p_\ell) \Big/ \frac{1}{2} \rho_1 W_1^2 \tag{A1}$$

$$C_{p2} = (p_\ell - p_1) \Big/ \frac{1}{2} \rho_1 W_1^2 \tag{A2}$$

where W is replaced by V in the case of stationary blades. The blade surface static pressures were calculated using the concept of rothalpy. Rothalpy defined as

$$H_R = h + \frac{W^2}{2} - \frac{U^2}{2} \tag{A3}$$

(ref. 25) is constant on a stream surface. The flow is assumed isentropic so the local static state can be related to the rothalpy state by the following relations

$$H_R - h = c_p(T_R - T) = \frac{W^2}{2} - \frac{U^2}{2} \tag{A4}$$

or

$$T = T_R - \frac{1}{c_p}\left(\frac{W^2}{2} - \frac{U^2}{2}\right) \tag{A5}$$

and

$$p = P_R\left(\frac{T}{T_R}\right)^{\gamma/\gamma-1} \tag{A6}$$

The rothalpy state is established from the known inlet absolute stagnation state, the known inlet velocities, isentropic relations, and the definition of rothalpy (A3). Using velocity triangle relations and (A3) it can be shown that

$$H_R = h_1 + \frac{V_1^2}{2} - U^2 + UW_\theta \tag{A7}$$

Subtracting the absolute stagnation enthalpy yields

$$H_R - H_1^o = h_1 + \frac{V_1^2}{2} - U^2 + UW_\theta - h_1 - \frac{V_1^2}{2} \tag{A8}$$

which reduces to

$$T_R = T_1^o - \frac{1}{c_p}(U^2 - UW_\theta) \tag{A9}$$

The pressure is given by

$$P_R = P_1^o(T_R/T_1^o)^{\gamma/\gamma-1} \tag{A10}$$

The pressure coefficients are calculated at points on the blade surface where horizontal and vertical mesh lines intersect the blade surface. The locations of these points are given in TSONIC and MAGNFY by their m- and θ-coordinates. For analysis purposes it is more desirable to locate them with respect to the blade chord (fig. 42). The calculation of blade surface locations as a fraction of chord were restricted to blade sections lying on cylindrical stream surfaces. The blade section was considered in the TSONIC coordinate system (fig. 43) to define fraction of chord locations.

$$\begin{aligned} \text{FRACC} &= \text{AM}/\text{AC} \\ &= (\text{AN} + \text{NM})/\text{AC} \end{aligned} \tag{A11}$$

Since triangles ANP, ACD, and LMN are similar,

$$\text{AN} = \text{AC}\,\frac{\text{AP}}{\text{AD}} \tag{A12}$$

$$\text{NM} = \text{LN}\,\frac{\text{CD}}{\text{AC}} \tag{A13}$$

Substituting (A12) and (A13) into (A11) gives

$$\text{FRACC} = \left(\text{AC}\,\frac{\text{AP}}{\text{AD}} + \text{LN}\,\frac{\text{CD}}{\text{AC}}\right)\Big/\text{AC} \tag{A14}$$

Each term in (A14) was evaluated as follows

$$\text{AP} = \text{m(J)} - \text{AQ} \tag{A15}$$

$$\text{AD} = \text{m(MBO)} - \text{F} - \text{AQ} \tag{A16}$$

$$\text{CD} = \text{R}\theta\text{(MBO,1)} \pm \text{G} + \text{OQ} \tag{A17}$$

$$\text{AC} = \sqrt{(\text{CD})^2 + (\text{AD})^2} \tag{A18}$$

$$\text{LN} = \text{LP} - \text{NP} \tag{A19}$$

$$\text{LP} = \text{R}\theta\text{(J, SURF)} - \text{(R) PIT(SURF)} + \text{OQ} \tag{A20}$$

$$\text{NP} = \text{CD}\,\frac{\text{AP}}{\text{AD}} \tag{A21}$$

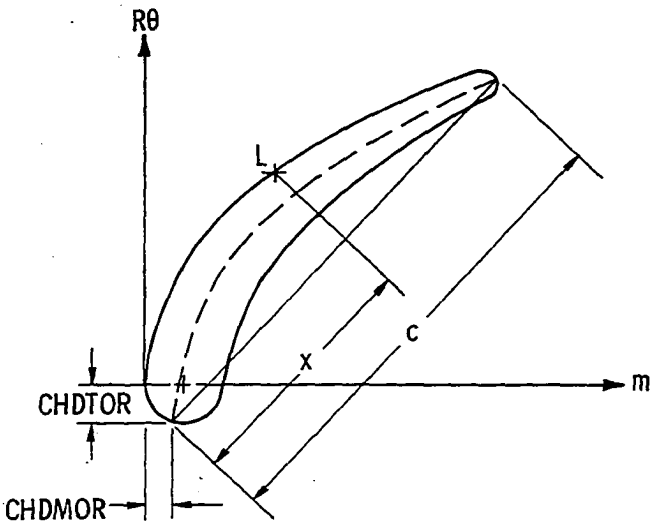

Figure 42. - Location of points on the blade surface with respect to the chord for a cylindrical stream surface.

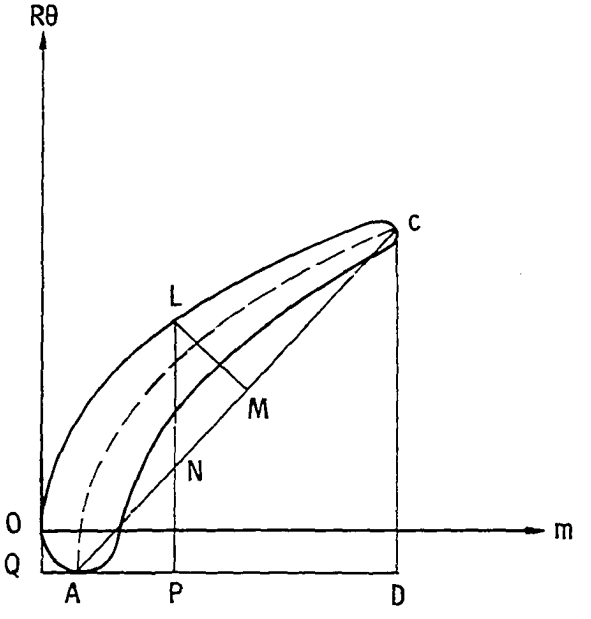

Figure 43. - Auxiliary geometrical quantities used in defining fraction of chord.

where PIT(1) = 0, PIT(2) = s. The quantities F and G were defined using figure 44.

$$F = RO - RO \cos(\eta_0 - \gamma^o), \qquad \eta_0 > \gamma^o \tag{A22}$$

$$G = RO \sin(\eta_0 - \gamma^o), \qquad \eta_0 > \gamma^o \tag{A23}$$

Similarly it can be shown that for the other case when $\eta_0 < \gamma^o$,

$$F = RO - RO \cos(\gamma^o - \eta_0), \qquad \eta_0 < \gamma^o \tag{A24}$$

$$G = RO \sin(\gamma^o - \eta_0), \qquad \eta_0 < \gamma^o \tag{A25}$$

Note that the sign on G in (A17) is + when $\eta_0 < \gamma^o$. The segments AQ and OQ were defined using figure 45 as

$$AQ = RI - RI \cos(\eta_I + \gamma^o) \tag{A26}$$

$$OQ = RI \sin(\eta_I + \gamma^o) \tag{A27}$$

Extra terms appear in the expressions for AP, AD, LP, and CD when the setting angle is large enough to require an artificial leading edge circle to be defined (appendix B). An example of this configuration is shown in figure 46. The only difference between the coordinate systems in figures 43 and 46 is a translation of axis. The magnitude of the translation can be evaluated by developing expressions for the location of the center of the original leading edge circle in the coordinate system of figure 46. An enlarged view of the leading edge circles is shown in figure 47. Comparing figures 46 and 47

$$CTRM = RLE + YCTRN/\sin \zeta - (XCTRN - RI + YCTRN/\tan \zeta)\cos \zeta \tag{A28}$$

$$CTRRT = (XCTRN - RI + YCTRN/\tan \zeta)\sin \zeta \tag{A29}$$

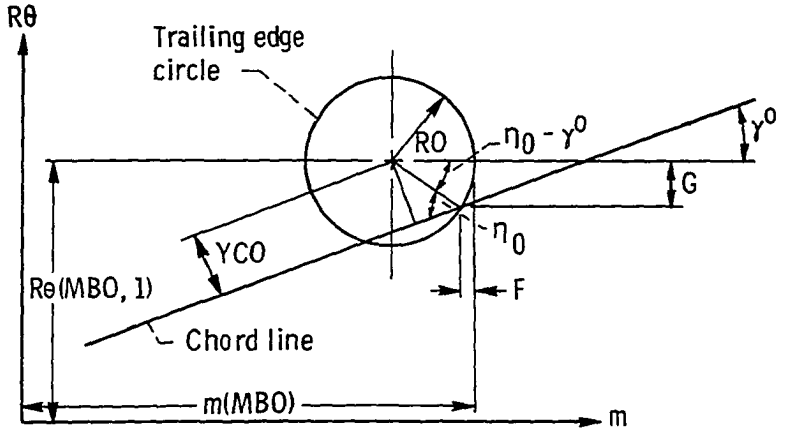

Figure 44. - Enlarged view of blade trailing edge circle.

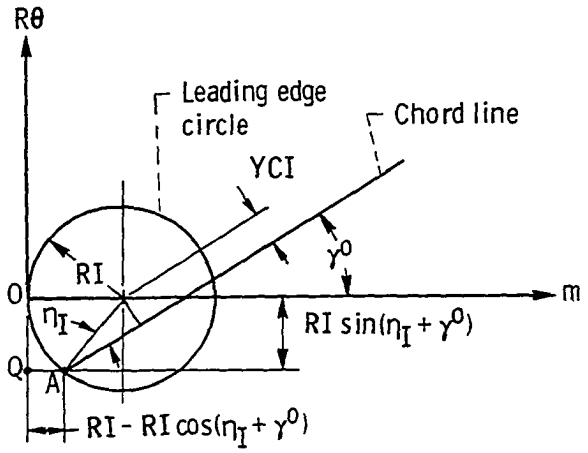

Figure 45. - Enlarged view of blade leading edge circle.

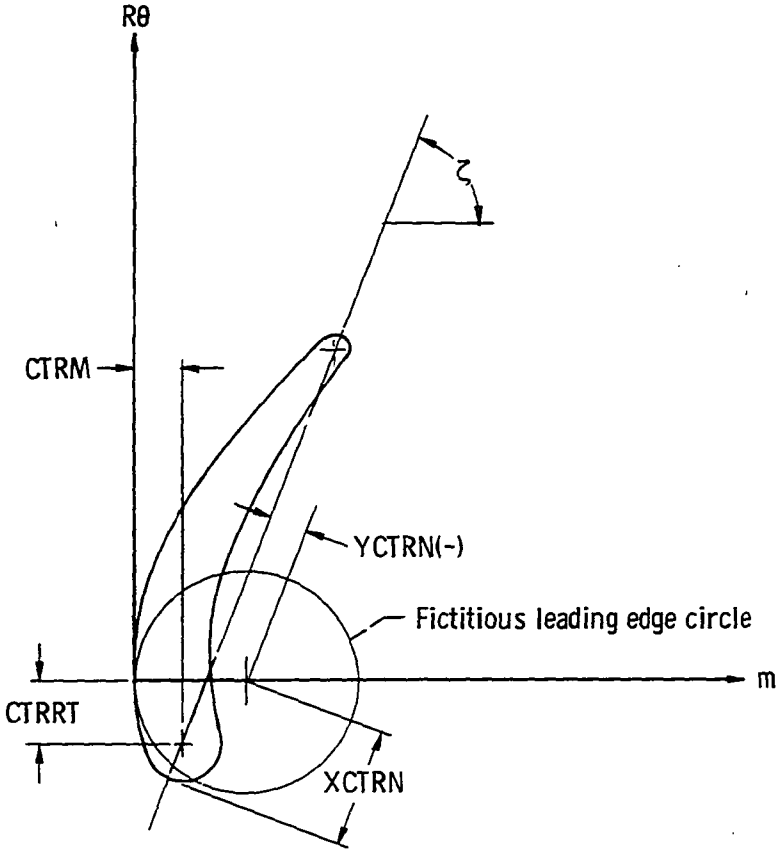

Figure 46. - Example of an artificial or fictitious leading edge circle.

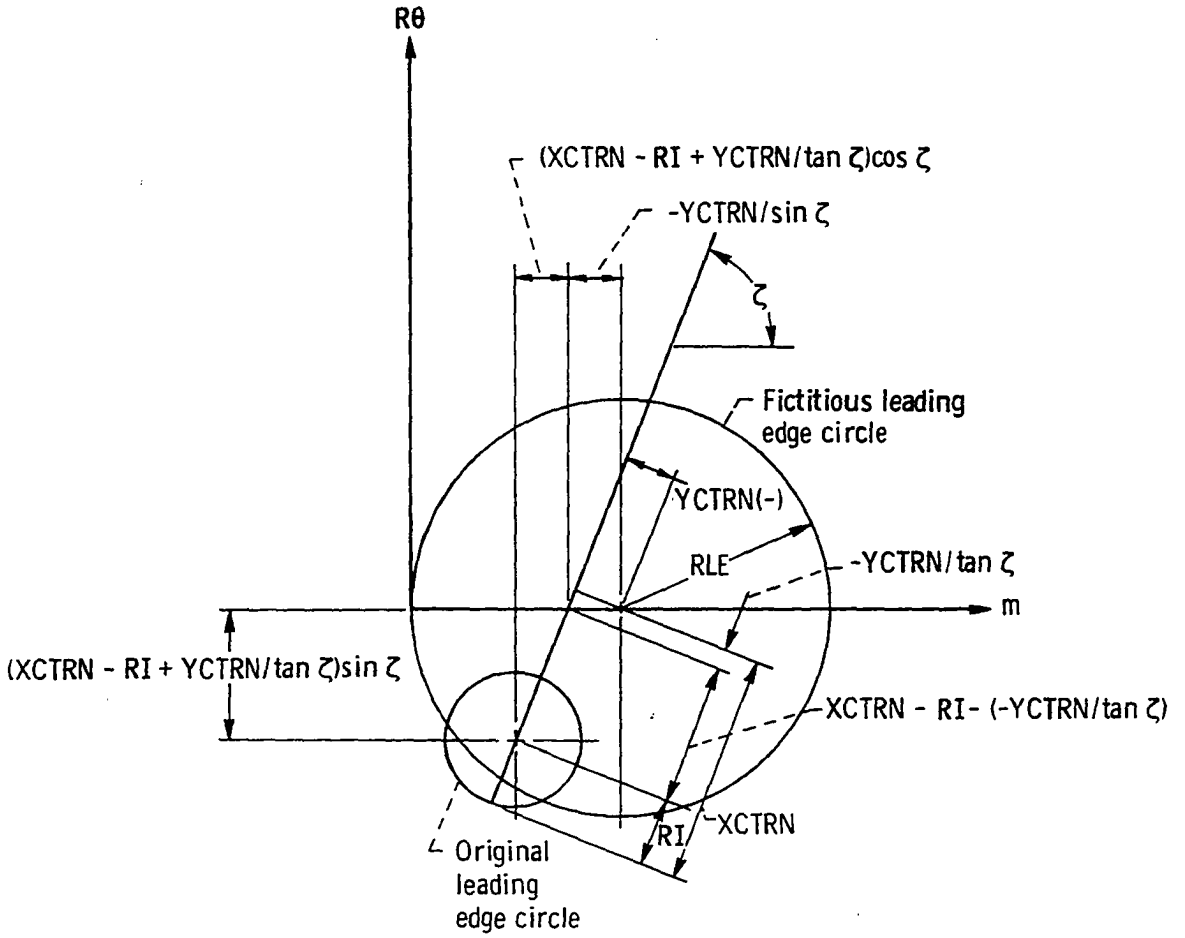

Figure 47. - Enlarged view of leading edge circles.

To calculate fraction of chord for the blade defined in figure 46 the following parameters are modified

$$AP = m(J) - AQ - CTRM + RI \tag{A30}$$

$$AD = m(MBO) - F - AQ - CTRM + RI \tag{A31}$$

$$CD = RO(MBO,1) \pm G + OQ + CTRRT \tag{A32}$$

$$LP = RO(J,SURF) - (R)PIT(SURF) + OQ + CTRRT \tag{A33}$$

Two extra input data cards must be added to the usual TSONIC and MAGNFY input data cards. They are shown schematically below.

1 10	11 20	21 30	31 40	41 50	51 60	61 70	71 80
KAPIN	KAPOUT	STDKIN	RLE	ORI	XCTRN	YCTRN	
ROTANG	YCI	YCO					

The input variables are defined as follows:

KAPIN inlet blade angle with respect to the meridional direction, deg

KAPOUT exit blade angle with respect to the meridional direction, deg

ORI radius of original leading edge, meters

RLE radius of artificially defined leading edge circle (fig. 47), meters

ROTANG angle between the chord line (AC, fig. 43) and the line connecting the centers of the original edge circles, deg Positive when the leading edge circle is larger than the

trailing edge circle

STDKIN angle between tangent to mean camber line at the leading edge and a line through the original edge circle centers, deg

XCTRN X-coordinate of center of artificially defined leading edge circle in coordinate system 2 (figs. 13 and 46), meters

YCI perpendicular distance between chord line and the center of the original leading edge circle (fig. 45), meters

YCTRN Y-coordinate of center of artificially defined leading edge circle in coordinate system 2 (figs. 13 and 46), meters

YCO perpendicular distance between chord line and the center of the trailing edge circle (fig. 44), meters

The source code for the two subprograms is given below. All new FORTRAN variables are defined. Existing variables which appear in the original TSONIC and MAGNFY programs (refs. 21 and 23) are not defined. Small changes required in existing subroutines are shown and referenced to the page of the original report where the coding appeared. Output is clearly labeled and self-explanatory.

```
IF (IEND.LE.0)  GO TO 30
CALL PRESCF
CALL TVELCY
```

page 48, ref. 21

```
      COMMON/PRETH/TH (50,2)
      COMMON SRW,ITER,IEND,LER(2),NER(2)
        .
        .
        .
      IM = MBI
      SURF = KODE + 1

   10 INTIND = 0
        .
        .
        .
      TI = FLOAT (ITV(IM) - ITO + IT + ITIND + KODE) + HT
      TH(J,SURF) + TI
      ITIND = ITIND + 1
```

page 86
ref. 21

SUBROUTINE PRESCF (for TSONIC)

```
      SUBROUTINE PRESCF
C
C
C  THIS SUBPROGRAM COMPUTES AND PRINTS VALUES OF TWO DIFFERENT
C  PRESSURE COEFFICIENTS.  THE CALCULATIONS ARE VALID FOR BOTH
C  ROTATING AND STATIONARY BLADE ROWS WITH OR WITHOUT RADIUS
C  CHANGE.
C
C
C  AC          LINE AC IN FIGURE 43.
C
C  AD          LINE AD IN FIGURE 43.
C
C  AP          LINE AP IN FIGURE 43.
C
C  ASET        ANGLE BETWEEN M-AXIS AND THE LINE CONNECTING THE
C              ORIGINAL EDGE CIRCLE CENTERS, RAD.
C
C  BETAI       AVERAGE VALUE OF FLOW ANGLE ALONG
C              THE VERTICAL GRID LINE AT THE LEADING EDGE.
C
C  FLN         LINE LN IN FIGURE 43.
C
C
C  CHMND       M-COORDINATE OF THE INTERSECTION OF THE MEAN LINE AND
C              THE TRAILING EDGE CIRCLE.
C
C  CHDMOR      M-COORDINATE OF THE INTERSECTION OF THE MEAN CAMBER
C              LINE AND THE LEADING EDGE CIRCLE.
C
C  CHDTOR      THETA-COORDINATE OF THE INTERSECTION OF THE MEAN
C              CAMBER LINE AND THE LEADING EDGE CIRCLE.
C
C  CTRM        M-COORDINATE OF THE CENTER OF THE ORIGINAL LEADING
C              EDGE CIRCLE.
C
C  CTRT        THETA-COORDINATE OF THE CENTER OF THE ORIGINAL
C              LEADING EDGE CIRCLE.
```

```
C   DELM        DIFFERENCE BETWEEN THE LARGEST M-COORDINATE AND CHMND.
C
C   DELTH       DIFFERENCE BETWEEN THETA-COORDINATES OF THE EXTREME
C               DOWNSTREAM EDGE OF THE BLADE AND THE END OF THE
C               MEANLINE. RAD.
C
C   ETAI        ANGLE BETWEEN CHORD (LINE CONNECTING ENDS OF MEAN LINE)
C               AND THE LINE CONNECTING THE LEADING EDGE CIRCLE CENTER
C               TO THE END OF THE MEANLINE, RAD.
C
C   ETAO        ANGLE BETWEEN CHORD AND THE LINE CONNECTING THE TRAILING
C               EDGE CIRCLE TO THE END OF THE MEANLINE, RAD.
C
C   FLN         LINE LN IN FIGURE 43.
C
C   FLP         LINE LP IN FIGURE 43.
C
C   FNP         LINE NP IN FIGURE 43.
C
C   FRACC       FRACTION OF CHORD FROM THE LEADING EDGE.
C
C   KAPIN       INLET BLADE ANGLE WITH RESPECT TO AXIAL
C               DIRECTION. DEG.
C
C   KAPOUT      EXIT BLADE ANGLE WITH RESPECT TO THE AXIAL
C               DIRECTION. DEG.
C
C   ORI         RADIUS OF ORIGINAL LEADING EDGE.
C
C   PCOEF1      PRESSURE COEFFICIENT. RATIO OF LOCAL
C               STAGNATION PRESSURE OF RELATIVE FLOW MINUS LOCAL
C               STATIC PRESSURE TO THE INLET VELOCITY PRESSURE.
C
C   PCOEF2      PRESSURE COEFFICIENT. RATIO OF LOCAL STATIC
C               PRESSURE MINUS INLET STATIC PRESSURE TO THE
C               INLET VELOCITY PRESSURE.
C
C   PIP         INLET STAGNATION PRESSURE.
C
C   PIT         EQUAL TO ZERO FOR BLADE SURFACE 1 AND EQUAL TO
C               PITCH FOR BLADE SURFACE 2.
C
C   PREL        RELATIVE TOTAL PRESSURE BASED ON ROTHALPY CONCEPT.
C
C   PSTAT       LOCAL STATIC PRESSURE ON BLADE SURFACE.
C
C   PSTAT1      INLET STATIC PRESSURE.
C
C   RCHDOR      RADIUS OF STREAM SURFACE AT (CHDMCR,CHDTOR).
C
C   RCHENC      STREAM SURFACE RADIUS AT M=CHMNC
C
C   RHOS1       INLET STATIC DENSITY.
C
C
C   RLE         RADIUS OF ARTIFICIALLY DEFINED LEADING EDGE CIRCLE.
C   ROTANG      ANGLE BETWEEN THE CHORD LINE AND THE LINE CONNECTING
C               CENTERS OF THE ORIGINAL EDGE CIRCLES.  POSITIVE WHEN
C               THE LEADING EDGE CIRCLE IS LARGER THAN THE TRAILING
C               EDGE CIRCLE.
C
C   SETANG      ANGLE BETWEEN CHORD (LINE CONNECTING ENDS OF MEAN LINE)
C               AND THE M-AXIS. DEG.
```

```
C   STDKIN      INLET BLADE ANGLE WITH RESPECT TO A LINE THROUGH
C               THE ORIGINAL EDGE CIRCLE CENTERS, DEG.
C
C   TH          THETA-COORDINATE OF HORIZONTAL MESH LINE INTERSECTING
C               BLADE SURFACE.
C
C   TIP         INLET ABSOLUTE STAGNATION TEMPERATURE.
C
C   TREL        RELATIVE TOTAL TEMPERATURE BASED ON ROTHALPY
C               CONCEPT.
C
C   TSTAT       LOCAL STATIC TEMPERATURE ON BLADE SURFACE.
C
C   TSTATI      INLET STATIC TEMPERATURE.
C
C   VI          AVERAGE VALUE OF VELOCITY ALONG
C               THE UPSTREAM BOUNDARY.
C
C   XCTRN       X-COORDINATE OF ARTIFICIALLY DEFINED LEADING EDGE CIRCLE
C               CENTER IN COORDINATE SYSTEM NUMBER 2.
C
C   YCI         PERPENDICULAR DISTANCE BETWEEN CHORD LINE AND THE CENTER
C               OF THE ORIGINAL LEADING EDGE CIRCLE.
C
C   YCO         PERPENDICULAR DISTANCE BETWEEN CHORD LINE AND THE CENTER
C               OF THE TRAILING EDGE CIRCLE.
C
C   YCTRN       Y-COORDINATE OF CENTER OF ARTIFICIALLY DEFINED
C               LEADING EDGE CIRCLE IN COORDINATE SYSTEM NUMBER 2.
C
C
C
      COMMON /CALCON/ACTWT,ACTOMG,ACTLAM,MBIM1,MBIP1,MBOM1,MBOP1,MMM1,
     1   HM1,HT,DTLR,DMLR,PITCH,CP,EXPON,TWW,CPTIP,TGROG,TBI,TBO,LAMBDA,
     2   TWL,ITMIN,ITMAX,NIP,IMS(2),BV(2),MV(100),IV(101),ITV(100,2),
     3   TV(100,2),DTDMV(100,2),BETAV(100,2),MH(40,2),DTDMH(40,2),
     4   BETAH(40,2),RMH(40,2),BEH(40,2),RM(100),BE(100),DBDM(100),
     5   SAL(100),AAA(100)
      COMMON /GEOMIN/ CHORD(2),STGR(2),XLE(2),THLE(2),RMI(2),RMO(2),
     1   RI(2),RO(2),BETI(2),BETO(2),NSPI(2),MSP(50,2),THSP(50,2)
      COMMON /INP/GAM,AR,TIP,RHOIP,WTFL,OMEGA,ORF,BETAI,BETAO,REDFAC,
     1   DENTOL,MBI,MBO,MM,NBBI,NBL,NRSP,MR(10),RMSP(10),BESP(10),
     2   BLCAT,AANOK,ERSOR,STRFN,SLCRD,INTVL,SURVL
      COMMON/PRETH/ TH(40,2)
      COMMON /SURVEL/ WTB(100,2),WMB(100,2),XDOWN(400),YACROS(400)
      DIMENSION CHOMND(1),CHOMOR(1),PIT(2),RCHEND(1),RCHOOR(1)
      REAL KAPIN,KAPOUT,MH,MV,LAMBDA
      INTEGER SURF
C
C
      II=5
      IO=6
      READ(II,5000) KAPIN,KAPOUT,STDKIN,RLE,ORI,XCTRN,YCTRN
      READ(II,5000) ROTANG,YCI,YCO
C
C  COMPUTE AVERAGE INLET VELOCITY AND FLOW ANGLE.
C
      VI=(LAMBDA/RM(MBI)-OMEGA*RM(MBI))/SIN(BETAI)
      BETAI=BETAI*57.295779
      WRITE(IO,5020) BETAI,VI
      WRITE(IO,5040) KAPIN,KAPOUT,STDKIN,ROTANG,RLE,ORI,XCTRN,YCTRN,YCI,
     1 YCO
```

```
      BETAI=BETAI/57.295779
      KAPIN=KAPIN/57.295779
      KAPOUT=KAPOUT/57.295779
      ROTANG= ROTANG/57.295779
      STOKIN=STOKIN/57.295779
      PI=3.1415927
C
C  COMPUTE RELATIVE TOTAL TEMPERATURE AND PRESSURE CONSISTENT
C  WITH ROTHALPY.
C
      PIP=RHOIP*AR*TIP
      TREL=TIP-(1./CP)*RM(MBI)*OMEGA*(RM(MBI)*OMEGA-VI*SIN(BETAI))
      PREL=PIP*((TREL/TIP)**(GAM*EXPON))
C
C  COMPUTE INLET STATIC TEMPERATURE, PRESSURE, AND DENSITY.
C
      TSTAT1=TIP-VI*VI*.5/CP
      PSTAT1=PIP*((TSTAT1/TIP)**(GAM*EXPON))
      RHOS1=PSTAT1/(AR*TSTAT1)
      WRITE(IO,5030) TREL,PREL,TSTAT1,PSTAT1,RHOS1
C
C  COMPUTE COORDINATES OF THE INTERSECTION OF THE MEAN CAMBER
C  LINE AND THE ORIGINAL LEADING EDGE CIRCLE.
C
      PIT(1)=0.
      PIT(2)=PITCH
      ASET=KAPIN-STOKIN
      IF(XCTRN) 150,100,150
  100 ORI=RI(2)
      CTRM=RI(2)
      GO TO 160
  150 CTRM=RLE+YCTRN/SIN(ASET)-(XCTRN+YCTRN/TAN(ASET)-ORI)*COS(ASET)
  160 ETAI= ASIN(YCI/ORI)
      ETAO= ASIN(YCO/RO(1))
      SETANG= ASET + ROTANG
      CHDMOR(1)= CTRM-ORI*COS(SETANG+ETAI)
      IF(XCTRN) 180,170,180
  170 RCHDOR(1)=RMI(1)
      CTRT=0.
      GO TO 190
  180 CALL SPLINT(MR,RMSP,NRSP,CHDMOR,1,RCHDOR,AAA(100))
      CTRT=-(XCTRN+YCTRN/TAN(ASET)-ORI)*SIN(ASET)/RCHDOR(1)
  190 CHDTOR=CTRT-ORI*SIN(SETANG+ETAI)/RCHDOR(1)
      IF(SETANG.GT.ETAO)  GO TO 240
      DELM=RO(1)*(1.-SIN(SETANG+PI/2.-ETAO))
      CHDMND(1)= MV(MBO)-DELM
      CALL SPLINT(MR,RMSP,NRSP,CHDMND,1,RCHEND,AAA(100))
      DELTH=-RO(1)*COS(SETANG+PI/2.-ETAO)/RCHEND(1)
      GO TO 250
  240 DELM= RO(1)*(1.-SIN(-SETANG+PI/2.+ETAO))
      CHDMND(1)= MV(MBO)-DELM
      CALL SPLINT(MR,RMSP,NRSP,CHDMND,1,RCHEND,AAA(100))
      DELTH= RO(1)*COS(-SETANG+PI/2.+ETAO)/RCHEND(1)
  250 AD= MV(MBO)-CHDMOR(1)-DELM
      CO=(TV(MBO,1)-CHDTOR+DELTH)*RCHEND(1)
      AC=SQRT(CO*CO+AD*AD)
      WRITE(IO,5300) AD,CO,AC,CHDMOR(1),DELM
C
C  COMPUTE LOCAL BLADE SURFACE STATIC TEMPERATURES, PRESSURES,
C  AND PRESSURE COEFFICIENTS BASED ON MERIDIONAL VELOCITY
C  COMPONENTS.
```

```
C
      DO 300 SURF=1.2
      WRITE(IO.5090) SURF
      DO 300 IM=MBIP1.MBOM1
      TSTAT=TREL-.5*(WMB(IM.SURF)*WMB(IM.SURF)-RM(IM)*OMEGA
     X *RM(IM)*OMEGA)/CP
      PSTAT=PREL*((TSTAT/TREL)**(GAM*EXPON))
      PCOEF1=(PIP-PSTAT)/(.5*RHOS1*VI*VI)
      PCOEF2=(PSTAT-PSTAT1)*2./(RHOS1*VI*VI)
      AP=MV(IM)-CHDMOR(1)
      FLP=(TV(IM.SURF)-CHDTOR-PIT(SURF))*RM(IM)
      FNP=CD*AP/AD
      FLN=FLP-FNP
      FRACC=AP/AD+FLN*CD/AC/AC
  300 WRITE(IO.5100) IM.MV(IM).FRACC.PCOEF1.PCOEF2.WMB(IM.SURF).
     1PSTAT.TV(IM.SURF)
C
C  COMPUTE LOCAL BLADE SURFACE STATIC TEMPERATURES. PRESSURES.
C  AND PRESSURE COEFFICIENTS BASED ON TANGENTIAL VELOCITY
C  COMPONENTS.
C
      DO 500 SURF=1.2
      IMSS=IMS(SURF)
      IF(IMSS.LT.1) GO TO 500
      WRITE(IO.5200) SURF
      DO 400 IHS=1.IMSS
      TSTAT=TREL-.5*(WTB(IHS.SURF)*WTB(IHS.SURF)-
     X RMH(IHS.SURF)*OMEGA*RMH(IHS.SURF)*OMEGA)/CP
      PSTAT=PREL*((TSTAT/TREL)**(GAM*EXPON))
      PCOEF1=(PIP-PSTAT)/(.5*RHOS1*VI*VI)
      PCOEF2=(PSTAT-PSTAT1)*2./(RHOS1*VI*VI)
      AP=MH(IHS.SURF)-CHDMOR(1)
      FLP=(TH(IHS.SURF)-CHDTOR-PIT(SURF))*RMH(IHS.SURF)
      FNP=CD*AP/AD
      FLN=FLP-FNP
      FRACC=AP/AD+FLN*CD/AC/AC
  400 WRITE(IO.5100) IHS.MH(IHS.SURF).FRACC.PCOEF1.PCOEF2.
     1 WTB(IHS.SURF).PSTAT.TH(IHS.SURF)
  500 CONTINUE
      RETURN
 5000 FORMAT (7F10.7)
 5020 FORMAT(1H1.////10X.7H BETAI=.F7.3.5X.5H  VI=.F7.3)
 5030 FORMAT(//5X.6H TREL=.F7.3.2X.6H PREL=.F12.2.2X.8H TSTAT1=.
     X F7.2.2X.8H PSTAT1=.F12.2.2X.7H RHOS1=.F7.4)
 5040 FORMAT(//10X.7H KAPIN=.F12.7.3X.8H KAPOUT=.F12.7.3X.8H STDKIN=.
     1 F12.7.3X.8H ROTANG=.F12.7.///.3X.5H RLE=.F11.8.3X.5H ORI=.F11.8.
     2 3X.7H XCTRN=.F11.8.3X.7H YCTRN=.F11.8.3X.5H YCI=.F11.8.3X.
     3 5H YCO=.F11.8)
 5090 FORMAT(1H1.////.10X.32H PRESSURE COEFFICIENTS AND BLADE
     1 31H SURFACE VELOCITIES FOR SURFACE.I2.20H BASED ON MERIDIONAL
     2 24H COMPONENTS OF VELOCITY.///7X.3H IM.8X.2H M.1X.
     3 10H FRAC CHRD.3X.7H PCOEF1.3X.7H PCOEF2.1X.9H VELOCITY.2X.
     4 10H STAT PRES.8X.6H THETA/)
 5100 FORMAT(I10.G11.4.F10.3.2F10.4.F10.2.F12.2.F14.8)
 5200 FORMAT(1H1.////10X.32H PRESSURE COEFFICIENTS AND BLADE
     1 31H SURFACE VELOCITIES FOR SURFACE.I2.20H BASED ON TANGENTIAL
     2 24H COMPONENTS OF VELOCITY. ///6X.4H IHS.8X.2H M.1X.
     3 10H FRAC CHRD.3X.7H PCOEF1.3X.7H PCOEF2.1X.9H VELOCITY.2X.
     4 10H STAT PRES.8X.6H THETA/)
 5300 FORMAT(//5X.4H AD=.F11.8.5X.4H CD=.F11.8.5X.4H AC=.F11.8.
     X 5X.6H CHDMOR=.F11.8.5X.6H DELM=.F11.8)
      END
```

```
      WRITE (6,1000) TIME
      IF (IEND.LE.0) GO TO 30
      CALL PRESCF
      GO TO 10
1000  FORMAT (8HLTIME =, F7.4, 5H MIN.)
```

page 42, ref. 23

```
      COMMON/PRETH/TH(40,2)
      COMMON SRW, ITER, IEND, LER(2), NER(1)
        .
        .
        .
      TI = FLOAT (ITV (IM + 1) - ITO - ITIND + KODE) *HT
      TH (J, KODE + 1) = TI
      ITIND = ITIND - 1
        .
        .
        .
      TI = FLOAT (ITV (IM) - ITO + ITIND + KODE) *HT
      TH (J,KODE+1) = TI
      ITIND = ITIND + 1
```

page 75 ref. 23

SUBROUTINE PRESCF (for MAGNFY)

```
      SUBROUTINE PRESCF
C
C
C  THIS SUBPROGRAM COMPUTES AND PRINTS VALUES OF TWO DIFFERENT
C  PRESSURE COEFFICIENTS.  THE CALCULATIONS ARE VALID FOR BOTH
C  ROTATING AND STATIONARY BLADE ROWS WITH OR WITHOUT RADIUS
C  CHANGE.
C
C
C  AC          LINE AC IN FIGURE 43.
C
C  AD          LINE AD IN FIGURE 43.
C
C  AP          LINE AP IN FIGURE 43.
C
C  ASET        ANGLE BETWEEN M-AXIS AND THE LINE CONNECTING THE
C              ORIGINAL EDGE CIRCLE CENTERS, RAD.
C
C  BETAI       AVERAGE VALUE OF FLOW ANGLE ALONG
C              THE VERTICAL GRID LINE AT THE LEADING EDGE.
C  CC          LINE CD IN FIGURE
C
C  CHMND       M-COORDINATE OF THE INTERSECTION OF THE MEAN LINE AND
C              THE TRAILING EDGE CIRCLE.
C
C  CHDMOR      M-COORDINATE OF THE INTERSECTION OF THE MEAN CAMBER
C              LINE AND THE LEADING EDGE CIRCLE.
C
C  CHDTOR      THETA-COORDINATE OF THE INTERSECTION OF THE MEAN
C              CAMBER LINE AND THE LEADING EDGE CIRCLE.
```

```
C
C   CTRM        M-COORDINATE OF THE CENTER OF THE ORIGINAL LEADING
C               EDGE CIRCLE.
C
C   CTRT        THETA-COORDINATE OF THE CENTER OF THE ORIGINAL
C               LEADING EDGE CIRCLE.
C
C   DELM        DIFFERENCE BETWEEN THE LARGEST M-COORDINATE AND CHMND.
C
C   DELTH       DIFFERENCE BETWEEN THETA-COORDINATES OF THE EXTREME
C               DOWNSTREAM EDGE OF THE BLADE AND THE END OF THE
C               MEANLINE. RAD.
C
C   ETA1        ANGLE BETWEEN CHORD (LINE CONNECTING ENDS OF MEAN LINE)
C               AND THE LINE CONNECTING THE LEADING EDGE CIRCLE CENTER
C               TO THE END OF THE MEANLINE, RAD.
C
C   ETAO        ANGLE BETWEEN CHORD AND THE LINE CONNECTING THE TRAILING
C               EDGE CIRCLE TO THE END OF THE MEANLINE, RAD.
C
C   FLN         LINE LN IN FIGURE 43.
C
C   FLP         LINE LP IN FIGURE 43.
C
C   FNP         LINE NP IN FIGURE 43.
C
C   FRACC       FRACTION OF CHORD FROM THE LEADING EDGE.
C
C   KAPIN       INLET BLADE ANGLE WITH RESPECT TO AXIAL
C               DIRECTION, DEG.
C
C   KAPOUT      EXIT BLADE ANGLE WITH RESPECT TO THE AXIAL
C               DIRECTION, DEG.
C
C   ORI         RADIUS OF ORIGINAL LEADING EDGE.
C
C   PCOEF1      PRESSURE COEFFICIENT, RATIO OF DIFFERENCE
C               BETWEEN STAGNATION PRESSURE AT RELATIVE FLOW
C               AND STATIC PRESSURE TO THE INLET VELOCITY PRESSURE.
C
C   PCOEF2      PRESSURE COEFFICIENT, RATIO OF LOCAL STATIC
C               PRESSURE MINUS INLET STATIC PRESSURE TO THE
C               INLET VELOCITY PRESSURE.
C
C   PIP         INLET STAGNATION PRESSURE.
C
C   PIT         EQUAL TO ZERO FOR BLADE SURFACE 1 AND EQUAL TO
C               PITCH FOR BLADE SURFACE 2.
C
C   PREL        RELATIVE TOTAL PRESSURE BASED ON ROTHALPY CONCEPT.
C
C   PSTAT       LOCAL STATIC PRESSURE ON BLADE SURFACE.
C
C   PSTAT1      INLET STATIC PRESSURE.
C
C   RCHDOR      RADIUS OF STREAM SURFACE AT (CHDMCR,CHDTOR).
C
C   RCHEND      STREAM SURFACE RADIUS AT M=CHMND
C
C   RHOS1       INLET STATIC DENSITY.
C
C   RLE         RADIUS OF ARTIFICIALLY DEFINED LEADING EDGE CIRCLE.
C
```

```
C   ROTANG      ANGLE BETWEEN THE CHORD LINE AND THE LINE CONNECTING
C               CENTERS OF THE ORIGINAL EDGE CIRCLES.  POSITIVE WHEN
C               THE LEADING EDGE CIRCLE IS LARGER THAN THE TRAILING
C               EDGE CIRCLE.
C
C   STGANG      ANGLE BETWEEN CHORD (LINE CONNECTING ENDS OF MEAN LINE)
C               AND THE M-AXIS. DEG.
C
C   STGKIN      INLET BLADE ANGLE WITH RESPECT TO A LINE THROUGH
C               THE ORIGINAL EDGE CIRCLE CENTERS, DEG.
C
C   TH          THETA-COORDINATE OF HORIZONTAL MESH LINE INTERSECTING
C               BLADE SURFACE.
C
C   TIP         INLET ABSOLUTE STAGNATION TEMPERATURE.
C
C   TREL        RELATIVE TOTAL TEMPERATURE BASED ON ROTHALPY
C               CONCEPT.
C
C   TSTAT       LOCAL STATIC TEMPERATURE ON BLADE SURFACE.
C
C   TSTATI      INLET STATIC TEMPERATURE.
C
C   VI          AVERAGE VALUE OF VELOCITY ALONG
C               THE UPSTREAM BOUNDARY.
C
C   XCTRN       X-COORDINATE OF ARTIFICIALLY DEFINED LEADING EDGE CIRCLE
C               CENTER IN COORDINATE SYSTEM NUMBER 2.
C
C   YCI         PERPENDICULAR DISTANCE BETWEEN CHORD LINE AND THE CENTER
C               OF THE ORIGINAL LEADING EDGE CIRCLE.
C
C   YCO         PERPENDICULAR DISTANCE BETWEEN CHORD LINE AND THE CENTER
C               OF THE TRAILING EDGE CIRCLE.
C
C   YCTRN       Y-COORDINATE OF CENTER OF ARTIFICIALLY DEFINED
C               LEADING EDGE CIRCLE IN COORDINATE SYSTEM NUMBER 2.
C
C
C
      COMMON /AUXRHO/ A(2000,4),U(2000),K(2000),RHO(2000)
      COMMON /INP/ GAM,AR,TIP,RHOIP,WTFL,WTFLSP,OMEGA,ORF,BETAI,BETAO,
     1NOBL,MBI,MPO,MBI2,MBC2,MM,NBBI,NBL,NRSP,MBDYF,MBDYL,ITF,ITL,
     2BLCAT,AANDK,ERSOR,STRFN,INTVL,SURVL,MAGFAC,
     3MR(50),RMSP(50),BESP(50)
      COMMON /CALCON/ MBII,MBOO,MMM,MBIIM1,MBIIP1,MBOOM1,MBOOP1,MMMM1,
     1HM1,HM2,HM3,HT,DTLR,DMLR,PITCH,CP,EXPON,TWW,CPTIP,TGROG,TBI,TBO,
     2LAMBDA,TWL,ITOR,ITMAX,NIP,IMS(4),BV(4),MV(100),IV(101),
     3UBV(100,4),RWBV(100,4),ITV(100,6),TV(100,4),DTDMV(100,4),
     4BETAV(100,4),MH(100,4),DTDMH(100,4),BETAH(100,4),RMH(100,4),
     5BEH(100,4),RM(100),BE(100),DBDM(100),SAL(100),AAA(100)
      COMMON /GEOMIN/ CHORD(4),STGR(4),XLE(4),THLE(4),RMI(4),RMO(4),
     1RI(4),RO(4),BETI(4),BETO(4),NSPI(4),MSP(50,4),THSP(50,4)
      COMMON/PRETH/ TH(40,2)
      DIMENSION CHDMND(1),CHDMOR(1),PIT(2),RCHEND(1),RCHDOR(1)
      DIMENSION WMB(100,4),WTB(100,4)
      EQUIVALENCE (A(1,4),WMB(1)),(A(401,4),WTB(1))
      REAL KAPIN,KAPOUT,MH,MV,LAMBDA
      INTEGER SURF
```

```
C
      II=5
      IO=6
      READ(II,5000) KAPIN,KAPOUT,STDKIN,RLE,ORI,XCTRN,YCTRN
      READ(II,5000) ROTANG,YCI,YCO
C
C  COMPUTE AVERAGE INLET VELOCITY AND FLOW ANGLE.
C
      VI=(LAMBDA/RMI(1)-OMEGA*RMI(1))/SIN(BETAI/57.295779)
      WRITE(IO,5020) BETAI,VI
      WRITE(IO,5040) KAPIN,KAPOUT,STDKIN,ROTANG,RLE,ORI,XCTRN,YCTRN,YCI,
     1 YCO
      BETAI=BETAI/57.295779
      KAPIN=KAPIN/57.295779
      KAPOUT=KAPOUT/57.295779
      ROTANG= ROTANG/57.295779
      STDKIN=STDKIN/57.295779
      PI=3.1415927
C
C  COMPUTE RELATIVE TOTAL TEMPERATURE AND PRESSURE CONSISTENT
C  WITH ROTHALPY.
C
      PIP=RHOIP*AR*TIP
      TREL=TIP-(1./CP)*RMI(1)*OMEGA*(RMI(1)*OMEGA-VI*SIN(BETAI))
      PREL=PIP*((TREL/TIP)**(GAM*EXPON))
C
C  COMPUTE INLET STATIC TEMPERATURE, PRESSURE, AND DENSITY.
C
      TSTAT1=TIP-VI*VI*.5/CP-(1./CP)*RMI(1)*OMEGA*(.5*RMI(1)*OMEGA
     1 -VI*SIN(BETAI))
      PSTAT1=PIP*((TSTAT1/TIP)**(GAM*EXPON))
      RHOS1=PSTAT1/(AR*TSTAT1)
      WRITE(IO,5030) TREL,PREL,TSTAT1,PSTAT1,RHOS1
C
C  COMPUTE COORDINATES OF THE INTERSECTION OF THE MEAN CAMBER
C  LINE AND THE ORIGINAL LEADING EDGE CIRCLE.
C
      PIT(1)=0.
      PIT(2)=PITCH
      ASET=KAPIN-STDKIN
      IF(XCTRN) 150,100,150
  100 ORI=RI(2)
      CTRM=RI(2)
      GO TO 160
  150 CTRM=RLE+YCTRN/SIN(ASET)-(XCTRN+YCTRN/TAN(ASET)-ORI)*COS(ASET)
  160 ETAI= ASIN(YCI/ORI)
      ETAC= ASIN(YCO/RC(1))
      SETANG= ASET + ROTANG
      CHDMOR(1)= CTRM-ORI*COS(SETANG+ETAI)
      IF(XCTRN) 180,170,180
  170 RCHDOR(1)=RMI(1)
      CTRT=0.
      GO TO 190
  180 CALL SPLINT(MR,RMSP,NRSP,CHDMOR,1,RCHDOR,AAA(100))
      CTRT=-(XCTRN+YCTRN/TAN(ASET)-ORI)*SIN(ASET)/RCHDOR(1)
  190 CHDTOR=CTRT-ORI*SIN(SETANG+ETAI)/RCHDOR(1)
      IF(SETANG.GT.ETAO)  GO TO 240
      DELM=RO(1)*(1.-SIN(SETANG+PI/2.-ETAC))
      CHDMND(1)= CHORD(1)-DELM
      CALL SPLINT(MR,RMSP,NRSP,CHDMND,1,RCHEND,AAA(100))
      DELTH=-RO(1)*COS(SETANG+PI/2.-ETAC)/RCHEND(1)
      GO TO 250
```

```
  240 DELM= RO(1)*(1.-SIN(-SETANG+PI/2.+ETAO))
      CHDMND(1)=CHORD(1)-DELM
      CALL SPLINT(MR,RMSP,NRSP,CHDMND,1,RCHEND,AAA(100))
      DELTH= RO(1)*COS(-SETANG+PI/2.+ETAO)/RCHEND(1)
  250 AD=CHORD(1)-CHDMOR(1)-DELM
      CD=(STGR(1)-CHDTOR+DELTH)*RCHEND(1)
      AC=SQRT(CD*CD+AD*AD)
      WRITE(IO,5300) AD,CD,AC,CHDMOR(1),DELM
C
C  COMPUTE LOCAL BLADE SURFACE STATIC TEMPERATURES, PRESSURES,
C  AND PRESSURE COEFFICIENTS BASED ON MERIDIONAL VELOCITY
C  COMPONENTS.
C
      MBOT=MINO(MMMM1,MBOO)
      IF(MBOT.LT.2) GO TO 320
      DO 300 SURF=1,2
      WRITE(IO,5090) SURF
      DO 300 IM=2,MBOT
      TSTAT=TREL-.5*(WMB(IM,SURF)*WMB(IM,SURF)-RM(IM)*OMEGA
     X *RM(IM)*OMEGA)/CP
      PSTAT=PREL*((TSTAT/TREL)**(GAM*EXPON))
      PCOEF1=(PIP-PSTAT)/(.5*RHOS1*VI*VI)
      PCOEF2=(PSTAT-PSTAT1)*2./(RHOS1*VI*VI)
      AP=MV(IM)-CHDMOR(1)
      FLP=(TV(IM,SURF)-CHDTOR-PIT(SURF))*RM(IM)
      FNP=CD*AP/AD
      FLN=FLP-FNP
      FRACC=AP/AD+FLN*CD/AC/AC
  300 WRITE(IO,5100) IM,MV(IM),FRACC,PCOEF1,PCOEF2,WMB(IM,SURF),
     X PSTAT,TV(IM,SURF)
  320 MBIT=MAXO(2,MBII)
      IF(MBIT.GT.MMMM1) GO TO 380
      MTEC=MBOYF+MBOO
      DO 350 SURF=3,4
      WRITE(IO,5090) SURF
      DO 350 IM=MBIT,MMMM1
      TSTAT=TREL-.5*(WMB(IM,SURF)*WMB(IM,SURF)-RM(IM)*OMEGA
     X *RM(IM)*OMEGA)/CP
      PSTAT=PREL*((TSTAT/TREL)**(GAM*EXPON))
      PCOEF1=(PIP-PSTAT)/(.5*RHOS1*VI*VI)
      PCOEF2=(PSTAT-PSTAT1)*2./(RHOS1*VI*VI)
      AP=MV(IM)-CHDMOR(1)
      FLP=(TV(IM,SURF)-CHDTOR-PIT(SURF))*RM(IM)
      FNP=CD*AP/AD
      FLN=FLP-FNP
      FRACC=AP/AD+FLN*CD/AC/AC
  350 WRITE(IO,5100) IM,MV(IM),FRACC,PCOEF1,PCOEF2,WMB(IM,SURF),
     X PSTAT,TV(IM,SURF)
C
C  COMPUTE LOCAL BLADE SURFACE STATIC TEMPERATURES, PRESSURES,
C  AND PRESSURE COEFFICIENTS BASED ON TANGENTIAL VELOCITY
C  COMPONENTS.
C
  380 DO 500 SURF=1,4
      IMSS=IMS(SURF)
      IF(IMSS.LT.1) GO TO 500
      WRITE(IO,5200) SURF
      DO 400 IHS=1,IMSS
      TSTAT=TREL-.5*(WTB(IHS,SURF)*WTB(IHS,SURF)-
     X RMH(IHS,SURF)*OMEGA*RMH(IHS,SURF)*OMEGA)/CP
      PSTAT=PREL*((TSTAT/TREL)**(GAM*EXPON))
      PCOEF1=(PIP-PSTAT)/(.5*RHOS1*VI*VI)
```

```
      PCOEF2=(PSTAT-PSTAT1)*2./(RHOS1*VI*VI)
      AP=MH(IHS,SURF)-CHDMOR(1)
      FLP=(TH(IHS,SURF)-CHDTOR-PIT(SURF))*RMH(IHS,SURF)
      FNP=CD*AP/AD
      FLN=FLP-FNP
      FRACC=AP/AD+FLN*CD/AC/AC
  400 WRITE(IO,5100) IHS,MH(IHS,SURF),FRACC,PCOEF1,PCOEF2,
     X WTB(IHS,SURF),PSTAT,TH(IHS,SURF)
  500 CONTINUE
      RETURN
 5000 FORMAT(7F10.7)
 5020 FORMAT(1H1,/////10X,7H BETAI=,F7.3,5X,5H  VI=,F7.3)
 5030 FORMAT(//5X,6H TREL=,F7.2,2X,6H PREL=,F12.2,2X,8H TSTAT1=,
     X F7.2,2X,8H PSTAT1=,F12.2,2X,7H RHOS1=,F7.4)
 5040 FORMAT(//10X,7H KAPIN=,F12.7,3X,8H KAPOUT=,F12.7,3X,8H STDKIN=,
     1 F12.7,3X,8H ROTANG=,F12.7,///,3X,5H RLE=,F11.8,3X,5H ORI=,F11.8,
     2 3X,7H XCTRN=,F11.8,3X,7H YCTRN=,F11.8,3X,5H YCI=,F11.8,3X,
     3 5H YCO=,F11.8)
 5090 FORMAT(1H1,/////,10X,32H PRESSURE COEFFICIENTS AND BLADE
     1 31H SURFACE VELOCITIES FOR SURFACE,I2,20H BASED ON MERIDIONAL
     2 24H COMPONENTS OF VELOCITY.///7X,3H IM,8X,2H M,1X,
     3 10H FRAC CHRD,3X,7H PCOEF1,3X,7H PCOEF2,1X,9H VELOCITY,2X,
     4 10H STAT PRES,8X,6H THETA/)
 5100 FORMAT(I10,G11.4,F10.3,2F10.4,F10.2,F12.2,F14.8)
 5200 FORMAT(1H1,/////10X,32H PRESSURE COEFFICIENTS AND BLADE
     1 31H SURFACE VELOCITIES FOR SURFACE,I2,20H BASED ON TANGENTIAL
     2 24H COMPONENTS OF VELOCITY. ///6X,4H IHS,8X,2H M,1X,
     3 10H FRAC CHRD,3X,7H PCOEF1,3X,7H PCOEF2,1X,9H VELOCITY,2X,
     4 10H STAT PRES,8X,6H THETA/)
 5300 FORMAT(//5X,4H AD=,F11.8,5X,4H CD=,F11.8,5X,4H AC=,F11.8,
     X 5X,8H CHDMOR=,F11.8,5X,6H DELM=,F11.8)
      END
```

Stream Function Interpolation in MAGNFY

Coding was added to SUBROUTINE SLAVBB of MAGNFY to furnish the coordinates at which several streamlines cross vertical mesh lines as output. The primary motivation for the change was to obtain coordinates of the stagnation or dividing streamline downstream of the trailing edge. No additional input data is required. Output is labeled and self-explanatory. The revised subroutine is listed below.

```
      SUBROUTINE SLAVBB(IM,UPPER,LOWER)
C
C  SLAVBB CALCULATES RHO*W-SUB-M ALONG VERTICAL MESH LINES
C
      COMMON SRW,ITER,IEND,LER(2),NER(1)
      COMMON /AUKRHO/ A(2000,4),U(2000),K(2000),RHO(2000)
      COMMON /INP/ GAM,AR,TIP,RHOIP,WTFL,WTFLSP,OMEGA,ORF,BETAI,BETAO,
     1NOBL,MBI,MBO,MBI2,MBO2,MM,NBBI,NBL,NRSP,MBOYF,MBOYL,ITF,ITL,
     2BLCAT,AANDK,ERSOR,STRFN,INTVL,SURVL,MAGFAC,
     3MR(50),RMSP(50),BESP(50)
      COMMON /CALCON/ MBII,MBOO,MMM,MBIIM1,MBIIP1,MBOOM1,MBOOP1,MMMM1,
     1HM1,HM2,HM3,HT,DTLR,DMLR,PITCH,CP,EXPON,TWW,CPTIP,TGROG,TBI,TBO,
     2LAMBDA,TWL,ITCR,ITMAX,NIP,IMS(4),BV(4),MV(100),IV(101),
     3UBV(100,4),RWBV(100,4),ITV(100,6),TV(100,4),DTDMV(100,4),
     4BETAV(100,4),MH(100,4),DTDMH(100,4),BETAH(100,4),RMH(100,4),
     5BEH(100,4),RM(100),BE(100),DBDM(100),SAL(100),AAA(100)
      COMMON /RHOS/ RHOHB(100,4),RHOVB(100,4),RBV(100,4)
      DIMENSION W(2000),RWM(2000),BETA(2000),WMB(100,4),WTB(100,4),
     1XDOWN(800),YACROS(800),TSL(400),TSP(100),USP(100),DUDT(100)
      DIMENSION UINT(5),TINT(5)
      EQUIVALENCE (A(1,1),W(1)),(A(1,2),RWM(1)),(A(1,3),BETA(1)),
     1(A(1,4),WMB(1)),(A(401,4),WTB(1)),(A(801,4),XDOWN(1)),
     2(K(1),YACROS(1)),(K(801),TSP(1)),
     3(K(901),USP(1)),(K(1001),DUDT(1))
      INTEGER BLDAT,AANDK,ERSOR,STRFN,SURVL,AATEMP,SURF,
     1FIRST,UPPER,SI,ST,SRW
      REAL K,KAK,LAMBDA,LMAX,MH,MLE,MR,MSP,MV,MVIM1
      ITVU= MAXO(ITV(IM,UPPER),2)
      ITVL= MINO(ITV(IM,LOWER),ITMAX-1)
      NSP= ITVL-ITVU+3
      IF(NSP.LT.3) RETURN
      TSP(1)= FLOAT(1-ITCR)*HT
      IF(ITV(IM,UPPER).LT.2.OR.UPPER.EQ.5) GO TO 10
      IF (TV(IM,UPPER).LT.TSP(1)) GO TO 10
      TSP(1)= TV(IM,UPPER)
      USP(1)= BV(UPPER)
      GO TO 20
```

```
   10 USP(1)= UBV(IM,1)
   20 TSP(NSP)= FLOAT(ITMAX-ITOR)*HT
      IF(ITV(IM,LOWER).GE.ITMAX.OR.LOWER.EQ.6) GO TO 30
      IF (TV(IM,LOWER).GE.TSP(NSP)) GO TO 30
      TSP(NSP)= TV(IM,LOWER)
      USP(NSP)= BV(LOWER)
      GO TO 40
   30 USP(NSP)= UBV(IM,2)
   40 NSPM1= NSP-1
      IT= 2
      IP= IPF(IM,ITVU)
      IPU= IP
   50 IF(IT.GT.NSPM1) GO TO 60
      TSP(IT)= FLOAT(IT-2+ITVU-ITOR)*HT
      USP(IT)= U(IP)
      IT= IT+1
      IP= IP+1
      GO TO 50
   60 IF (IEND.LT.0) GO TO 67
C
C  INTERPOLATE FOR STREAMLINE COORDINATES
C
      IF ((IM.EQ.2).AND.(UPPER.EQ.5)) WRITE (6,1000)
      NI=5
      IF (IM.GT.MBOC) GO TO 62
      IF (LOWER.EQ.6) GO TO 61
      UINT(1)=-.03
      UINT(2)=-.025
      UINT(3)=-.02
      UINT(4)=-.01
      UINT(5)=0.
      GO TO 63
   61 UINT(1)=0.
      UINT(2)=.01
      UINT(3)=.02
      UINT(4)=.025
      UINT(5)=.03
      GO TO 63
   62 UINT(1)= -.03
      UINT(2)=-.01
      UINT(3)=0.
      UINT(4)=.01
      UINT(5)=.03
   63 CALL SPLINT (USP,TSP,NSP,UINT,NI,TINT,AAA)
      DO 66 J=1,5
   66 AAA(J)=RMSP(1)*TINT(J)
      WRITE(6,1010) MV(IM),(UINT(J),TINT(J),AAA(J),J=1,5)
C
C  CALCULATE RHO*W-SUB-M IN THE REGION, AND RHO*W AT VERTICAL
C  MESH LINE INTERSECTIONS ON THE BLADE SURFACES, OR RHO
C  ON THE HORIZONTAL BOUNDARIES
C
   67 CALL SPLINE(TSP,USP,NSP,DUDT,AAA)
      IPL= IP-1
      IT= 2
      IP= IPU
   70 IF(IP.GT.IPL) GO TO 80
      RWM(IP)= DUDT(IT)*WTFL/BE(IM)/RM(IM)
      IP= IP+1
      IT= IT+1
      GO TO 70
```

```
   80 IF(ITV(IM,UPPER).LT.2.OR.UPPER.EQ.5) GO TO 90
      IF (TV(IM,UPPER).LT.FLOAT(1-ITOR)*HT) GO TO 90
C  UPPER BLADE SURFACE
      WMB(IM,UPPER)= DUDT(1)*WTFL/BE(IM)/RM(IM)
      RMDTU2 = (RM(IM)*DTDMV(IM,UPPER))**2
      IF(RMDTU2.GT.10000.) WMB(IM,UPPER)=0.
      WMB(IM,UPPER) = ABS(WMB(IM,UPPER))*SQRT(1.+RMDTU2)
      GO TO 100
C  LOWER BOUNDARY
   90 RWMBV = DUDT(1)*WTFL/BE(IM)/RM(IM)
      RW= SQRT(RWBV(IM,1)**2+RWMBV**2)
      TWLMR= 2.*OMEGA*LAMBDA-(OMEGA*RM(IM))**2
      LER(1) = 1
C     DENSTY CALL NO. 1
      CALL DENSTY(RW,RBV(IM,1),ANS,TWLMR,CPTIP,EXPON,RHOIP,GAM,AR,TIP)
  100 IF(ITV(IM,LOWER).GE.ITMAX.OR.LOWER.EQ.6) GO TO 110
      IF (TV(IM,LOWER).GE.FLOAT(ITMAX-ITOR)*HT) GO TO 110
C  LOWER BLADE SURFACE
      WMB(IM,LOWER)= DUDT(NSP)*WTFL/BE(IM)/RM(IM)
      RMDTL2 = (RM(IM)*DTDMV(IM,LOWER))**2
      IF(RMDTL2.GT.10000.) WMB(IM,LOWER)=0.
      WMB(IM,LOWER) = ABS(WMB(IM,LOWER))*SQRT(1.+RMDTL2)
      RETURN
C  UPPER BOUNDARY
  110 RWMBV = DUDT(NSP)*WTFL/BE(IM)/RM(IM)
      RW= SQRT(RWBV(IM,2)**2+RWMBV**2)
      TWLMR= 2.*OMEGA*LAMBDA-(OMEGA*RM(IM))**2
      LER(1) = 2
C     DENSTY CALL NO. 2
      CALL DENSTY(RW,RBV(IM,2),ANS,TWLMR,CPTIP,EXPON,RHOIP,GAM,AR,TIP)
      RETURN
 1000 FORMAT(1H1,30X,22HSTREAMLINE COORDINATES///4X,12HM COORDINATE,
     X 2(7X,10HSTREAM FN.,10X,5HTHETA,4X,10X,6HRTHETA,3X)//)
 1010 FORMAT (1X,7G18.7/(19X,6G18.7))
      END
```

Miscellaneous Coding Changes

A number of miscellaneous coding changes were made to correct incorrect coding in TSONIC and MAGNFY. The changes to TSONIC (ref. 21) are listed below.

1. In INPUT (page 48, ref. 21) changed BLANK to NLANK in the 15th and 16th statements to conform to FORMAT statement variable type

2. In SOR (page 61, ref. 21) replaced statement 100 and the next two statements with the coding below to avoid subscripts out of range

```
100 IF (IM.EQ.1) GO TO 101
      IF (IM.EQ.MM) GO TO 102
    IP3=IPF(IM-1,IT3)
    IP4=IPF(IM+1,IT4)
    GO TO 103
101 IP4=IPF(IM+1,IT4)
    IP3=IP4-NBBI
    GO TO 103
102 IP3=IPF(IM-1,IT3)
    IP4=IP3+NBBI
103 IF (ORF.GT.1.) GO TO 110
```

3. In TANG (pages 66 and 67, ref. 21) changed AAA to AAA (1) in all ROOT calls.

4. In MAIN (page 47, ref. 21) added "SRW = 0." because it is not initialized for use in SPLINT

5. In ROOT (page 87, ref. 21) added the coding below to handle the case where the root occurs at the left end of the interval.

```
   IF(ABS(Y-FX1).GT.TOLERY) GO TO 5
   X=X1
   RETURN
 5 X2 = B
```

The following changes were made to MAGNFY (ref. 23).

1. In TANG (page 65, ref. 23) changed AAA to AAA(1) in all ROOT calls.
2. Initialized SRW = 0. in MAIN (page 41, ref. 23) because it is undefined in SPLINT
3. In INPUT (page 47, ref. 23) add "IM = 1" after statement 220, and add "IF (KBDRY.EQ.4) IM = MMM" after "DO 230 KBDRY = 3,4," to avoid an undefined subscript
4. In PRECAL (page 51, ref. 23) after "DO 190 SURF = 1.4", inserted "IF (IMS (SURF) . LE.0) GO TO 190" to avoid a zero subscript.
5. In HRB (page 55, ref. 23) replaced the 8th through the 16th arithmetic statements with the coding below to avoid zero and out-of-range subscripts.

```
      IF (IT.EQ.2) GO TO 10
      R(1)= RHO(IP-1)
      GO TO 20
   10 R(1)=RBV(IM,1)
   20 IF (IT.EQ.ITMAX-1) GO TO 30
      R(2)= RHO(IP+1)
      GO TO 40
   30 R(2)=RBV(IM,2)
   40 IF (IM.EQ.2) GO TO 50
      R(3)= RHO(IP3)
      GO TO 60
   50 R(3)=RBV(IT,3)
   60 IF (IM.EQ.MMM1) GO TO 70
      R(4)= RHO(IP4)
      GO TO 80
   70 R(4)=RBV(IT,4)
   80 BZ= BE(IM)
```

6. In SOR (page 58, ref. 23) added "IF (IPI.LE.0) IP1 = 1" after "IP1 = IP - 1" and changed "IF (IM.EQ.2) IP3 = 0" to "IF (IM.EQ.2) IP3 = 1" and "IF(IM.EQ.MMMM1) IP4 = 0" to "IF (IM.EQ.MMMM1) IP4 = 1" to avoid zero subscripts. The coefficients of V(0) are always zero so V(1) can replace it with no error.
7. In SPLINT (page 79, ref. 23) added "C(N) = 0." after "C(1) = -.5".

APPENDIX B. ARBITRARY BLADE PROFILE GEOMETRY PROGRAM (ARBBP)

The ARBBP program was written to calculate geometrical input parameters (fig. 12) for the TSONIC and MAGNFY programs. It was written by making extensive modifications and additions to a similar program (ref. 28) to expand its applicability to any profile shape described in one of the three coordinate systems shown in figure 13. The only restrictions on the profiles are that the leading and trailing edges must be either circular or sharp and that the profile must lie on a right circular cylinder or a plane.

Three major tasks are performed by the ARBBP program. The input coordinates are transformed into the staggered position in the coordinate system shown in figure 12; the transformed coordinates are interpolated at regular intervals to provide additional coordinate points; and the tangency points and directions at the edge circles are determined for the suction and pressure surfaces. The tangency directions are determined in coordinate system 2 (fig. 13). A parabola is fitted to the three input coordinate points nearest the edge circle, and the XX-coordinate is determined for which the slopes of the parabola and the edge circle differ by less than a given tolerance.

The transformed input coordinates are listed in the ARBBP output and often are the best points to use for TSONIC and MAGNFY input. These transformed coordinates normally are defined in the coordinate system of figure 12, but occasionally when the blade setting angle is quite large the suction surface will be a double-valued curve in that coordinate system. To avoid this problem an artificial or fictitious leading edge

circle is defined and the coordinates are transformed to the coordinate system shown in figure 46. The "pressure" surface now includes part of the original suction surface and the original leading edge arc. Input data for TSONIC and MAGNFY are treated as usual except that two leading edge radii are used (RI1 and RI2, fig. 12) rather than the original leading edge radius.

The interpolation of coordinates is done in coordinate system 2 (fig. 13(b)) using a piecewise cubic spline fit (ref. 29). Input parameters ISPP and ISPS are provided to allow different subsets of the input coordinate points to be used in calculating the spline fit. These input parameters can be very helpful in obtaining a spline fit with smoothly varying curvatures. The interpolated coordinate points appear in the output twice, once with respect to coordinate system 2 (fig. 13(b)) and once with respect to the coordinate system of figure 12.

Many of the FORTRAN variable names in ARBBP are the same ones used in reference 29 for the same quantity. Slight differences exist in some cases, however, because coordinate system 2 (fig. 13(b)) is used as the basic coordinate system in ARBBP while coordinate system 1 was the basic coordinate system used in reference 29. Major differences in variable definitions occur when a fictitious leading edge circle (fig. 46) is necessary, although analogous definitions are used.

The arrangement of the input data cards is shown in figure 48. The input variables are defined below.

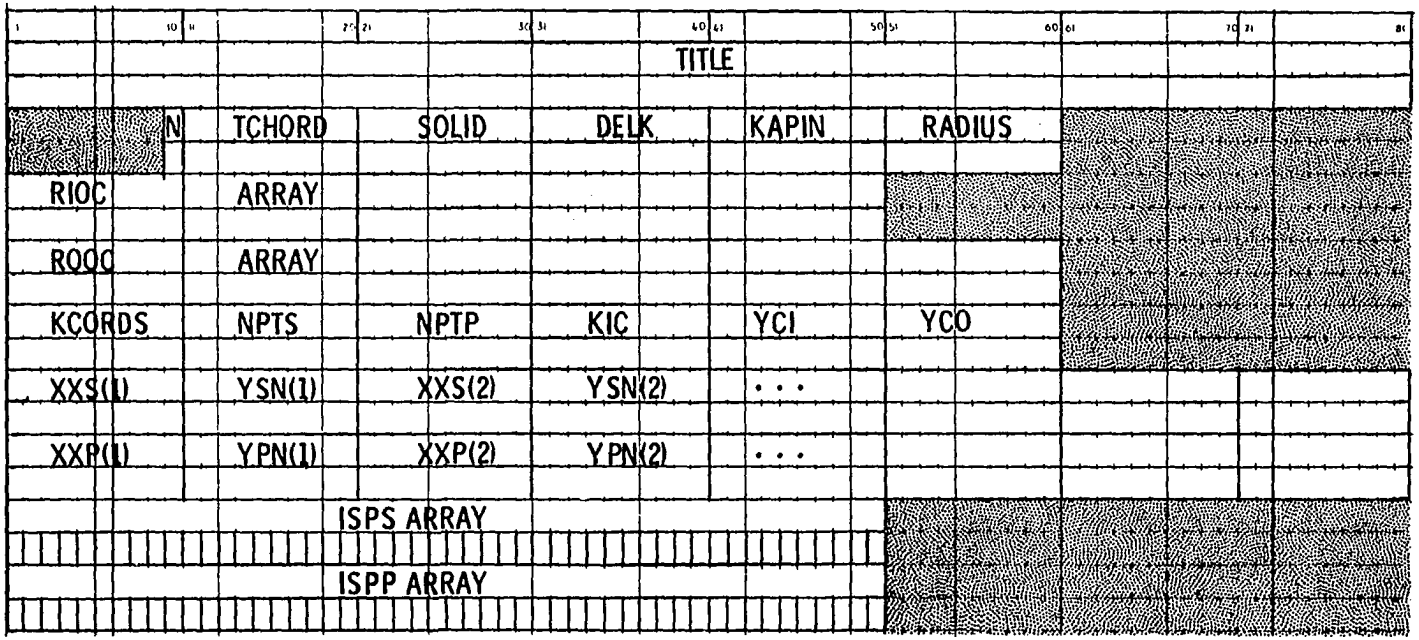

Figure 48. - ARBBP input data.

DELK camber angle, ϕ°, deg

ISPP, ISPS spline fit option parameter: if ISPP(K) = 0 (ISPS(K) = 0), the Kth pressure (suction) surface coordinate point is not used in the spline fit; if ISPP(K) = 1 (ISPS(K) = 1), the Kth pressure (suction) surface coordinate point is used in the spline fit

KAPIN blade inlet angle in staggered position, κ_1 (fig. 3), deg

KCORDS input coordinate system option parameters,

1: coordinate system 1, dimensional coordinates

2: coordinate system 1, coordinates normalized by chord

3: coordinate system 2, dimensional coordinates

4: coordinate system 2, coordinates normalized by chord

5: coordinate system 3, dimensional coordinates

6: coordinate system 3, coordinates normalized by chord

KIC inlet blade angle with respect to chord line (fig. 13), deg

N number of blade segments comprising the blade section, must be 1

NPTP number of (XXP, YPN) pressure surface coordinate pairs to be read as input

NPTS number of (XXS, YSN) suction surface coordinate pairs to be read as input

RADIUS radius from axis of rotation to cylindrical surface containing blade profile, meters (RADIUS is only used to convert tangential coordinates, $R\theta$, to θ-coordinates in radians)

RIOC ratio of leading edge radius to chord

ROOC ratio of trailing edge radius to chord

SOLID solidity, σ

TCHORD chord, c (figs. 13 and 42), meters

TITLE identifying information

XXP coordinate of pressure surface parallel to chord (fig. 13), meters

XXS coordinate of suction surface parallel to chord (fig. 13), meters

YCI dimensional distance between chord line and the center of the leading edge circle (fig. 45), meters

YCO dimensional distance between chord line and the center of the trailing edge circle (fig. 44), meters

YPN coordinate of pressure surface normal to chord (fig. 13), meters

YSN coordinate of suction surface normal to chord (fig. 13), meters

Output format for ARBBP is very similar to the output of reference 29 with some additions and a few deletions. The first two pages list the input data using the variable names as titles. These variables were defined above and will not be repeated. The next page contains the input coordinate arrays in dimensional form. The next four pages contain intermediate results from the tangency point calculations. The headings are variable names which are defined at the beginning of the listing of subroutine ANGITR.

If a fictitious leading edge circle is defined, the next two pages will contain intermediate results from calculations which determine the center and radius of the fictitious circle. The locations of the point which will fall on the origin in figure 46 and the tangency points on the fictitious circle are also given (with respect to coordinate system 2).

The tangency points are located so that the tangent angles in figure 46 are $\pm 88^{\circ}$. The headings on these two pages are variables which are defined on comment cards in the listings of subroutines ANGSER and LEDGE.

The next page of output contains the input coordinate points transformed into the coordinate system used in TSONIC and MAGNFY. They are referenced either to the coordinate system of figure 12 or figure 46. The headings are variable names which are defined on comment cards in subroutine BLDCD1.

The next four pages list overall blade parameters and information about the blade in coordinate system 2 (fig. 13(b)). In case a fictitious leading edge circle has been defined, the XX-axis of coordinate system 2 passes through its center rather than the center of the original leading edge circle. Some of the input quantities defined earlier are repeated under the heading of overall blade parameters. The other headings are defined below and in figure 49.

CHORD distance between extreme left and right edges of blade in coordinate system 2 (fig. 49), meters

CURVIP pressure surface curvature

CURVIS suction surface curvature

KIC angle between the tangent to the mean camber line at the leading edge and the line connecting the edge circle centers (fig. 13(b)), deg

KIP slope of the pressure surface at the leading edge tangency point (fig. 49), deg

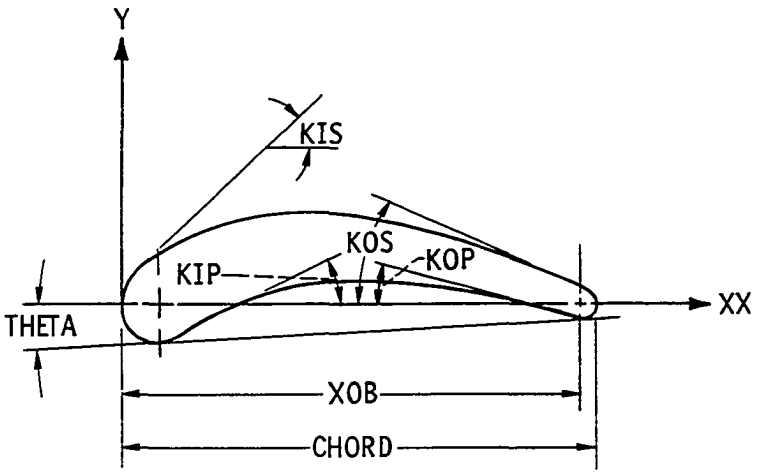

Figure 49. - Output variables in coordinate system 2.

KIS slope of the suction surface at the leading edge tangency point (fig. 49), deg

KOC angle between the tangent to the mean camber line at the trailing edge and the line connecting the edge circle centers (fig. 13(b)), deg

KOP slope of the pressure surface at the trailing edge tangency point (fig. 49), deg

KOS slope of the suction surface at the trailing edge tangency point (fig. 49), deg

PHIC camber angle, ϕ^{o}, deg

PHIP pressure surface camber angle, KIP + KOP, deg

PHIS suction surface camber angle, KIS + KOS, deg

PITCH blade pitch, s, meters

RI radius of either the original or the fictitious leading edge circle, meters

RI1 radius of a fictitious arc from the origin of figure 46 to the tangency point on the suction surface (see also fig. 12), meters

RI2 radius of a fictitious arc from the origin of figure 46 to the tangency point on the pressure surface (see also fig. 12), meters

RO radius of the trailing edge circle, meters

THETA angle between line connecting edge circle centers and line tangent to edge circles (fig. 49), deg

XP XX-coordinate of interpolated point on pressure surface, coordinate system 2, meters

XS XX-coordinate of interpolated point on suction surface, coordinate system 2, meters

YP interpolated Y-coordinate of point on pressure surface, coordinate system 2, meters

YS interpolated Y-coordinate of point on suction surface, coordinate system 2, meters

The last four pages of output are intended for direct use as input for the inviscid flow programs. The output headings are defined graphically in figures 50 and 51 which were adapted from figures 15 and 16 of reference 28. Quantities required as input for TSONIC and MAGNFY are defined below.

BETIP (BETOP) angle with respect to z-direction at tangent point of leading (trailing) edge radius with pressure surface (fig. 51), deg

BETIS (BETOS) angle with respect to z-direction at tangent point of leading (trailing) edge radius with suction surface (fig. 51), deg

MCHORD length of blade in z-direction (figs. 50 and 51), meters

MSPP (MSPS) z-coordinates of points on the pressure (suction) surface at which blade coordinates (THSPP and THSPS) are given (fig. 51), meters

RI (RO) leading (trailing) edge radius (fig. 51), meters

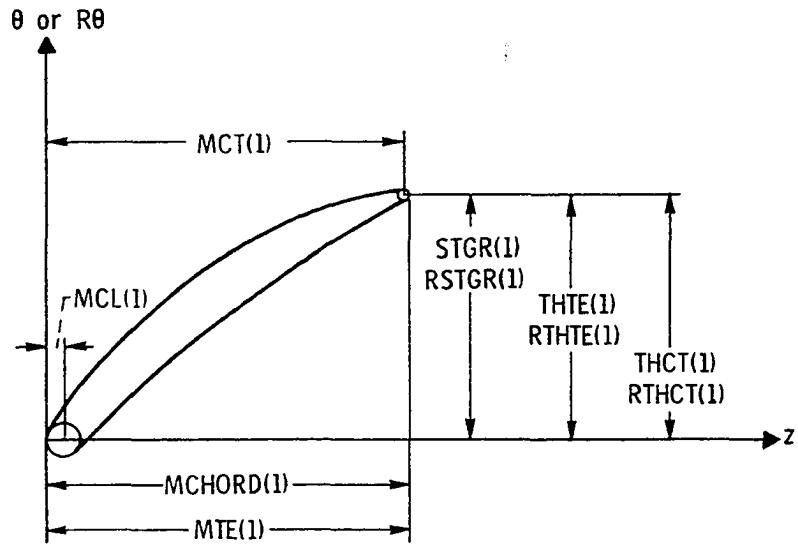

Figure 50. - Blade section output variables used for inviscid flow programs (refs. 19, 21, 23, and 24).

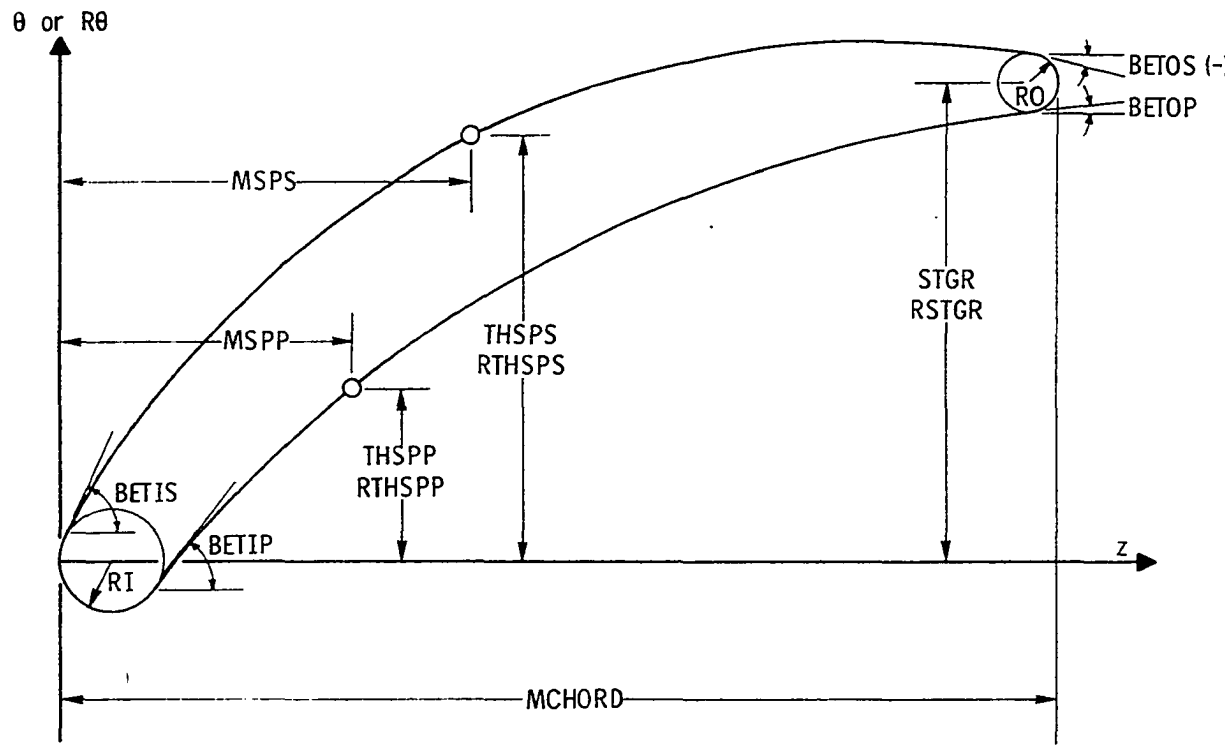

Figure 51. - Blade segment output variables used for inviscid flow programs (refs. 19, 21, 23, and 24).

THSPP (THSPS) θ-coordinates of points on the pressure (suction) surface (fig. 51), meters

A complete listing of the ARBBP program follows.

```
      COMMON/INPUT/N,TCHORD,SOLID,DELK,KAPIN,RADIUS,
     1 RIOC(5),ROOC(5),TITLE(12)
      COMMON/OUTPUT/CHORD(5),GAMR(5),PHIC(5),PITCH
      COMMON/COM1/RI(1),RO(1),THETA(1),X1(1),Y1(1),X2(1),Y2(1),
     1 KIC(1),KOC(1),KIS(1),KOS(1),PHIS(1),KIP(1),KOP(1),PHIP(1),
     2 NDEL(1),XX(1,300),YS(1,300),YP(1,300)
      COMMON/COM2/GAMS,MCHORD(1),RSTGR(1),STGR(1),MLE(1),RTHLE(1),
     1THLE(1),MTE(1),RTHTE(1),THTE(1),MCL(1),RTHCL(1),THCL(1),MCT(1),
     1RTHCT(1),THCT(1),BETIS(1),BETOS(1),BETIP(1),BETOP(1),MSPS(1,300),
     1RTHSPS(1,300),THSPS(1,300),MSPP(1,300),RTHSPP(1,300),THSPP(1,300)
      REAL KIC,KOC,KIS,KOS,KIP,KOP,KAPIN
      REAL MLE,MTE,MCL,MCT,MCHORD,MSPS,MSPP
   10 CALL BLDCD1
      CALL IFINPT
      GO TO 10
      END



      SUBROUTINE ANGIT(XC1,XC2,XC3,YC1,YC2,YC3,X1ST,ER,XCTR,SIGN,
     1 ANGANS,XCIR,YCIR,J)
C
C  THIS SUBPROGRAM CALCULATES THE SURFACE-EDGE CIRCLE TRANSITION
C  POINTS BY FITTING A PARABOLA TO THE FIRST OR LAST THREE POINTS
C  AND SOLVING FOR THE POINT HAVING EQUAL SLOPES ON THE
C  PARABOLA AND THE EDGE CIRCLE.
C  THE TANGENT ANGLE AT THE TRANSITION POINT IS
C  OBTAINED BY DIFFERENTIATING THE EQUATION OF THE EDGE CIRCLE.
C
C
C
C  A,B,C        COEFFICIENTS OF THE LAGRANGIAN INTERPOLATING
C               POLYNOMIAL FITTING THE SURFACE COORDINATES.
C
C  ANGANS       ANGLE BETWEEN TANGENT AT EDGE CIRCLE-BLADE SURFACE
C               TRANSITION POINT WITH RESPECT TO CHORD LINE THROUGH
C               EDGE CIRCLE CENTERS.
C
C  DYDXC        SLOPE OF TANGENT TO EDGE CIRCLE
C
C  DYDXP        SLOPE OF TANGENT TO PARABOLA FITTED THROUGH
C               THREE BLADE SURFACE POINTS.
C
C  FPS(L)       DIFFERENCE BETWEEN SLOPES ON THE BLADE SURFACE
C               AND EDGE CIRCLE AT ESTIMATED XX LOCATION OF
C               TRANSITION POINT.
C
C  ER           RADIUS OF EDGE CIRCLE.
```

```
C   FL          VARIABLE DIVISOR USED TO ADJUST X(I) WHEN IT FALLS
C               OUTSIDE THE EDGE CIRCLE.
C
C   X(I)        ESTIMATED XX LOCATION OF SURFACE-EDGE CIRCLE
C               TRANSITION POINT.
C
C   XCIR        XX LOCATION OF SURFACE-EDGE CIRCLE TRANSITION POINT.
C
C   XCTR        XX LOCATION OF EDGE CIRCLE CENTER
C
C   XC1,XC2,    ABSCISSAS OF THREE BLADE SURFACE POINTS NEAREST TO THE
C   XC3         EDGE CIRCLE.
C
C   XNXT        VALUE OF XX OBTAINED BY INTERPOLATION USING EPS=0.
C
C   XX(J,K)     COORDINATES ALONG LINE TANGENT TO EDGE CIRCLES
C
C   XIST        INITIAL GUESS AT XX LOCATION OF SURFACE-EDGE
C               TRANSITION POINT
C
C   YCIR        ORDINATE OF EDGE CIRCLE AT X(I).
C
C   YC1,YC2,    ORDINATES OF THREE BLADE SURFACE POINTS NEAREST TO THE
C   YC3         EDGE CIRCLE.
C
C   YPAR        ORDINATE OF BLADE SURFACE AT X(I).
C
C
      COMMON/INOUT/ II,IO
      DIMENSION EPS(2),ER(1),X(2)
C
C   CALCULATE SURFACE PARABOLA COEFFICIENTS
C
      A = YC1/((XC1-XC2)*(XC1-XC3))+YC2/((XC2-XC1)*(XC2-XC3))
     1 +YC3/((XC3-XC1) *(XC3-XC2))
      B=-YC1*(XC2+XC3)/((XC1-XC2)*(XC1-XC3))
     1  -YC2*(XC1+XC3)/((XC2-XC1)*(XC2-XC3))
     2 -YC3*(XC1+XC2)/((XC3-XC1)*(XC3-XC2))
      C=YC1*XC2*XC3/((XC1-XC2)*(XC1-XC3))
     1 +YC2*XC1*XC3/((XC2-XC1)*(XC2-XC3))
     2 +YC3*XC1*XC2/((XC3-XC1)*(XC3-XC2))
C
C   BEGIN TRANSITION LOCATION ITERATION
C
      WRITE(IO,5000)
      X(2)= XIST
      DO 200  I=1,20
      X(1)= X(2)-.04*ER(J)
      DO 100  L=1,2
      FL=23-I-L
      IF(ABS(X(L)-XCTR).GT.ER(J)) X(L)=XCTR+ER(J)/FL
      YCIR=SIGN*SQRT(ER(J)*ER(J)-(X(L)-XCTR)*(X(L)-XCTR))
      DYDXC=-SIGN*(X(L)-XCTR)/SQRT(ER(J)*ER(J)-(X(L)-XCTR)
     1 *(X(L)-XCTR))
      DYDXP=2.*A*X(L)+B
      YPAR=A*X(L)*X(L)+B*X(L)+C
      EPS(L)=DYDXP-DYDXC
      WRITE(IO,5010) L,X(L),DYDXP,DYDXC,EPS(L),YPAR,YCIR
      IF(ABS(EPS(L)) .LE..000001) GO TO 300
  100 CONTINUE
C
C   INTERPOLATE FOR XX AT WHICH EPS=0.
```

```
      CALL FITLIN (XNXT,0.,X,EPS)
      WRITE(10,5030) XNXT
      IF (XNXT.GE.0.) GO TO 200
      X1ST=X1ST/4.
      XNXT=X1ST
  200 X(2)= XNXT
      WRITE(10,5020)
  300 ANGANS=ATAN(DYDXP)
      XCIR=X(L)
      RETURN
 5000 FORMAT(///9X,1HL,8X,4HX(L),7X,5HDYDXP,7X,5HDYDXC
     1 ,9X,3HEPS,7X,5H YPAR,7X,5H YCIR/)
 5010 FORMAT(I10,6F12.8)
 5020 FORMAT(//10X,44HTRANSITION POINT ITERATION DID NOT CONVERGE
     1 ,11HIN 20 TRIES//)
 5030 FORMAT(/10X,6H XNXT=,F11.8)
 5050 FORMAT(/5X,6HX1ST= ,F11.8,3X,7HER(J)= ,F11.8,3X,6HX(1)= ,F11.8,3X,
     1 6HX(2)= ,F11.8/)
 5060 FORMAT(/10X,3HA= ,F10.7,3X,3HB= ,F10.7,3X,3HC= ,F10.7,3X,6HXCTR= ,
     1 F10.7/)
      END



      SUBROUTINE ANGSER(XANS,YANS,ANGVAL,CURANS)
C
C  THIS SUBROUTINE CALCULATES THE COORDINATES, (XANS,YANS),
C  OF THE POINT ON THE SURFACE DESCRIBED BY (XSPS,YSPS)
C  WHERE THE SURFACE TANGENT ANGLE EQUALS ANGVAL.  THE
C  CURVATURE OF THE SURFACE IS ALSO COMPUTED AT THAT POINT.
C
C  ANGVAL      SPECIFIED SURFACE ANGLE, RAD.
C
C
C  CURANS      CURVATURE AT XANS.
C
C  CTDMN       FIRST DERIVATIVE OF SPLINE CURVE AT XNEW.
C
C  CYDXS(L)    FIRST DERIVATIVE OF SUCTION SURFACE AT SPLINE POINT.
C
C  EMNEW       SECOND DERIVATIVE OF SPLINE CURVE AT XNEW.
C
C  FPSL(I)     DIFFERENCE BETWEEN DESIRED SURFACE SLOPE AND
C              THE SURFACE SLOPE AT XCR(I).
C
C  FDERIV      TANGENT OF ANGVAL.
C
C  XANS        X-COORDINATE WHERE THE SURFACE ANGLE IS EQUAL
C              TO ANGVAL.
C
C  XCR(I)      ESTIMATED XXS-LOCATION WHERE THE SURFACE ANGLE
C              IS EQUAL TO ANGVAL.
C
C  XNEW        NEXT BEST ESTIMATE FOR XXS-LOCATION WHERE THE
C              SURFACE ANGLE IS EQUAL TO ANGVAL.
C
C  YANS        ORDINATE AT XANS.
C
C  YNEW        ORDINATE OF SPLINE CURVE AT XNEW.
C
```

```
      COMMON/BLOK A/ GAMS,PI,RI1,RI2
      COMMON/COORD/ CURVIP(100),CURVIS(100),CURVP(50),CURVS(50),
     1 DYDXP(20),DYDXS(20),EMP(20),EMP1(20),EMS(20),EMS1(20),RTHP(50),
     2 RTHS(50),TP(50),TS(50),XMP(50),XMS(50),XP(100),XS(100),XSPP(100),
     3 XSPS(100),XXP(50),XXS(50),YPI(50),YPN(50),YSI(50),YSN(50),
     4 YSPP(100),YSPS(100)
      COMMON/INOUT/ II,IO
      COMMON/INTEGR/ KROT,LMAXP,LMAXS,NDELJ,NDELJP,NDELJS,NPTP,
     1 NPTPP,NPTS,NPTSS
      DIMENSION CURANS(1),DTDMN(1),EPSL(2),XCR(2),XNEW(1),YNEW(1)
C
C
C  SEARCH FOR SPLINE POINTS WHOSE SLOPES BRACKET ANGVAL
C
      FDERIV= TAN(ANGVAL)
      DO 800  L=2,LMAXS
      IF(FDERIV.GT.DYDXS(L))   GO TO 900
  800 CONTINUE
  900 XCR(1)= XSPS(L-1)
      XCR(2)= XSPS(L)
      EPSL(1)= FDERIV-DYDXS(L-1)
      EPSL(2)= FDERIV-DYDXS(L)
      DO 1000  I=1,2
      IF(ABS(EPSL(I)) .LE. .00001) GO TO 1200
 1000 CONTINUE
      WRITE(IO,9100)
      DO 1100 KL=1,25
      WRITE(IO,9200) (KL,XCR(I),EPSL(I),I=1,2)
C
C  INTERPOLATE FOR NEW BEST ESTIMATE OF XANS
      CALL FITLN (XNEW,0.,XCR,EPSL)
      IF(XNEW(1).LE.XSPS(L-1)) XNEW(1)=(XCR(1)+XSPS(L-1))/2.
      IF(XNEW(1).GT.XSPS(L)) XNEW(1)=(XCR(1)+XSPS(L))/2.
C
C  INTERPOLATE SPLINE CURVE FIT FOR SLOPE AT XNEW
      CALL SPLN (XNEW,YNEW,XSPS,YSPS,EMS,DTDMN,CURANS,
     1 LMAXS,1)
      WRITE(IO,9300) XNEW,YNEW,FDERIV,DTDMN
      IF(ABS(FDERIV-DTDMN(1)) .LE. .00001) GO TO 1400
      XCR(2)= XCR(1)
      XCR(1)= XNEW(1)
      EPSL(2)= EPSL(1)
 1100 EPSL(1)= FDERIV-DTDMN(1)
      WRITE(IO,9400)
      STOP
 1200 XANS= XCR(I)
      IF(I .EQ. 2)  GO TO 1300
      YANS= YSPS(L-1)
      CURANS(1)= CURVIS(L-1)
      RETURN
 1300 YANS= YSPS(L)
      CURANS(1)= CURVIS(L)
      RETURN
 1400 XANS= XNEW(1)
      YANS=YNEW(1)
      RETURN
 9100 FORMAT(17X,3H KL,9X,4H XCR,8X,5H EPSL//)
 9200 FORMAT (11X,I10,2F13.8)
 9300 FORMAT(10X,6H XNEW=,F10.7,7H  YNEW=,F10.7,9H  FDERIV=,F10.7,
     1 8H  DTDMN=,F10.7//)
  400 FORMAT(////,20X,23H FDERIV CALCULATION DID,
     1 31H NOT CONVERGE IN 25 ITERATIONS.)
      END
```

```
      SUBROUTINE BLDCD1
C
C
C   THIS SUBPROGRAM CALCULATES BLADE SURFACE COORDINATES WITH RESPECT
C   TO A CHORD LINE THROUGH THE CENTERS OF THE LEADING AND TRAILING EDGE
C   CIRCLES AND A LINE NORMAL TO THE CHORD AND TANGENT TO THE LEADING
C   EDGE CIRCLE.  BLADE SURFACE TANGENT ANGLES ARE ALSO OBTAINED AT
C   THE POINTS WHERE THE SURFACES ARE TANGENT TO THE EDGE CIRCLES.
C   PERMISSIBLE BLADE PROFILES MUST HAVE CIRCULAR OR SHARP EDGES.
C   COORDINATE SYSTEMS FOR INPUT BLADE COORDINATES MUST HAVE ONE AXIS
C   PASSING THROUGH THE CENTERS OF THE EDGE CIRCLES, TANGENT TO THE
C   EDGE CIRCLES, OR PASSING THROUGH THE INTERSECTIONS OF THE
C   MEAN CAMBER LINE AND THE EDGE CIRCLES.  INPUT COORDINATES MAY
C   BE NORMALIZED BY THE CHORD LENGTH IF DESIRED (SEE DEFINITION
C   OF KCORDS).
C
C
C   ANGANS      ANGLE OF SURFACE TANGENT AT LEADING OR TRAILING
C               EDGE TRANSITION POINTS
C
C   CHORD(J)    LENGTH OF CHORD LINE THROUGH EDGE CIRCLE CENTERS.
C
C   CHRD        LENGTH OF CHORD LINE TANGENT TO EDGE CIRCLES
C
C   CURVIP      CURVATURE AT INTERPOLATED POINTS ON PRESSURE SURFACE.
C
C   CURVIS      CURVATURE AT INTERPOLATED POINTS ON SUCTION SURFACE.
C
C   CURVP       CURVATURE AT INPUT POINTS ON PRESSURE SURFACE.
C
C   CURVS       CURVATURE AT INPUT POINTS ON SUCTION SURFACE.
C
C   DYDXP(L)    FIRST DERIVATIVE OF PRESSURE SURFACE AT SPLINE POINT.
C
C   DYDXS(L)    FIRST DERIVATIVE OF SUCTION SURFACE AT SPLINE POINT.
C
C   D2YDXP      SECOND DERIVATIVE ON PRESSURE SURFACE.
C
C   D2YDXS      SECOND DERIVATIVE ON SUCTION SURFACE.
C
C   EMP         SECOND DERIVATIVE ON PRESSURE SURFACE AT SPLINE POINT
C               OBTAINED USING A DOUBLE SPLINE FIT PROCEDURE.
C
C   EMS         SECOND DERIVATIVE ON SUCTION SURFACE AT SPLINE POINT
C               OBTAINED USING A DOUBLE SPLINE FIT PROCEDURE.
C
C   EMP1        SECOND DERIVATIVE ON PRESSURE SURFACE AT SPLINE POINT
C               OBTAINED USING A SINGLE SPLINE FIT PROCEDURE.
C
C   EMS1        SECOND DERIVATIVE ON SUCTION SURFACE AT SPLINE POINT
C               OBTAINED USING A SINGLE SPLINE FIT PROCEDURE.
C
C   ER(J)       RADIUS OF EDGE CIRCLE
C
C   FKISA       ANGLE OF SUCTION SURFACE AT LEADING EDGE
C               TRANSITION POINT WITH RESPECT TO THE CHORD
C               LINE THROUGH THE EDGE CIRCLE CENTERS.
C
C   FKIPA       ANGLE OF PRESSURE SURFACE AT LEADING EDGE
C               TRANSITION POINT WITH RESPECT TO THE CHORD
C               LINE THROUGH THE EDGE CIRCLE CENTERS.
C
```

```
C   FKOPA       ANGLE OF PRESSURE SURFACE AT TRAILING EDGE
C               TRANSITION POINT WITH RESPECT TO THE CHORD
C               LINE THROUGH THE EDGE CIRCLE CENTERS.
C
C   FKOSA       ANGLE OF SUCTION SURFACE AT TRAILING EDGE
C               TRANSITION POINT WITH RESPECT TO THE CHORD
C               LINE THROUGH THE EDGE CIRCLE CENTERS.
C
C   GAMS        BLADE SETTING ANGLE PLUS ROTANG.
C
C
C   II          CARD READER REFERENCE NUMBER
C
C   IO          LINE PRINTER REFERENCE NUMBER
C
C   ISPP(K).    OPTION PARAMETERS PERMITTING CHOICE OF INPUT
C   ISPS(K)     COORDINATES TO BE USED IN SPLINE FIT INTERPOLATION.
C               ISPP(K)=0 = KTH COORDINATE ON PRESSURE SURFACE
C                         NOT USED
C                       =1 = KTH COORDINATE ON PRESSURE SURFACE
C                         IS USED
C               ISPS(K)=0 = KTH COORDINATE ON SUCTION SURFACE
C                         NOT USED
C                       =1 = KTH COORDINATE ON SUCTION SURFACE
C                         IS USED
C
C   KCORDS      1= DIMENSIONAL COORDINATES FROM LINE TANGENT TO EDGE CIRCLES
C               2= NONDIMENSIONAL COORDINATES FROM LINE TANGENT TO EDGE CIRCLES
C               3= DIMENSIONAL COORDINATES FROM LINE THRU EDGE CIRCLE CENTERS
C               4= NONDIMENSIONAL COORDINATES FROM LINE THRU EDGE CIRCLE CENTERS
C               5= DIMENSIONAL COORDINATES FROM LINE THROUGH
C                  INTERSECTIONS OF EDGE CIRCLES AND MEAN CAMBER
C                  LINES.
C               6= NONDIMENSIONAL COORDINATES FROM LINE
C                  THROUGH INTERSECTIONS OF MEAN CAMBER LINE
C                  AND EDGE CIRCLES.
C               (COORDINATES NORMALIZED BY THE CHORD LENGTH)
C
C   KIC(J)      INLET BLADE ANGLE WITH RESPECT TO CHORD LINE, DEG
C
C   KROT        0= IF SUCTION SURFACE DOES NOT EXTEND UPSTREAM OF
C                  THE LEADING EDGE CIRCLE.
C               1= IF SUCTION DOES EXTEND UPSTREAM OF THE
C                  LEADING EDGE CIRCLE.
C
C   LMAXS       NUMBER OF SUCTION SURFACE COORDINATES USED
C               IN SPLINE FIT INTERPOLATION.
C
C   LMAXP       NUMBER OF PRESSURE SURFACE COORDINATES USED
C               IN SPLINE FIT INTERPOLATION.
C
C   NPTP        NUMBER OF (XXPN,YPN) PRESSURE SURFACE COORDINATE PAIRS TO BE READ
C
C   NPTPM1      NPTP MINUS 1.
C
C   NPTS        NUMBER OF (XXSN,YSN) SUCTION SURFACE COORDINATE PAIRS TO BE READ
C
C   NPTSM1      NPTS MINUS 1.
C
C   PI          THE CONSTANT 3.14159265.
C
```

```
C  RANG          ANGLE BETWEEN LINE CONNECTING EDGE CIRCLE CENTERS
C                AND CHORD LINE TANGENT TO EDGE CIRCLES.
C
C  RCTANG        ANGLE BETWEEN INPUT CHORD LINE AND CHORD LINE
C                THROUGH CENTERS OF EDGE CIRCLES.
C
C  RTHP          PRESSURE SURFACE R X THETA COORDINATE IN IDEAL
C                FLOW PROGRAM COORDINATE SYSTEM.
C
C  RTHS          SUCTION SURFACE R X THETA COORDINATE IN IDEAL
C                FLOW PROGRAM COORDINATE SYSTEM.
C
C  SIGN          +1 ON SUCTION SURFACE. -1. ON PRESSURE SURFACE
C
C  TKIP          TANGENT TO THE XSPP-YSPP CURVE AT THE
C                FIRST XSPP POINT.
C
C  TKOS          TANGENT TO THE XSPS-YSPS CURVE AT THE
C                LAST XSPS POINT.
C
C  TKIS          TANGENT TO THE XSPS-YSPS CURVE AT THE
C                FIRST XSPS POINT.
C
C  TKOP          TANGENT TO THE XSPP-YSPP CURVE AT THE
C                LAST XSPP POINT.
C
C  TP(K)         PRESSURE SURFACE THETA COORDINATE IN IDEAL FLOW
C                PROGRAM COORDINATE SYSTEM.
C
C  TS(K)         SUCTION SURFACE THETA COORDINATE IN IDEAL FLOW
C                PROGRAM COORDINATE SYSTEM.
C
C  XCI(XCO)      DISTANCE BETWEEN THE END OF THE CHORD LINE AND A LINE
C                NORMAL TO THE CHORD PASSING THROUGH THE CENTER OF THE
C                LEADING (TRAILING) EDGE CIRCLE.
C
C  XC1.XC2.      CHORDWISE POSITION OF SURFACE POINTS
C  XC3
C
C  XMP(K)        PRESSURE SURFACE MERIDIONAL COORDINATE IN
C                INVISCID FLOW PROGRAM COORDINATE SYSTEM.
C
C  XMS(K)        SUCTION SURFACE MERIDIONAL COORDINATE IN
C                INVISCID FLOW PROGRAM COORDINATE SYSTEM.
C
C  XSPP(K)       INPUT COORDINATES USED IN SPLINE INTERPOLATION
C                ON PRESSURE SURFACE.
C
C  XSPS(K)       INPUT COORDINATES USED IN SPLINE INTERPOLATION
C                ON SUCTION SURFACE.
C
C  XXOC(K)       BLADE COORDINATE ALONG CHORD NORMALIZED BY
C                CHORD LENGTH.
C
C  XXP(K).       COORDINATE OF PRESSURE SURFACE POINT PARALLEL TO CHORD
C  XXPN(K)
C
C  XXS(K).       COORDINATE OF SUCTION SURFACE POINT PARALLEL TO CHORD
C  XXSN(K)
C
C  YCI           DIMENSIONAL DISTANCE BETWEEN CHORD LINE AND
C                CENTER OF LEADING EDGE CIRCLE.
```

```
C   YCO          DIMENSIONAL DISTANCE BETWEEN CHORD LINE AND
C                CENTER OF TRAILING EDGE CIRCLE.
C
C   YC1,YC2,     DISTANCE FROM THE CHORD OF SURFACE POINTS
C   YC3
C
C   YMAX         APPROXIMATE MAXIMUM ORDINATE OF SUCTION SURFACE
C                WITH RESPECT TO CHORD LINE.
C
C   YPN(K)       COORDINATE OF PRESSURE SURFACE POINT NORMAL TO CHORD
C
C   YPOC(K)      DISTANCE FROM CHORD LINE TO PRESSURE SURFACE
C                NORMALIZED BY CHORD LENGTH.  CHORD LINE IS TANGENT
C
C   YSN(K)       COORDINATE OF SUCTION SURFACE POINT NORMAL TO CHORD
C
C   YSPP(K)      INPUT COORDINATES USED IN SPLINE INTERPOLATION
C                ON PRESSURE SURFACE.
C
C   YSPS(K)      INPUT COORDINATES USED IN SPLINE INTERPOLATION
C                ON SUCTION SURFACE.
C
C   YSOC(K)      DISTANCE FROM CHORD LINE TO SUCTION SURFACE
C                NORMALIZED BY CHORD LENGTH.
C
C
      COMMON/INPUT/N,TCHORD,SOLID,DELK,KAPIN,RADIUS,
     1 RIOC(5),ROOC(5),TITLE(12)
      COMMON/INADD/ YC1,YCO
       COMMON/OUTPUT/CHORD(5),GAMR(5),PHIC(5),PITCH
      COMMON/COM1/RI(1),RO(1),THETA(1),XL(1),YL(1),X2(1),Y2(1),
     1 KIC(1),KOC(1),KIS(1),KOS(1),PHIS(1),KIP(1),KOP(1),PHIP(1),
     2 NDEL(1),XX(1,300),YS(1,300),YP(1,300)
      COMMON/BLOK A/ GAMS,PI,RI1,RI2
      COMMON/COORD/ CURVIP(100),CURVIS(100),CURVP(50),CURVS(50),
     1 DYDXP(20),DYDXS(20),EMP(20),EMP1(20),EMS(20),EMS1(20),RTHP(50),
     2 RTHS(50),TP(50),TS(50),XMP(50),XMS(50),XP(100),XS(100),XSPP(100),
     3 XSPS(100),XXP(50),XXS(50),YPI(50),YPN(50),YSI(50),YSN(50),
     4 YSPP(100),YSPS(100)
      COMMON/INOUT/ II,IO
      COMMON/INTEGR/ KROT,LMAXP,LMAXS,NDELJ,NDELJP,NDELJS,NPTP,
     1 NPTPP,NPTS,NPTSS
      COMMON/OPT/ ISPP(50),ISPS(50),KCORDS
      DIMENSION                    XXOC(300),YPOC(300),YSOC(300),
     1 DYDXIP(300),DYDXIS(300)
      REAL KIC,KOC,KIS,KOS,KIP,KOP,KAPIN
C
C
      CALL INPUT1
C
C   INITIALIZE VARIABLES AND CONVERT UNITS
C
      J=1
      DELK = DELK/57.295779
      KIC(J)=KIC(J)/57.295779
      PITCH= TCHORD/SOLID
      CHRD=TCHORD
      CHORD(J) = TCHORD
      KROT=0
      PI=3.14159265
      RI(J) = RIOC(J) * TCHORD
      RO(J) = ROOC(J) * TCHORD
```

```
C  CHECK INPUT BLADE COORDINATE SYSTEM
C
      IF ((KCORDS.EQ.2).OR.(KCORDS.EQ.4).OR.(KCORDS.EQ.6)) GO TO 300
      IF(KCORDS.EQ.3) GO TO 920
      IF (KCORDS.EQ.5) GO TO 650
      GO TO 730
C
C  CONVERT NONDIMENSIONAL COORDINATES TO DIMENSIONAL COORDINATES
C
  300 DO 500  K=1,NPTS
      XXS(K) = TCHORD*XXS(K)
  500 YSN(K) = TCHORD*YSN(K)
      DO 600  K=1,NPTP
      XXP(K) = TCHORD*XXP(K)
  600 YPN(K) = TCHORD*YPN(K)
      WRITE(IO,4045)
      WRITE(IO,4047) (K,XXS(K),YSN(K),K=1,NPTS)
      WRITE(IO,4060) (K,XXP(K),YPN(K),K=1,NPTP)
      IF (KCORDS.EQ.2) GO TO 730
      IF(KCORDS.EQ.4) GO TO 920
C
C  MAP COORDINATES INTO COORDINATE SYSTEM WITH ONE AXIS
C  THROUGH THE EDGE CENTERS AND THE OTHER AXIS TANGENT TO
C  THE LEADING EDGE.
C
  650 XCI=SQRT(RI(J)*RI(J)-YCI*YCI)
  660 XCO= SQRT(RO(J)*RC(J)-YCO*YCO)
      ROTANG=ATAN((YCI-YCC)/(TCHORD-XCI-XCO))
      CHORD(J)= (TCHORD-XCI-XCO)/COS(ROTANG)+RI(J)+RC(J)
      KIC(J)=KIC(J)+ROTANG
      DO 700 K=1,NPTS
      XXS(K)=(XXS(K)-XCI)*COS(ROTANG)-(YSN(K)-YCI)
     1 *SIN(ROTANG)+RI(J)
  700 YSN(K)=(XXS(K)-XCI)*SIN(ROTANG)+(YSN(K)-YCI)
     1 *COS(ROTANG)
      DO 720 K=1,NPTP
      XXP(K)=(XXP(K)-XCI)*COS(ROTANG)-(YPN(K)-YCI)
     1 *SIN(ROTANG)+RI(J)
  720 YPN(K)=(XXP(K)-XCI)*SIN(ROTANG)+(YPN(K)-YCI)
     1 *COS(ROTANG)
      GO TO 920
C
C  MAP COORDINATES INTO COORDINATE SYSTEM WITH ONE AXIS
C  THROUGH THE EDGE CENTERS AND THE OTHER AXIS TANGENT TO
C  THE LEADING EDGE.
C
  730 RANG=ASIN((RI(J)-RO(J))/(CHRD-RI(J)-RC(J)))
      CHORD(J)=(CHRD-RI(J)-RC(J))/COS(RANG)+RI(J)+RO(J)
      KIC(J)=KIC(J)+RANG
      DO 840 K=1,NPTS
      XXS(K)=(XXS(K)-RI(J))*COS(RANG)-(YSN(K)-RI(J))*SIN(RANG)+RI(J)
  840 YSN(K)=(XXS(K)-RI(J))*SIN(RANG)+(YSN(K)-RI(J))*COS(RANG)
      DO 860 K=1,NPTP
      XXP(K)=(XXP(K)-RI(J))*COS(RANG)-(YPN(K)-RI(J))*SIN(RANG)+RI(J)
  860 YPN(K)=(XXP(K)-RI(J))*SIN(RANG)+(YPN(K)-RI(J))*COS(RANG)
C
C  INITIALIZATION OF VARIABLES FOR SPECIAL CASE N=1
C
  920 PHIC(J) = DELK
      GAMR(J) = 0.
      THETA(J) = ATAN((RI(J)-RO(J))/(CHORD(J)-RI(J)-RC(J)))
      X1(J) = 0.
```

```
      Y1(J) = 0.
      X2(J)=CHORD(J)
      Y2(J)=0.
C
C  CALCULATE BLADE SURFACE TANGENT ANGLES AT LEADING AND TRAILING
C  EDGE TRANSITION POINTS
C
C  SUCTION SURFACE, LEADING EDGE*
C
      X1ST = RI(J) * (1.-SIN(KIC(J)))
      XCTR = RI(J)
      WRITE(IO,6100)
 6100 FORMAT(1H1////10X,26H TANGENCY POINT ITERATIONS///)
      WRITE(IO,6200)
 6200 FORMAT(10X,30H SUCTION SURFACE, LEADING EDGE)
      WRITE(IO,5050) X1ST,RI(J)
      CALL ANGIT(XXS(2),XXS(3),XXS(4),YSN(2),YSN(3),YSN(4),
     1 X1ST,RI,XCTR,1.,FKISA,XXS(1),YSN(1),J)
      KIS(J) =FKISA
C
C  PRESSURE SURFACE, LEADING EDGE*
C
      WRITE(IO,6300)
 6300 FORMAT(1H1////10X,31H PRESSURE SURFACE, LEADING EDGE)
      X1ST = RI(J) * (1.-SIN(KIC(J)))
      CALL ANGIT(XXP(2),XXP(3),XXP(4),YPN(2),YPN(3),YPN(4),
     1 X1ST,RI,XCTR,-1.,FKIPA,XXP(1),YPN(1),J)
      KIP(J) =FKIPA
C
C  SUCTION SURFACE, TRAILING EDGE*
C
      WRITE(IO,6400)
 6400 FORMAT(1H1////10X,31H SUCTION SURFACE, TRAILING EDGE)
      KOC(J) = KIC(J) - DELK
      X1ST= CHORD(J) -RO(J)*(1.-SIN(-KOC(J)))
      XCTR= CHORD(J) - RO(J)
      CALL ANGIT(XXS(NPTS-3),XXS(NPTS-2),XXS(NPTS-1),YSN(NPTS-3),
     1 YSN (NPTS-2),YSN(NPTS-1),X1ST,RO,XCTR,1.,FKOSA,
     2 XXS(NPTS),YSN(NPTS),J)
      KOS(J) =FKOSA
C
C  PRESSURE SURFACE, TRAILING EDGE*
C
      WRITE(IO,6500)
 6500 FORMAT(1H1////10X,32H PRESSURE SURFACE, TRAILING EDGE)
      X1ST=CHORD(J)-RO(J)*(1.-SIN(-KOC(J)))
      CALL ANGIT(XXP(NPTP-3),XXP(NPTP-2),XXP(NPTP-1),YPN(NPTP-3),
     1 YPN(NPTP-2),YPN(NPTP-1),X1ST,RO,XCTR,-1.,FKOPA,
     2 XXP(NPTP),YPN(NPTP),J)
      KOP(J) =FKOPA
C
C  ROTATE COORDINATES INTO INVISCID FLOW PROGRAM COORDINATE SYSTEM.
C
      GAMS=(KAPIN/57.295779)-KIC(J)
      IF((PI/2.-KIS(J)).LT.GAMS) KROT=1
      IF(KROT.EQ.1) GO TO 1400
      DO 1300 K=1,NPTS
      XMS(K)=(XXS(K)-RI(J))*COS(GAMS)-YSN(K)*SIN(GAMS)+RI(J)
      RTHS(K)=(XXS(K)-RI(J))*SIN(GAMS)+YSN(K)*COS(GAMS)
 1300 TS(K)=RTHS(K)/RADIUS
      DO 1320 K=1,NPTP
      XMP(K)=(XXP(K)-RI(J))*COS(GAMS)-YPN(K)*SIN(GAMS)+RI(J)
      RTHP(K)=(XXP(K)-RI(J))*SIN(GAMS)+YPN(K)*COS(GAMS)
```

```
 1320 TP(K)=RTHP(K)/RADIUS
      WRITE(IO,4050) (K,XXS(K),YSN(K),XMS(K),TS(K),RTHS(K),K=1,NPTS)
      WRITE(IO,4065) (K,XXP(K),YPN(K),XMP(K),TP(K),RTHP(K),K=1,NPTP)
C
C  SELECT INPUT COORDINATES TO BE USED IN SPLINE FIT
C
 1400 L=1
      NPTSM1=NPTS-1
      DO 1420 K=2,NPTSM1
      IF(ISPS(K).EQ.0) GO TO 1420
      L=L+1
      XSPS(L)=XXS(K)
      YSPS(L)=YSN(K)
 1420 CONTINUE
      XSPS(1)=XXS(1)
      YSPS(1)=YSN(1)
      LMAXS=L+1
      XSPS(LMAXS)=XXS(NPTS)
      YSPS(LMAXS)=YSN(NPTS)
      L=1
      NPTPM1=NPTP-1
      DO 1430 K=2,NPTPM1
      IF(ISPP(K).EQ.0) GO TO 1430
      L=L+1
      XSPP(L)=XXP(K)
      YSPP(L)=YPN(K)
 1430 CONTINUE
      XSPP(1)=XXP(1)
      YSPP(1)=YPN(1)
      LMAXP=L+1
      XSPP(LMAXP)=XXP(NPTP)
      YSPP(LMAXP)=YPN(NPTP)
C
C  INTERPOLATE FOR ORDINATES AT REGULAR INTERVALS ALONG THE CHORD
C
C  SUCTION SURFACE*
C
      TKIS=TAN(KIS(J))
      TKOS=TAN(KOS(J))
      TKIP=TAN(KIP(J))
      TKOP=TAN(KOP(J))
      CALL SPLFIT (XX,YS,DYDXS,EMS,EMS1,XSPS,YSPS,LMAXS,TKIS,TKOS,
     1 CURVS,CURVIS,DYDXIS,NDEL)
      NDELJ=NDEL(J)
C
C  PRESSURE SURFACE*
C
      CALL SPLFIT (XX,YP,DYDXP,EMP,EMP1,XSPP,YSPP,LMAXP,TKIP,TKOP,
     1 CURVP,CURVIP,DYDXIP,NDEL)
C
C  CHECK FOR POINTS ON SUCTION SURFACE WHICH WILL EXTEND TO
C  THE LEFT OF THE Y-AXIS.
C
      IF((PI/2.-KIP(J)).GT.GAMS) GO TO 1440
      WRITE(IO,5015)
      STOP
 1440 IF(KROT.NE.1) GO TO 1450
      CALL LEDGE
      THETA(J)=ATAN((RI(J)-RC(J))/(X2(J)-RI(J)-RO(J)))
      CHORD(J)=X2(J)
      WRITE(IO,1000)
      WRITE(IO,5040)
```

```
      WRITE(IO,5020) (K,XMS(K),TS(K),RTHS(K),CURVS(K),K=1,NPTSS)
      WRITE (IO,5030) (K,XMP(K),TP(K),RTHP(K),CURVP(K),K=1,NPTPP)
C
C  PREPARE OUTPUT VARIABLES
C
 1450 PHIS(J)=KIS(J)-KOS(J)
      PHIP(J) = KIP(J)-KOP(J)
      IF(KROT.EQ.1) GO TO 1580
      DO 1500   K=1,NDELJ
      XXOC(K) = XX(J,K)/CHORD(J)
      YSOC(K) = YS(J,K)/CHORD(J)
 1500 YPOC(K) = YP(J,K)/CHORD(J)
C
C  PUT OUTPUT ANGLES IN DEGREES
C
 1580 DELK = DELK*57.295779
      DO 1590 J=1,N
      THETA(J)=THETA(J)*57.295779
      PHIC(J) = PHIC(J)*57.295779
      PHIS(J) = PHIS(J)*57.295779
      PHIP(J) = PHIP(J)*57.295779
      KIC(J) = KIC(J)*57.295779
      KIS(J) = KIS(J)*57.295779
      KIP(J) = KIP(J)*57.295779
      KOC(J) = KOC(J)*57.295779
      KOS(J) = KOS(J)*57.295779
 1590 KOP(J) = KOP(J)*57.295779
C
C  CHANGE SIGN OF SELECTED OUTPUTS
C
      DO 1600 J=1,N
      KOS(J)= -KOS(J)
      KOC(J)= -KOC(J)
 1600 KOP(J)= -KOP(J)
C
C  PRINT OUTPUT
C
      WRITE(6,1000)
      IF(KROT.EQ.1) WRITE(IO,5040)
      WRITE(6,1140) N,TCHORD,PITCH,SOLID,DELK,KAPIN
      DO 1620 J=1,N
      WRITE(6,1150) J
      WRITE(6,1160) CHORD(J),RI(J),RO(J),THETA(J)
      WRITE(6,1180) X1(J),Y1(J),X2(J),Y2(J),GAMR(J)
      WRITE(6,1190) PHIS(J),                    KIS(J),KOS(J)
      WRITE(6,1200) PHIC(J),                    KIC(J),KOC(J)
      WRITE(6,1210) PHIP(J),                    KIP(J),KOP(J)
      IF(KROT.EQ.1) GO TO 1700
      NDELJ = NDEL(J)
 1610 WRITE(6,1230) NDEL(J)
 1620 WRITE(6,1240) (K,XX(J,K),YS(J,K),YP(J,K),XXOC(K),YSOC(K),
     1 YPOC(K),CURVIS(K),CURVIP(K),K=1,NDELJ)
      RETURN
 1700 WRITE(IO,5060) RI1,RI2
      WRITE(IO,5070)
      WRITE(IO,5080) (K,XS(K),YS(J,K),CURVIS(K),K=1,NDELJS)
      WRITE(IO,5090)
      WRITE(IO,5080) (K,XP(K),YP(J,K),CURVIP(K),K=1,NDELJP)
      RETURN
```

```
C  FORMAT STATEMENTS
C
 1000 FORMAT(1H1///)
 1140 FORMAT(10X,24HOVERALL BLADE PARAMETERS/14X,1HR,6X,6HTCHORD,7X,
     15HPITCH,6X,5HSOLID,7X,4HDELR,7X,5HKAPIN,
     2 /13X,I2,5X,F8.5,4X,F8.5,4X,F7.4,3X,F8.3,3X,F9.4)
 1150 FORMAT(///10X,18HBLADE SEGMENT NO. ,I2)
 1160 FORMAT(/16X,5HCHORD,9X,2HRI,11X,2HRO,10X,5HTHETA/10X,4(F12.8,1X))
 1180 FORMAT(/14X,2HX1,8X,2HY1,8X,2HX2,8X,2HY2,7X,4HGAMR/
     110X,5(F9.5,1X))
 1190 FORMAT(/13X,4HPHIS,7X,2HRS,8X,2HHS,8X,2HBS,7X,3HKIS,7X,3HKOS/
     110X,F9.5,1X,30X,2(F9.5,1X))
 1200 FORMAT(/13X,4HPHIC,7X,2HRC,8X,2HHC,8X,2HBC,7X,3HKIC,7X,3HKOC/
     110X,F9.5,1X,30X,2(F9.5,1X))
 1210 FORMAT(/13X,4HPHIP,7X,2HRP,8X,2HHP,8X,2HBP,7X,3HKIP,7X,3HKOP/
     110X,F9.5,1X,30X,2(F9.4,1X))
 1230 FORMAT(/9X,5X,7HNDEL = ,I2,//12X,2HXX,8X,2HYS,8X,2HYP,7X,3HXOC,6X,
     1 4HYSOC,6X,4HYPOC,3X,7H CURVIS,4X,7H CURVIP)
 1240 FORMAT (1X,I3,1X,8F10.5)
 4045 FORMAT(1H1,//10X,10H UNROTATED)
 4047 FORMAT(10X,24H DIMENSIONAL COORDINATES,//9X,1HK,8X,4H XXS,
     1 7X,5H  YSN,//(I10,2F12.7))
 4050 FORMAT(1H1,//6X,30H DIMENSIONAL INPUT COORDINATES,
     1 4X,26H INPUT COORDINATES ROTATED/
     2 40X,41H INTO INVISCID FLOW PROGRAM COORD. SYSTEM,
     3 //9X,1HK,10X,4H XXS,
     4 9X,5H  YSN,9X,5H  XMS,11X,3H TS,9X,5H RTHS,//(I10,5F14.9))
 4060 FORMAT(//9X,1HK,8X,4H XXP,8X,4H YPN,//(I10,2F12.7))
 4065 FORMAT(//9X,1HK,10X,4H XXP,10X,4H YPN,9X,5H  XMP,11X,3H TP,
     1 9X,5H RTHP,//(I10,5F14.9))
 5015 FORMAT(1H1,////,10X,27H PRESSURE SURFACE WILL BE A,
     1 20H DOUBLE VALUED CURVE)
 5020 FORMAT(10X,45H INPUT COORDINATES ROTATED INTO INVISCID FLOW
     1 26H PROGRAM COORDINATE SYSTEM.///20X,16H SUCTION SURFACE,
     2 //,25X,4H XMS,11X,3H TS,9X,5H RTHS,6X,6H CURVS,//,
     3 (I15,3F14.9,F12.5))
 5030 FORMAT(///20X,17H PRESSURE SURFACE,//,25X,4H XMP,11X,3H TP,
     1 9X,5H RTHP,6X,6H CURVP,//(I15,3F14.9,F12.5))
 5040 FORMAT(5X,37H THIS OUTPUT WAS OBTAINED USING A NEW,
     1 50H ARTIFICIALLY DEFINED LEADING EDGE CIRCLE IN PLACE,
     2 37H OF THE ORIGINAL LEADING EDGE CIRCLE.//)
 5050 FORMAT(/5X,6HX1ST= ,F10.8,3X,7HRI(J)= ,F10.8,3X/)
 5060 FORMAT (//10X,5H RI1=,F14.9,5X,5H RI2=,F14.9)
 5070 FORMAT(//18X,2H K,9X,3H XS,9X,3H YS,5X,7H CURVIS/)
 5080 FORMAT(15X,I5,2F12.7,F12.5)
 5090 FORMAT(1H1,//18X,2H K,9X,3H XP,9X,3H YP,5X,7H CURVIP/)
 9500 FORMAT (//10X,2H K,5X,7H EMS(K),7X,5H XSPS,7X,5H YSPS,//
     1 (I12,3F12.8))
      END



      SUBROUTINE FITLIN (XA,YA,XB,YB)
C
C
C  THIS SUBROUTINE FITS A STRAIGHT LINE THROUGH TWO (XB,YB)
C  POINT PAIRS AND INTERPOLATES OR EXTAPOLATES TO FIND THE
C  XA VALUE CORRESPONDING TO A GIVEN YA VALUE.
C
C
      DIMENSION XB(1),YB(1)
C
```

```
      SLOPE=(XB(2)-XB(1))/(YB(2)-YB(1))
      XINTCP=XB(1)-SLOPE*YB(1)
      XA=SLOPE*YA+XINTCP
      RETURN
      END



      SUBROUTINE IFINPT
      COMMON/INPUT/N,TCHORD,SOLID,DELK,KAPIN,RADIUS,
     1 RIOC(5),ROOC(5),TITLE(12)
       COMMON/OUTPUT/CHORD(5),GAMR(5),PHIC(5),PITCH
      COMMON/COM1/RI(1),RO(1),THETA(1),X1(1),Y1(1),X2(1),Y2(1),
     1 KIC(1),KOC(1),KIS(1),KOS(1),PHIS(1),KIP(1),KOP(1),PHIP(1),
     2 NDEL(1),XX(1,300),YS(1,300),YP(1,300)
      COMMON/COM2/GAMS,MCHORD(1),RSTGR(1),STGR(1),MLE(1),RTHLE(1),
     1THLE(1),MTE(1),RTHTE(1),THTE(1),MCL(1),RTHCL(1),THCL(1),MCT(1),
     1RTHCT(1),THCT(1),BETIS(1),BETOS(1),BETIP(1),BETOP(1),MSPS(1,300),
     1RTHSPS(1,300),THSPS(1,300),MSPP(1,300),RTHSPP(1,300),THSPP(1,300)
      COMMON/COORD/ CURVIP(100),CURVIS(100),CURVP(50),CURVS(50),
     1 DYDXP(20),DYDXS(20),EMP(20),EMP1(20),EMS(20),EMS1(20),RTHP(50),
     2 RTHS(50),TP(50),TS(50),XMP(50),XMS(50),XP(100),XS(100),XSPP(100),
     3 XSPS(100),XXP(50),XXS(50),YPI(50),YPN(50),YSI(50),YSN(50),
     4 YSPP(100),YSPS(100)
      COMMON/INTEGR/ KROT,LMAXP,LMAXS,NDELJ,NDELJP,NDELJS,NPTP,
     1 NPTPP,NPTS,NPTSS
      REAL KIC,KOC,KIS,KOS,KIP,KOP,KAPIN
      COMMON/INOUT/ II,IO
      REAL MLE,MTE,MCL,MCT,MCHORD,MSPS,MSPP
C
C
C  COMPUTATION OF GEOMETRICAL INPUT FOR INVISCID FLOW PROGRAM
C
C  CHANGE SIGN OF SELECTED PARAMETERS
C
      DO 10 J=1,N
      KOS(J)= -KOS(J)
      KOC(J)= -KOC(J)
      KOP(J)= -KOP(J)
      Y1(J)= -Y1(J)
   10 Y2(J)= -Y2(J)
C
C  LOCATICN OF CENTERS OF LEADING EDGE CIRCLES
C
      GAMS = (KAPIN-KIC(1))/57.295779
      DO 20 J=1,N
      GAMR(J) = GAMR(J)/57.295779
      GAMJ = GAMS-GAMR(J)
      TEM1 = (X1(J)-RI(1))*COS(GAMS)-Y1(J)*SIN(GAMS)+RI(1)
      TEM2 = (X1(J)-RI(1))*SIN(GAMS)+Y1(J)*COS(GAMS)
      MCL(J) = TEM1+RI(J)*COS(GAMJ)
      RTHCL(J) = TEM2+RI(J)*SIN(GAMJ)
   20 THCL(J) = RTHCL(J)/RADIUS
C
C  LOCATION OF CENTERS OF TRAILING EDGE CIRCLES
C
      DO 30 J=1,N
      GAMJ = GAMS-GAMR(J)
      TEM2 = (X2(J)-RI(1))*SIN(GAMS)+Y2(J)*COS(GAMS)
      MCT(J)=(X2(J)-RI(J))*COS(GAMS)+RI(J)-RO(J)*COS(GAMS)
      RTHCT(J) = TEM2-RO(J)*SIN(GAMJ)
```

```
   30 THCT(J) = RTHCT(J)/RADIUS
C
C  LOCATION OF LEADING EDGES
C
      DO 40 J=1,N
      MLE(J) = MCL(J)-RI(J)
      RTHLE(J) = RTHCL(J)
   40 THLE(J) = THCL(J)
C
C  LOCATION OF TRAILING EDGES
C
      DO 50 J=1,N
      MTE(J) = MCT(J)+RC(J)
      RTHTE(J) = RTHCT(J)
   50 THTE(J) = THCT(J)
C
C  LOCATION OF LOCAL BLADE CHORDS AND STAGGERS
C
      DO 60 J=1,N
      MCHORD(J) = MTE(J)-MLE(J)
      RSTGR(J) = RTHTE(J)-RTHLE(J)
   60 STGR(J) = THTE(J)-THLE(J)
C
C  LOCATION OF SPLINE CURVE ANGLES
C
      DO 70 J=1,N
      GAMJ = GAMS-GAMR(J)
      BETIS(J) = KIS(J)+GAMJ*57.295779
      BETOS(J) = KOS(J)+GAMJ*57.295779
      BETIP(J) = KIP(J)+GAMJ*57.295779
   70 BETOP(J) = KOP(J)+GAMJ*57.295779
C
C  LOCATION OF SPLINE POINTS ON BLADES
C
      DO 80 J=1,N
      GAMJ = GAMS-GAMR(J)
      TEM1 = (X1(J)-RI(1))*COS(GAMS)-Y1(J)*SIN(GAMS)+RI(1)
      TEM2 = (X1(J)-RI(1))*SIN(GAMS)+Y1(J)*COS(GAMS)
      IF(KROT.EQ.1) GO TO 100
      NDELJ = NDEL(J)
      DO 80 K=1,NDELJ
      MSPS(J,K) = TEM1+XX(J,K)*COS(GAMJ)-YS(J,K)*SIN(GAMJ)-MLE(J)
      MSPP(J,K) = TEM1+XX(J,K)*COS(GAMJ)-YP(J,K)*SIN(GAMJ)-MLE(J)
      RTHSPS(J,K) = TEM2+XX(J,K)*SIN(GAMJ)+YS(J,K)*COS(GAMJ)-RTHLE(J)
      RTHSPP(J,K) = TEM2+XX(J,K)*SIN(GAMJ)+YP(J,K)*COS(GAMJ)-RTHLE(J)
      THSPS(J,K) = RTHSPS(J,K)/RADIUS
   80 THSPP(J,K) = RTHSPP(J,K)/RADIUS
C
C  PRINT OUTPUT
C
      WRITE(6,1000)
   85 WRITE(6,1010)
      WRITE(6,1020) (J,MCHORD(J),STGR(J),RSTGR(J),RI(J),RO(J),
     1MLE(J),THLE(J),RTHLE(J),MTE(J),THTE(J),RTHTE(J),J=1,N)
      WRITE(6,1030)
      WRITE(6,1040) (J,BETIS(J),BETOS(J),BETIP(J),BETOP(J),
     1MCL(J),THCL(J),RTHCL(J),MCT(J),THCT(J),RTHCT(J),J=1,N)
      IF(KROT.EQ.1) GO TO 400
      DO 90 J=1,N
      WRITE(6,1050) J
      WRITE(6,1060)
      NDELJ = NDEL(J)
```

```
   90 WRITE(6,1070) (K,MSPS(J,K),THSPS(J,K),RTHSPS(J,K),
     1MSPP(J,K),THSPP(J,K),RTHSPP(J,K),K=1,NDELJ)
      RETURN
C
C  LOCATION OF SPLINE POINTS ON REDEFINED BLADE SURFACES
C
  100 DO 200 K=1,NDELJS
      MSPS(J,K)=TEM1+XS(K)*COS(GAMJ)-YS(J,K)*SIN(GAMJ)-MLE(J)
      RTHSPS(J,K)=TEM2+XS(K)*SIN(GAMJ)+YS(J,K)*COS(GAMJ)-RTHLE(J)
  200 THSPS(J,K)=RTHSPS(J,K)/RADIUS
      DO 300 K=1,NDELJP
      MSPP(J,K)=TEM1+XP(K)*COS(GAMJ)-YP(J,K)*SIN(GAMJ)-MLE(J)
      RTHSPP(J,K)=TEM2+XP(K)*SIN(GAMJ)+YP(J,K)*COS(GAMJ)-RTHLE(J)
  300 THSPP(J,K)=RTHSPP(J,K)/RADIUS
      WRITE(IO,1080)
      GO TO 85
  400 WRITE(IO,1090)
      WRITE(IO,1100) (K,MSPS(J,K),THSPS(J,K),RTHSPS(J,K),
     1 K=1,NDELJS)
      WRITE(IO,1110)
      WRITE(IO,1100) (K,MSPP(J,K),THSPP(J,K),RTHSPP(J,K),
     1 K=1,NDELJP)
      RETURN
C
C  FORMAT STATEMENTS
C
 1000 FORMAT(1H1/////10X,41HCOMPUTED INPUT FOR INVISCID FLOW PROGRAMS
     1 ////)
 1010 FORMAT(6X,5HBLADE,8X,6HMCHORD,7X,4HSTGR,9X,5HRSTGR,6X,2HRI,8X,
     12HRO,8X,3HMLE,6X,4HTHLE,6X,5HRTHLE,6X,3HMTE,6X,4HTHTE,6X,5HRTHTE)
 1020 FORMAT(7X,I2,3X,3F13.9,8F10.7)
 1030 FORMAT(////6X,5HBLADE,5X,5HBETIS,5X,5HBETCS,5X,5HBETIP,5X,5HBETOP
     1,16X,3HMCL,6X,4HTHCL,6X,5HRTHCL,6X,3HMCT,6X,4HTHCT,6X,5HRTHCT)
 1040 FORMAT(7X,I2,3X,4F10.5,10X,6F10.5)
 1050 FORMAT(///10X,18HBLADE SEGMENT NO. ,I2)
 1060 FORMAT(/18X,4HMSPS,10X,5HTHSPS,8X,6HRTHSPS,19X,4HMSPP,10X,
     15HTHSPP,8X,6HRTHSPP)
 1070 FORMAT((5X,I5,3F14.9,10X,3F14.9))
 1080 FORMAT(1H1,/////,10X,33H COMPUTED INPUT FOR INVISCID FLOW,
     1  9H PROGRAMS,/,5X,31H THIS OUTPUT WAS OBTAINED USING,
     2 50H A NEW ARTIFICIALLY DEFINED LEADING EDGE CIRCLE IN,
     3 43H PLACE OF THE ORIGINAL LEADING EDGE CIRCLE.///)
 1090 FORMAT(////10X,16H SUCTION SURFACE,//,18X,4HMSPS,10X,5HTHSPS,
     1 8X,6HRTHSPS)
 1100 FORMAT(5X,I5,3F14.9)
 1110 FORMAT(1H1,////,10X,17H PRESSURE SURFACE,//,18X,4HMSPP,
     1 10X,5HTHSPP,8X,6HRTHSPP)
      END



      SUBROUTINE INPUT1
      COMMON/INPUT/N,TCHORD,SOLID,DELK,KAPIN,RADIUS,
     1 RIOC(5),ROOC(5),TITLE(12)
      COMMON/INADD/ YCI,YCO
      COMMON/COM1/RI(1),RO(1),THETA(1),X1(1),Y1(1),X2(1),Y2(1),
     1 KIC(1),KOC(1),KIS(1),KOS(1),PHIS(1),KIP(1),KOP(1),PHIP(1),
     2 NDEL(1),XX(1,300),YS(1,300),YP(1,300)
```

```
      COMMON/COORD/ CURVIP(100),CURVIS(100),CURVP(50),CURVS(50),
     1 DYDXP(20),DYDXS(20),EMP(20),EMP1(20),EMS(20),EMS1(20),RTHP(50),
     2 RTHS(50),TP(50),TS(50),XMP(50),XMS(50),XP(100),XS(100),XSPP(100),
     3 XSPS(100),XXP(50),XXS(50),YPI(50),YPN(50),YSI(50),YSN(50),
     4 YSPP(100),YSPS(100)
      COMMON/INOUT/ II,IO
      COMMON/INTEGR/ KROT,LMAXP,LMAXS,NDELJ,NDELJP,NDELJS,NPTP,
     1 NPTPP,NPTS,NPTSS
      COMMON/OPT/ ISPP(50),ISPS(50),KCORDS
C
C   READ AND PRINT INPUT
C
      II = 5
      IO = 6
   10 WRITE(6,1000)
      READ (5,1250) (TITLE(I),I=1,12)
      WRITE(6,1260) (TITLE(I),I=1,12)
      READ (5,1020) N,TCHORD,SOLID,DELK,KAPIN,RADIUS
      WRITE(6,1030) N,TCHORD,SOLID,DELK,KAPIN,RADIUS
      READ (5,1010) (RIOC(J),J=1,N)
      WRITE(6,1100) (RIOC(J),J=1,N)
      READ (5,1010) (ROOC(J),J=1,N)
      WRITE(6,1110) (ROOC(J),J=1,N)
C
C   READ AND PRINT BLADE COORDINATES
C
      J = 1
      READ (II,4000) KCORDS,NPTS,NPTP,KIC(J),YCI,YCO
      WRITE (IO,4010) KCORDS,NPTS,NPTP,KIC(J),YCI,YCO
      NPTS=NPTS+1
      NPTP= NPTP+1
      READ(II,4020) (XXS(K),YSN(K),K=2,NPTS)
      READ (II,4020) (XXP(K), YPN(K), K=2,NPTP)
      READ (II,4080) (ISPS(K), K=2,NPTS)
      READ (II,4080) (ISPP(K), K=2,NPTP)
      WRITE(IO,4090)
      WRITE(IO,5000) (ISPS(K),K=2,NPTS)
      WRITE(IO,5010)
      WRITE(IO,5000) (ISPP(K),K=2,NPTP)
      WRITE(IO,4015)
      WRITE(IO,4030) (K,XXS(K),YSN(K), K=2,NPTS)
      WRITE (IO,4040) (K,XXP(K), YPN(K), K=2,NPTP)
      NPTS= NPTS+1
      NPTP= NPTP+1
      XXS(1)=0.
      XXS(NPTS)=0.
      YSN(1)= 0.
      YSN(NPTS)=0.
      XXP(1)=0.
      XXP(NPTP)=0.
      YPN(1)= 0.
      YPN(NPTP)= 0.
      RETURN
C
C   FORMAT STATEMENTS
C
 1000 FORMAT(1H1///)
 1010 FORMAT(8F10.5)
 1020 FORMAT(I10,5F10.5)
 1030 FORMAT(//6X,1HN,6X,6HTCHORD,6X,5HSOLID,6X,4HDELK,6X,5HKAPIN,5X,
     16HRADIUS/5X,I2,5X,F8.5,3X,F8.4,3X,F7.3,4X,F7.3,3X,F8.5)
 1100 FORMAT(/6X,10HRI/C ARRAY/(9X,5(F9.5,1X)))
```

```
 1110 FORMAT(/6X,10HRO/C ARRAY/(9X,5(F9.5,1X)))
 1250 FORMAT(12A6)
 1260 FORMAT(1X,12A6)
 4000 FORMAT(3I10,3F10.3)
 4010 FORMAT(1H1,///3X,7H KCORDS,5X,5H NPTS,5X,5H NPTP,3X,7H KIC(J),
     1 6X,4H YCI,6X,4H YCO,
     2 //3I10,F10.3,4F10.7)
 4015 FORMAT (//10X,18H INPUT COORDINATES/)
 4020 FORMAT(8F10.7)
 4030 FORMAT(//8X,2H K,5X,7H XXS(K),5X,7H YSN(K),//(I10,2F12.7))
 4040 FORMAT(//8X,2H K,5X,7H XXP(K),5X,7H YPN(K),//(I10,2F12.7))
 4080 FORMAT(50I1)
 4090 FORMAT(//10X,25H  ISPS(K), K=2,3,....,NPTS/)
 5000 FORMAT(10X,50I2)
 5010 FORMAT(//10X,25H  ISPP(K), K=2,3,....,NPTP/)
      END



      SUBROUTINE LEDGE
C
C  THIS SUBROUTINE LOCATES THE LEFTMOST POINT OF THE BLADE IN
C  THE STAGGERED POSITION.  A PAIR OF NEW LEADING EDGE CIRCULAR
C  ARCS ARE DEFINED WITH CENTERS ON A LINE NORMAL TO THE SURFACE
C  AT THE LOCATED POINT.  THE BLADE SUCTION AND PRESSURE
C  SURFACES ARE REDEFINED ACCORDINGLY.  THE SURFACE COORDINATES
C  ARE MAPPED INTO A COORDINATE SYSTEM WITH THE X-AXIS THROUGH THE
C  CENTERS OF THE NEW LEADING EDGE CIRCLE AND THE TRAILING EDGE CIRCLE,
C  AND THE Y-AXIS TANGENT TO THE NEW LEADING EDGE CIRCLE.
C
C
C  ACRIT       SURFACE ANGLE EQUAL TO PI/2 MINUS GAMS, RAD.
C
C  AEPS        ANGULAR DISTANCE BETWEEN THE ORIGIN AND THE
C              FIRST SPLINE POINTS (TRANSITION POINTS) ON THE
C              REDEFINED SUCTION AND PRESSURE SURFACES.
C
C  ALE         ANGULAR LOCATION OF POINT ON THE ORIGINAL
C              LEADING EDGE CIRCLE, RAD.
C
C  ALFN        ANGLE BETWEEN A, THE LINE CONNECTING THE CENTERS OF THE
C              ORIGINAL LEADING AND TRAILING EDGE CIRCLES AND B, THE
C              LINE CONNECTING THE CENTERS OF THE NEW LEADING EDGE
C              CIRCLE AND THE ORIGINAL TRAILING EDGE CIRCLE, RAD.
C
C  AMINUS      ANGLE WHERE SUCTION SURFACE IS TANGENT TO THE
C              NEW LEADING EDGE CIRCLE, RAD.
C
C  APLUS       ANGLE WHERE PRESSURE SURFACE IS TANGENT TO THE
C              NEW LEADING EDGE CIRCLE, RAD.
C
C  CCRIT       CURVATURE AT XCRIT.
C
C  CMINUS      CURVATURE AT XMINUS.
C
C  CPLUS       CURVATURE AT XPLUS
C
C  DANG        ONE-EIGHTH OF THE ANGULAR DISTANCE AROUND THE
C              ORIGINAL LEADING EDGE.
```

```
C  KL          INDEX OF FIRST XX  VALUE TO THE LEFT OF XPLUS.
C
C  KLP1        KL PLUS 1.
C
C  KLP7        KL + 7 POINTS ON ORIGINAL LEADING EDGE CIRCLE.
C
C  KR          INDEX OF THE FIRST MEMBER OF THE XX(K) ARRAY
C              TO THE RIGHT OF XMINUS.
C
C  NDELJP      NUMBER OF COORDINATES ON REDEFINED PRESSURE
C              SURFACE.
C
C  NDELJS      NUMBER OF COORDINATES ON THE REDEFINED SUCTION
C              SURFACE.
C
C  RI1         RADIUS OF NEW LEADING EDGE CIRCLE ON THE SUCTION
C              SURFACE.
C
C  RI2         RADIUS OF NEW LEADING EDGE CIRCLE ON THE PRESSURE
C              SURFACE.
C
C  RLE         RADIUS OF CIRCLE TANGENT TO SUCTION SURFACE AT
C              (XCRIT,YCRIT).
C
C  XCRIT       X-COORDINATE WHERE THE SUCTION SURFACE ANGLE IS
C              EQUAL TO ACRIT.
C
C  XCTRN       X-COORDINATE OF CENTER OF CIRCLE TANGENT TO THE
C              SUCTION SURFACE AT (XCRIT,YCRIT).
C
C  XCTR1       X-COORDINATE OF CENTER OF NEW SUCTION SURFACE
C              LEADING EDGE CIRCLE.
C
C  XCTR2       X-COORDINATE OF CENTER OF NEW PRESSURE SURFACE
C              LEADING EDGE CIRCLE.
C
C  XMINUS      X-COORDINATE OF POINT WHERE THE SUCTION SURFACE
C              MEETS THE NEW LEADING EDGE CIRCLE.
C
C  XP          X-COORDINATE OF PRESSURE SURFACE ARRAY.
C
C  XPL         ABSCISSA OF POINT ON ORIGINAL LEADING EDGE.
C
C  XPLUS       X-COORDINATE OF POINT WHERE THE PRESSURE SURFACE
C              MEETS THE NEW LEADING EDGE CIRCLE.
C
C  XS          X-COORDINATE OF SUCTION SURFACE ARRAY.
C
C  YCRIT       Y-COORDINATE OF SUCTION SURFACE AT XCRIT.
C
C  YCTRN       Y-COORDINATE OF CENTER OF CIRCLE TANGENT TO THE
C              SUCTION SURFACE AT (XCRIT,YCRIT).
C
C  YCTR1       Y-COORDINATE OF CENTER OF NEW SUCTION SURFACE
C              LEADING EDGE CIRCLE.
C
C  YCTR2       Y-COORDINATE OF CENTER OF NEW PRESSURE SURFACE
C              LEADING EDGE CIRCLE.
C
C  YMINUS      ORDINATE AT XMINUS.
C
C  YPL         ORDINATE OF POINT ON ORIGINAL LEADING EDGE.
```

```
C  YPLUS      ORDINATE AT XPLUS.
C
C
      COMMON/COM1/RI(1),RO(1),THETA(1),X1(1),Y1(1),X2(1),Y2(1),
     1 KIC(1),KOC(1),KIS(1),KOS(1),PHIS(1),KIP(1),KOP(1),PHIP(1),
     2 NDEL(1),XX(1,300),YS(1,300),YP(1,300)
      COMMON/INPUT/N,TCHORD,SOLID,DELK,KAPIN,RADIUS,
     1 RIOC(5),ROOC(5),TITLE(12)
       COMMON/OUTPUT/CHORD(5),GAMR(5),PHIC(5),PITCH
      COMMON/INOUT/ II,IO
      COMMON/INTEGR/ KROT,LMAXP,LMAXS,NDELJ,NDELJP,NDELJS,NPTP,
     1 NPTPP,NPTS,NPTSS
      COMMON/COORD/ CURVIP(100),CURVIS(100),CURVP(50),CURVS(50),
     1 DYDXP(20),DYDXS(20),EMP(20),EMP1(20),EMS(20),EMS1(20),RTHP(50),
     2 RTHS(50),TP(50),TS(50),XMP(50),XMS(50),XP(100),XS(100),XSPP(100),
     3 XSPS(100),XXP(50),XXS(50),YPI(50),YPN(50),YSI(50),YSN(50),
     4 YSPP(100),YSPS(100)
      COMMON/BLOK A/ GAMS,PI,RI1,RI2
      DIMENSION CCRIT(1),CMINUS(1),CPLUS(1),CURANS(1),DTDMN(1),
     1 SCRTCH (50),XNEW(1),YNEW(1)
      REAL KIC,KIP,KIS,KOP,KOS,KOC
C
C
      J=1
C
C  CHECK FOR LIMITING CASE WHERE BETI FOR THE SUCTION SURFACE
C  WILL BE WITHIN 2 DEGREES OF VERTICAL IN THE STAGGERED
C  POSITION
C
      IF(GAMS-PI/2.+KIS(J)-2./57.295779) 500,600,700
  500 WRITE(IO,9000)
      STOP
C
C  CASE WHERE KIS + GAMS EQUALS 92 DEGREES
C
  600 ACRIT=PI/2.-GAMS
      AEPS=1./57.295779
      APLUS=ACRIT+AEPS
      AMINUS=ACRIT-AEPS
      GO TO 800
C
C  CASE WHERE KIS + GAMS IS GREATER THAN 92 DEGREES
C
  700 ACRIT= PI/2.-GAMS
      AEPS=2./57.295779
      APLUS=ACRIT+AEPS
      AMINUS=ACRIT-AEPS
C
C  CALCULATE LOCATIONS ON THE SUCTION SURFACE WHERE THE SURFACE
C  ANGLE EQUALS ACRIT, APLUS, AND AMINUS
C
  800 WRITE(IO,9500)
 9500 FORMAT(1H1///,10X,42H CALCULATION OF NEW ORIGIN AND NEW LEADING
     1 21H EDGE TANGENCY POINTS/)
      WRITE(IO,9600)
 9600 FORMAT(//10X,16H ORIGIN LOCATION)
      CALL ANGSER (XCRIT,YCRIT,ACRIT,CCRIT)
      WRITE(IO,9700)
 9700 FORMAT(///10X,17H PRESSURE SURFACE)
      CALL ANGSER (XPLUS,YPLUS,APLUS,CPLUS)
      WRITE(IO,9800)
 9800 FORMAT(1H1//////10X,16H SUCTION SURFACE)
      CALL ANGSER (XMINUS,YMINUS,AMINUS,CMINUS)
```

```
C  CALCULATE RADII AND CENTERS FOR NEW LEADING EDGE CIRCLES
C
      RLE=-1./CCRIT(1)
      XCTRN= XCRIT+RLE*SIN(ACRIT)
      YCTRN= YCRIT-RLE*COS(ACRIT)
      RI1=SQRT((XMINUS-XCRIT)**2+(YMINUS-YCRIT)**2)/(2.*SIN(AEPS/2.)
      RI2=SQRT((XPLUS-XCRIT)**2+(YPLUS-YCRIT)**2)/(2.*SIN(AEPS/2.))
      XCTR1=XCRIT+RI1*SIN(ACRIT)
      XCTR2=XCRIT+RI2*SIN(ACRIT)
      YCTR1=YCRIT-RI1*COS(ACRIT)
      YCTR2=YCRIT-RI2*COS(ACRIT)
C
C  PRINT COORDINATES OF ORIGIN OF INVISCID FLOW PROGRAM COORDINATE
C  SYSTEM
C
      WRITE(IO,9300) XCTRN,YCTRN,CCRIT,CPLUS,CMINUS
      WRITE (IO,9400) XCRIT,YCRIT,XPLUS,YPLUS,XMINUS,YMINUS
C
C  REDEFINE THE SUCTION SURFACE AS BEGINNING AT (XMINUS,YMINUS),
C  AND REDEFINE THE PRESSURE SURFACE AS BEGINNING AT (XPLUS,YPLUS)
C
C  SEARCH FOR FIRST XX(J,K) TO THE LEFT OF XPLUS
C
      DO 900  K=1,NDELJ
      IF(XX(J,K) .GE. XPLUS)  GO TO 1000
  900 CONTINUE
      WRITE(IO,9100) XPLUS
      STOP
 1000 KL= K-1
      KLP7 = KL+7
      NDELJP= NDELJ+KLP7
C
C  CALCULATE THE ANGLE OF ROTATION NEEDED TO ORIENT THE CENTERS OF
C  THE TRAILING EDGE CIRCLE AND THE NEW LEADING EDGE CIRCLE ON
C  THE X-AXIS
C
      ALFN=ATAN(YCTRN/(CHORD(J)-RC(J)-XCTRN))
C
C  MAP INTERPOLATED COORDINATES INTO SYSTEM WITH X-AXIS THROUGH THE
C  CENTERS OF THE NEW LEADING EDGE CIRCLE AND ORIGINAL TRAILING EDGE
C  CIRCLE.  THE Y-AXIS IS TANGENT TO THE NEW LEADING EDGE CIRCLE.
C
      DO 1100  KK=1,NDELJ
      K= NDELJ-KK+1
      L= NDELJP-KK+1
      XP(L)=(XX(J,K)-XCTRN)*COS(ALFN)-(YP(J,K)-YCTRN)*SIN(ALFN)
     1 + RLE
      YP(J,L)=(XX(J,K)-XCTRN)*SIN(ALFN)+(YP(J,K)-YCTRN)*COS(ALFN)
 1100 CURVIP(L)= CURVIP(K)
      DO 1200  L=1,KL
      K= KL-L+1
      XP(L)= (XX(J,K)-XCTRN)*COS(ALFN)-(YS(J,K)-YCTRN)*SIN(ALFN)
     1 +RLE
      YP(J,L)=(XX(J,K)-XCTRN)*SIN(ALFN)+(YS(J,K)-YCTRN)*COS(ALFN)
 1200 CURVIP(L)= CURVIS(K)
C
C  POINTS ON THE ORIGINAL LEADING EDGE ARC
C
      KLP1= KL+1
      DANG=(PI-KIS(J)+KIP(J))/8.
      ALE= KIS(J)
```

```
      DO 1300  L=KLP1,KLP7
      ALE= ALE+DANG
      XPL=RI(J)*(1.-SIN(ALE))
      YPL=RI(J)*COS(ALE)
      XP(L)=(XPL-XCTRN)*COS(ALFN)-(YPL-YCTRN)
     1 *SIN(ALFN)+RLE
      YP(J,L)=(XPL-XCTRN)*SIN(ALFN)+(YPL-YCTRN)*COS(ALFN)
 1300 CURVIP(L)=1./RI(J)
C
C   SEARCH FOR FIRST XX(J,K) TO THE RIGHT OF XMINUS
C
      DO 1400  K=1,NDELJ
      IF(XX(J,K) .GT. XMINUS) GO TO 1500
 1400 CONTINUE
      WRITE(IO,9200)
      STOP
 1500 KR= K
      NDELJS =NDELJ-KR+1
      DO 1600  L=1,NDELJS
      K= KR+L-1
      XS(L)=(XX(J,K)-XCTRN)*COS(ALFN)-(YS(J,K)-YCTRN)
     1 *SIN(ALFN)+RLE
      YS(J,L)=(XX(J,K)-XCTRN)*SIN(ALFN)+(YS(J,K)-YCTRN)*COS(ALFN)
 1600 CURVIS(L)= CURVIS(K)
C
C   SEARCH FOR FIRST XXS(K) TO THE LEFT OF THE XPLUS
C
      DO 1700  K=1,NPTS
      IF(XXS(K) .GE. XPLUS) GO TO 1800
 1700 CONTINUE
 1800 KL= K-1
      NPTPP= NPTP+KL
C
C   CALCULATE CURVATURES FOR INPUT COORDINATES
C
      CALL SPLN (XXS,YSI,XSPS,YSPS,EMS,SCRTCH,CURVS,
     1 LMAXS,NPTS)
      CALL SPLN (XXP,YPI,XSPP,YSPP,EMP,SCRTCH,CURVP,
     1 LMAXP,NPTP)
C
C   MAP INPUT COORDINATES INTO INVISCID FLOW PROGRAM COORDINATE
C   SYSTEM
C
      DO 1900  KK=1,NPTP
      K= NPTP-KK+1
      L= NPTPP-KK+1
      XMP(L)= (XXP(K)-XCTRN)*COS(GAMS)-(YPN(K)-YCTRN)
     1 *SIN(GAMS)+RLE
      RTHP(L)= (XXP(K)-XCTRN)*SIN(GAMS)+(YPN(K)-YCTRN)*COS(GAMS)
      TP(L)= RTHP(L)/RADIUS
 1900 CURVP(L)= CURVP(K)
      DO 2000  L=1,KL
      K= KL-L+1
      XMP(L)=(XXS(K)-XCTRN)*COS(GAMS)-(YSN(K)-YCTRN)*SIN(GAMS)
     1 + RLE
      RTHP(L)=(XXS(K)-XCTRN)*SIN(GAMS)+(YSN(K)-YCTRN)*COS(GAMS)
      TP(L)= RTHP(L)/RADIUS
 2000 CURVP(L)= CURVS(K)
C
C   SEARCH FOR FIRST XXS(K) TO THE RIGHT OF XMINUS
C
```

```
      DO 2100  K=1,NPTS
      IF(XXS(K) .GT. XMINUS) GO TO 2200
 2100 CONTINUE
 2200 KR= K
      NPTSS= NPTS-KR+1
C
C  MAP INPUT COORDINATES INTO INVISCID FLOW PROGRAM COORDINATE
C  SYSTEM
C
      DO 2300  L=1,NPTSS
      K= KR+L-1
      XMS(L)= (XXS(K)-XCTRN)*COS(GAMS)-(YSN(K)-YCTRN)*
     1 SIN(GAMS)+RLE
      RTHS(L)= (XXS(K)-XCTRN)*SIN(GAMS)+(YSN(K)-YCTRN)*COS(GAMS)
      TS(L)= RTHS(L)/RADIUS
 2300 CURVS(L)= CURVS(K)
      KIS(J)= AMINUS+ALFN
      KIP(J)=-PI+APLUS+ALFN
      RI(J)= RLE
      KOC(J)=KOC(J)+ALFN
      KOS(J)= KOS(J)+ALFN
      KOP(J)=KOP(J)+ALFN
      KIC(J)= KIC(J)+ALFN
      X2(J)=YCTRN/SIN(ALFN)+RLE+RO(J)
      RETURN
 9000 FORMAT(////5X,36H MAXIMUM SUCTION SURFACE BLADE ANGLE,
     1 30H IS BETWEEN 90 AND 92 DEGREES.)
 9100 FORMAT (1H1,////,10X,7H XPLUS=,F10.7,16H IS NOT ON BLADE)
 9200 FORMAT (1H1,////,10X,23H XMINUS IS NOT ON BLADE)
 9300 FORMAT(//10X,7H XCTRN=,F10.7,3X,7H YCTRN=,F10.7,
     1 8H  CCRIT=,F11.6,8H  CPLUS=,F11.6,9H  CMINUS=,F11.6)
 9400 FORMAT (//7H XCRIT=,F11.8,8H  YCRIT=,F11.8,8H  XPLUS=,F11.8,
     1 8H  YPLUS=,F11.8,9H  XMINUS=,F11.8,9H  YMINUS=,F11.8)
      END



      SUBROUTINE SPLFIT (XX,YS,DTDM,EM,EM1,MSP,THSP,NSP,SLPI,SLPO,CURV,
     1 CURVI,DYDX,NDEL)
C
C  THIS SUBPROGRAM INTERPOLATES THE MSP-THSP ARRAYS FOR YS VALUES
C  AT GIVEN XX VALUES.  CURVATURES ARE ALSO COMPUTED.  A SPLINE
C  FIT IS USED.
C
C
C
C  CURVI(K)   CURVATURE AT COORDINATE POINT (XX,YS) OR (XX,YP).
C
C  CURV(KK)   CURVATURE AT COORDINATE POINT (MSP,THSP).
C
C  DTDM(KK)   FIRST DERIVATIVE AT COORDINATE POINT (MSP,THSP).
C
C  DYDX       FIRST DERIVATIVE AT COORDINATE POINT (XX,YS).
C
C  D2YDX2     SECOND DERIVATIVE AT COORDINATE POINT (XX,YS).
C
C  EM(KK)     SECOND DERIVATIVE AT COORDINATE POINT (MSP,THSP)
C             OBTAINED WITH A DOUBLE SPLINE FIT PROCEDURE.
C
C  EM1(K)     SECOND DERIVATIVE AT COORDINATE POINT (MSP,THSP)
C             OBTAINED WITH A SINGLE SPLINE FIT PROCEDURE.
C  MSP(KK)    THE ARRAY OF ABSCISSA VALUES.
C
```

```
C  SLPI        SLOPE OF THE THSP VERSUS MSP CURVE AT
C              THE FIRST MSP POINT.
C
C  SLPO        SLOPE OF THE THSP VERSUS MSP CURVE AT
C              THE LAST MSP POINT.
C
C  TANGI       TANGENT OF THE DTDM VERSUS MSP CURVE AT
C              THE FIRST MSP POINT.
C
C  TANGO       TANGENT OF THE DTDM VERSUS MSP CURVE AT
C              THE LAST MSP POINT.
C
C  THSP(KK)    ARRAY OF ORDINATE VALUES.
C
C  XX(K)       THE INTERPOLATE.
C
C  YS(K)       THE INTERPOLATED ANSWER.
C
      COMMON/INPUT/N,TCHORD,SOLID,DELK,KAPIN,RADIUS,
     1 RIOC(5),ROOC(5),TITLE(12)
      COMMON/INOUT/ II,IO
       COMMON/OUTPUT/CHORD(5),GAMR(5),PHIC(5),PITCH
      COMMON/INTEGR/ KRDT,LMAXP,LMAXS,NDELJ,NDELJP,NDELJS,NPTP,
     1 NPTPP,NPTS,NPTSS
      DIMENSION XX(1,1),YS(1,1), MSP(1), THSP(1),DTDM(1),EM(1),
     1 CURV(1), CURVI(1),NDEL(1),SCRTCH(20),EM1(1),DYDX(1)
      REAL MMMSP, MSP, MSPMM
C
C  CALCULATE FIRST AND SECOND DERIVATIVES AND CURVATURES AT
C  INPUT CORRDINATE POINTS.
C
      CALL SPLN22(MSP,THSP,SLPI,SLPO,NSP,DTDM,EM1)
      TANGI= EM1(1)
      TANGO=EM1(NSP)
      CALL SPLN22(MSP,DTDM,TANGI,TANGO,NSP,EM,SCRTCH)
      DO 10 K=1,NSP
   10 CURV(K)= EM(K)/(1.+DTDM(K)*DTDM(K))**1.5
C
C  BLADE SECTION COORDINATES AT DELX INCREMENTS
C
      DO 45 J=1,N
      TEM = CHORD(J)/20./10000.
      NEXP = 0
   20 NEXP = NEXP+1
      TEM = 10.*TEM
      IF (TEM-1..LT.0.) GO TO 20
      M = TEM
      IF (M.GE.2) GO TO 25
      M = 1
      GO TO 35
   25 IF (M.GE.5) GO TO 30
      M = 2
      GO TO 35
   30 M = 5
      M=2
   35 DELX = FLOAT(M)*10.**(4-NEXP)
      J=1
      NDEL(J)= CHORD(J)/DELX+1.
      XX(J,1)=0.
      NDELJ = NDEL(J)
      IF (NDELJ.LE.100) GO TO 40
      WRITE(IO,1280) NDELJ
      NDELJ=100
```

```
   40 DO 45 K=1,NDELJ
   45 XX(J,K+1)= XX(J,K)+DELX
C
C   INTERPOLATE FOR YS VALUES CORRESPONDING TO XX VALUES.
C
      KK= 2
      DO 100  K=1,NDELJ
      IF((XX(J,K) .LT. MSP(1)).OR.(XX(J,K).GT.MSP(NSP))) GO TO 100
C
C   SEARCH FOR COORDINATE POINTS BRACKETING XX(K)
C
   50 IF(XX(J,K) .LE. MSP(KK)) GO TO 60
      IF(KK .GE. NSP) GO TO 200
      KK= KK+1
      GO TO 50
C
C   CALCULATE SPLINE INTERPOLATION EQUATION COEFFICIENTS
C
   60 S= MSP(KK)-MSP(KK-1)
      EMKM1= EM(KK-1)
      EMK= EM(KK)
      MSPMM= MSP(KK)-XX(J,K)
      MMMSP= XX(J,K)-MSP(KK-1)
      THK= THSP(KK)/S
      THKM1= THSP(KK-1)/S
C
C   CALCULATE ORDINATE (YS), FIRST DERIVATIVE, SECOND DERIVATIVE,
C   AND CURVATURE
C
      YS(J,K)=EMKM1*MSPMM**3/6./S+EMK*MMMSP**3/6./S+(THK-EMK*S/6.)
     1 *MMMSP+(THKM1-EMKM1*S/6.)*MSPMM
      DYDX(K)= -EMKM1*MSPMM**2/2./S+EMK*MMMSP**2/2./S
     1 +THK-THKM1-(EMK-EMKM1)*S/6.
      D2YDX2= EMKM1*MSPMM/S+EMK*MMMSP/S
      CURVI(K)= D2YDX2/(1.+DYDX(K)*DYDX(K))**1.5
      KK= 2
  100 CONTINUE
      RETURN
C
C   ERROR RETURN
C
  200 WRITE(IO,500) XX(J,K)
  500 FORMAT (1H1,/////10X,34H XX COORDINATE IS NOT WITHIN BLADE,
     1 /10X,4H XX=,F10.5)
      RETURN
 1280 FORMAT(//10X,7H NDELJ=,I6,33H WHICH IS LARGER THAN DIMENSIONED
     1 ,12H ARRAY SIZES //)
      END



      SUBROUTINE SPLN (X,Y,XB,YB,EMB,FDERV,CURV,LMAXS,KLIM)
C
C   THIS SUBROUTINE FITS A CUBIC SPLINE CURVE TO THE (XB,YB)
C   COORDINATE ARRAYS AND INTERPOLATES TO FIND Y-VALUES WHICH
C   CORRESPOND TO THE GIVEN X-VALUES.  THE FIRST DERIVATIVE
C   AND THE CURVATURE AT X ARE ALSO RETURNED TO THE CALLING
C   PROGRAM.
C
C
      COMMON/INOUT/ II,IO
      DIMENSION CURV(1),DTDMB(1),EMB(1),FDERV(1),X(1),XB(1),
     1 Y(1),YB(1)
```

```
      REAL MMMSP,MSPMM
C
C
      KK= 2
      DO 100  K=1,KLIM
      IF((X(K) .LT. XB(1)) .OR. (X(K) .GT. XB(LMAXS))) GO TO 100
C
C  SEARCH FOR COORDINATE POINTS BRACKETING X
C
   50 IF(X(K) .LE. XB(KK)) GO TO 60
      IF(KK .GE. LMAXS)  GO TO 200
      KK= KK+1
      GO TO 50
C
C  CALCULATE SPLINE INTERPOLATION EQUATION COEFFIENTS
C
   60 S= XB(KK)-XB(KK-1)
      EMKM1= EMB(KK-1)
      EMK= EMB(KK)
      MSPMM= XB(KK)-X(K)
      MMMSP=X(K)-XB(KK-1)
      THK= YB(KK)/S
      THKM1= YB(KK-1)/S
C
C  CALCULATE ORDINATE, FIRST DERIVATIVE, SECOND DERIVATIVE,
C  AND CURVATURE
C
      Y(K)= EMKM1*MSPMM**3/6./S+EMK*MMMSP**3/6./S+(THK-EMK*S/6.)
     1 *MMMSP+(THKM1-EMKM1*S/6.)*MSPMM
      FDERV(K)= -EMKM1*MSPMM**2/2./S+EMK*MMMSP**2/2./S
     1 + THK-THKM1-(EMK-EMKM1)*S/6.
      SDERV=EMKM1*MSPMM/S+EMK*MMMSP/S
      CURV(K)=SDERV/(1.+FDERV*FDERV)**1.5
  100 CONTINUE
      RETURN
C
C  ERROR RETURN
C
  200 WRITE(IO,500) X(K)
  500 FORMAT(1H1,////,10X,33H X COORDINATE IS NOT WITHIN BLADE,
     1 /,10X,3H X=,F10.5)
      STOP
      END



      SUBROUTINE SPLN22 (X,Y,Y1P,YNP,N,SLOPE,EM)
C
C  SPLN22 CALCULATES FIRST AND SECOND DERIVATIVES AT SPLINE POINTS
C  END CONDITION - DERIVATIVES SPECIFIED AT END POINTS
C
      COMMON SRW
      COMMON /BOX/ G(100),SB(100)
      DIMENSION X(N),Y(N),EM(N),SLOPE(N)
      INTEGER SRW
      SB(1) = .5
      F = (Y(2)-Y(1))/(X(2)-X(1))-Y1P
      G(1) = F*3./(X(2)-X(1))
      NC=N-1
      IF(NC.LT.2) GO TO 20
```

```
      DO 10 I=2,NO
      A = (X(I)-X(I-1))/6.
      C = (X(I+1)-X(I))/6.
      W = 2.*(A+C)-A*SB(I-1)
      SB(I) = C/W
      F = (Y(I+1)-Y(I))/(X(I+1)-X(I))-(Y(I)-Y(I-1))/(X(I)-X(I-1))
   10 G(I) = (F-A*G(I-1))/W
   20 F = YNP-(Y(N)-Y(N-1))/(X(N)-X(N-1))
      W = (X(N)-X(N-1))/6.*(2.-SB(N-1))
      EM(N) = (F-(X(N)-X(N-1))*G(N-1)/6.)/W
      DO 30 I=2,N
      K = N+1-I
   30 EM(K) = G(K)-SB(K)*EM(K+1)
      SLOPE(1) = (X(1)-X(2))/6.*(2.*EM(1)+EM(2))+(Y(2)-Y(1))/(X(2)-X(1))
      DO 40 I=2,N
   40 SLOPE(I) = (X(I)-X(I-1))/6.*(2.*EM(I)+EM(I-1))+(Y(I)-Y(I-1))/
     1    (X(I)-X(I-1))
      IF(SR.EQ.18) WRITE (6,1000) N,(X(I),Y(I),SLOPE(I),EM(I),I=1,N)
      RETURN
 1000 FORMAT (2X,15HNO. OF POINTS =,I3/10X,1HX,19X,1HY,19X,5HSLOPE,15X,
     12HEM/(4G20.8))
      END
```

APPENDIX C. INPUT BLADE GEOMETRY CHECKING PROGRAM (INCHK)

The INCHK program was developed to expedite the selection of a suitable set of blade coordinates for use as TSONIC and MAGNFY input data. INCHK has two major functions; it calculates curvatures of the blade surfaces at the input coordinate points, and it rotates the calculated blade surface angles into a standard reference position for comparison with surface angles calculated for the same profile at other setting angles. The curvatures are useful in deciding where points should be added or removed. The blade surface angles in the reference position (fig. 16) are used when calculations are made for the same blade profile at different blade setting angles to maintain a reasonably consistent blade description.

Several subroutines from TSONIC were used intact or in modified form in writing INCHK. Consequently the input to INCHK consists of all the input data for TSONIC described in reference 21 followed by one additional data card described in figure 52.

Definitions of the input parameters shown in figure 52 are given below:

KAPIN inlet blade angle in the staggered position, κ_1 (fig. 3), deg

KIC inlet blade angle in the reference position, deg

RLED radius of leading edge circle (the fictitious leading edge circle if one has been defined), meters

XCTRN XX-coordinate of the center of the fictitious leading edge circle (fig. 46), equals zero if fictitious edge circle is not defined, meters

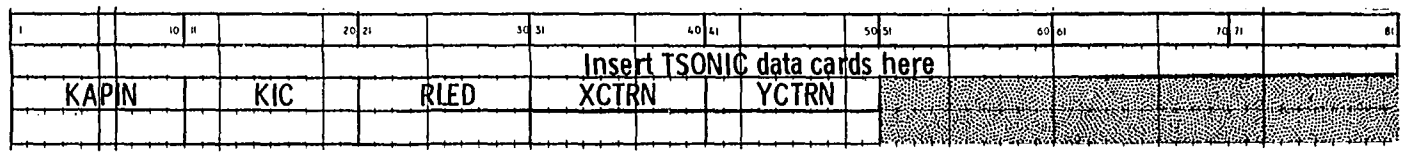

Figure 52. - INCHK input data.

YCTRN Y-coordinate of the center of the fictitious leading edge circle (fig. 46), equals zero if fictitious edge circle is not defined, meters

The output consists of the first few pages of TSONIC output (ref. 21) plus additional output containing blade surface curvatures and blade geometry in the reference position chosen (where κ_1 = KIC). The curvature output is valid for general stream surfaces of revolution, but the reference position geometry output is valid only for cylindrical stream surfaces. The output is clearly labeled, but key headings are defined below for completeness.

CURV blade surface curvature

M meridional coordinate, m (fig. 16), meters

RTHETA tangential coordinate (fig. 16), meters

SURF ANG blade surface angle in reference position, deg

A complete listing of the source cards for INCHK follows.

```
      COMMON SRW,ITER,IEND,LER(2),NER(2)
      COMMON /INP/GAM,AR,TIP,RHOIP,WTFL,OMEGA,ORF,BETAI,BETAO,REDFAC,
     1   DENTOL,MBI,MBO,MM,NBBI,NBL,NRSP,MR(10),RMSP(10),BESP(10),
     2   BLDAT,AANDK,ERSOR,STRFN,SLCRD,INTVL,SURVL
      COMMON /CALCON/ACTWT,ACTOMG,ACTLAM,MBIM1,MBIP1,MBOM1,MBOP1,MMM1,
     1   RM1,RT,DTLR,UMLR,PITCH,CP,EXPON,TWW,CPTIP,TGROG,TBI,TBO,LAMBDA,
     2   TWL,ITMIN,ITMAX,NIP,IMS(2),BV(2),MV(100),IV(101),ITV(100,2),
     3   TV(100,2),DTDMV(100,2),BETAV(100,2),MH(100,2),DTDMH(100,2),
     4   BETAH(100,2),RMH(100,2),BEH(100,2),RP(100),BE(100),DBDM(100),
     5   SAL(100),AAA(100)
      COMMON /GEOMIN/ CHORD(2),STGR(2),MLE(2),THLE(2),RMI(2),RMO(2),
     1   RI(2),RO(2),BETI(2),BETO(2),NSPI(2),MSP(50,2),THSP(100,2)
      COMMON /D2TDM2/ D2TDM2(100,2)
      DIMENSION CURV(100,2),FMV(50,2)
      INTEGER BLDAT,AANDK,ERSOR,STRFN,SLCRD,SURVL,AATEMP,SURF,FIRST,
     1   UPPER,S1,ST,SRW
      REAL K,KAK,LAMBDA,LMAX,MH,MLE,MR,MSL,MSP,MV,MVIM1
      EXTERNAL BL1,BL2
C
C
      II=5
      IO=6
      CALL INPUT
```

```
C  CALCULATE TV, ITV, IV, DTDMV, AND BETAV ARRAYS
C
C  TV, ITV, AND DTDMV ON BLADE
      DO 120 IM=MBI,MBO
      LER(2)=1
C     BLCO CALL NO. 1
      CALL BL1(MV(IM),TV(IM,1),DTDMV(IM,1),INF)
      LER(2)=2
C     BLCO CALL NO. 2
      CALL BL2(MV(IM),TV(IM,2),DTDMV(IM,2),INF)
  120 CONTINUE
C
C  BETAV ARRAY
C
      DO 200 SURF=1,2
      DO 200 IM=MBI,MBO
      CURV(IM,SURF) = (RM(IM)*D2TDM2(IM,SURF)+SAL(IM)*DTDMV(IM,SURF)) /
     1   (1.+(RM(IM)*DTDMV(IM,SURF))**2)**1.5
  200 BETAV(IM,SURF) = ATAN(DTDMV(IM,SURF)*RM(IM))*57.295779
      WRITE (6,1070)
      WRITE (6,1080) (MV(IM),TV(IM,1),DTDMV(IM,1),CURV(IM,1),TV(IM,2),
     1   DTDMV(IM,2),CURV(IM,2),IM=MBI,MBO)
C
C  ROTATE COORDINATES TO STANDARD POSITION.
C
      DO 300 IM=MBI,MBO
      FMV(IM,1)=MV(IM)
  300 FMV(IM,2)=MV(IM)
      WRITE (6,1250)
      PIT=0.
      WRITE(6,5200)
 5200 FORMAT (///30H SUCTION SURFACE, INTERSECTION,
     1 23H OF VERTICAL MESH LINES//)
      CALL ROTATE (FMV,TV,DTDMV,D2TDM2,MBIP1,MBCM1,1,PIT)
      WRITE(6,1250)
      PIT=PITCH
      WRITE (6,5300)
 5300 FORMAT (///31H PRESSURE SURFACE, INTERSECTION,
     1 23H OF VERTICAL MESH LINES//)
      CALL ROTATE (FMV,TV,DTDMV,D2TDM2,MBIP1,MBCM1,2,PIT)
      STOP
 1070 FORMAT (1H1,6X,62HBLADE DATA AT INTERSECTIONS OF VERTICAL MESH LIN
     1ES WITH BLADES)
 1080 FORMAT (1HL,22X,15HBLADE SURFACE 1,30X,15HBLADE SURFACE 2/7X,
     1   1HM,14X,2HTV,11X,5HDTDMV,11X,4HCURV,12X,2HTV,11X,5HDTDMV,11X,
     2   4HCURV/(7G15.5))
 1250 FORMAT(1H1,////10X,23H BLADE GEOMETRY ROTATED
     1 46H INTO COORDINATE SYSTEM WITH INLET BLADE ANGLE
     2 14H EQUAL TO KIC. )
 5000 FORMAT (2F10.5)
 5100 FORMAT (//10X,8H STRFAC=,F10.5,10X,8H YSTRFC=,F10.5)
      END



      SUBROUTINE BLCO
C
C  BLCO CALCULATES BLADE THETA COORDINATE AS A FUNCTION OF M
C
      COMMON SRW,ITER,IEND,LER(2),NER(2)
```

```
      COMMON /INP/GAM,AR,TIP,RHOIP,WTFL,OMEGA,ORF,BETAI,BETAO,REDFAC,
     1    DENTOL,MBI,MBO,MM,NBBI,NBL,NRSP,MR(10),RMSP(10),BESP(10),
     2    BLCAT,AANDK,ERSOR,STRFN,SLCRD,INTVL,SURVL
      COMMON /CALCON/ACTWT,ACTUMG,ACTLAM,MBIM1,MBIP1,MBOM1,MBOP1,MMM1,
     1    HM1,HT,DTLR,DMLR,PITCH,CP,EXPON,TWW,CPTIP,TGROG,TBI,TBO,LAMBDA,
     2    TWL,ITMIN,ITMAX,NIP,IMS(2),BV(2),MV(100),IV(101),ITV(100,2),
     3    TV(100,2),DTDMV(100,2),BETAV(100,2),MH(100,2),DTDMH(100,2),
     4    BETAH(100,2),RMH(100,2),BEH(100,2),RM(100),BE(100),DBDM(100),
     5    SAL(100),AAA(100)
      COMMON /GEOMIN/ CHORD(2),STGR(2),RLE(2),THLE(2),RMI(2),RMO(2),
     1    RI(2),RO(2),BETI(2),BETO(2),NSPI(2),MSP(50,2),THSP(100,2)
      COMMON /BLCOCM/ EM(100,2),INIT(2)
      COMMON /D2TDM2/ D2TDM2(100,2)
C
      ENTRY  BL1(M,THETA,DTDM,INF)
C
      INTEGER BLCAT,AANDK,ERSOR,STRFN,SLCRD,SURVL,AATEMP,SURF,FIRST,
     1    UPPER,S1,ST,SRW
      REAL K,KAK,LAMBDA,LMAX,MH,MLE,MR,MSL,MSP,MV,MVIM1
      REAL M,MMLE,MSPMM,MMMSP
      REAL MSPR
      SURF= 1
      SIGN= 1.
      GO TO 10
      ENTRY  BL2(M,THETA,DTDM,INF)
      SURF= 2
      SIGN=-1.
   10 INF = 0
      IM = 1
      DO 15 I=MBI,MBO
   15 IF(ABS(MV(I)-M).LE.DMLR) IM=I
      NSP= NSPI(SURF)
      IF (INIT(SURF).EQ.13) GO TO 30
      INIT(SURF)= 13
C
C  INITIAL CALCULATION OF FIRST AND LAST SPLINE POINTS ON BLADE
C
      AA = BETI(SURF)/57.295779
      AA = SIN(AA)
      MSP(1,SURF) =  RI(SURF)*(1.-SIGN*AA)
      BB = SQRT(1.-AA**2)
      THSP(1,SURF) = SIGN*BB*RI(SURF)/RMI(SURF)
      BETI(SURF) = AA/BB/RMI(SURF)
      AA = BETO(SURF)/57.295779
      AA = SIN(AA)
      MSP(NSP,SURF) = CHORD(SURF)-RO(SURF)*(1.+SIGN*AA)
      BB = SQRT(1.-AA**2)
      THSP(NSP,SURF) = STGR(SURF)+SIGN*BB*RO(SURF)/RMO(SURF)
      BETO(SURF) = AA/BB/RMO(SURF)
      DO 20 IA=1,NSP
      MSP(IA,SURF)=(MSP(IA,SURF)+RLE(SURF))
   20 THSP(IA,SURF)=(THSP(IA,SURF)+THLE(SURF))
      CALL SPLN22(MSP(1,SURF),THSP(1,SURF),BETI(SURF),BETO(SURF),NSP,
     1 AAA,EM(1,SURF))
      IF(BLCAT.LE.0) GO TO 30
      WRITE(6,1000)
      WRITE(6,1010) SURF
      WRITE (6,1020) (MSP(IA,SURF),THSP(IA,SURF),AAA(IA),
     1 EM(IA,SURF), IA=1,NSP)
C
C  ROTATE COORDINATES TO STANDARD POSITION.
C
```

```
      WRITE (6,1050)
      IF(SURF.EQ.2) GO TO 22
      PIT=0.
      WRITE(6,1060)
 1060 FORMAT(////37H SUCTION SURFACE, INPUT SPLINE POINTS//)
      GO TO 25
   22 PIT= PITCH
      WRITE(6,1070)
 1070 FORMAT (////38H PRESSURE SURFACE, INPUT SPLINE POINTS//)
   25 CALL ROTATE(MSP,THSP,AAA,EM,1,NSP,SURF,PIT)
C
C  BLADE COORDINATE CALCULATION
C
   30 KK = 2
      IF (M.GT.MSP(1,SURF)) GO TO 50
C
C  AT LEADING EDGE RADIUS
C
      MMLE= M-MLE(SURF)
      IF (MMLE.LT.-DMLR) GO TO 90
      MMLE= AMAX1(0.,MMLE)
      THETA= SQRT(MMLE*(2.*RI(SURF)-MMLE))*SIGN
      IF (THETA.EQ.0.) GO TO 40
      RMM= RI(SURF)-MMLE
      DTDM=(RMM/THETA/RMI(SURF)/STRFAC)
      THETA = THETA/RMI(SURF)
      D2TDM2(IM,SURF) = (-THETA-RMM*DTDM)/(RMI(SURF)*THETA)**2
      THETA =(THETA+THLE(SURF))
      RETURN
   40 INF= 1
      DTDM = 1.E10*SIGN
      THETA= THLE(SURF)
      D2TDM2(IM,SURF) = 0.
      RETURN
C
C  ALONG SPLINE CURVE
C
   50 IF (M.LE.MSP(KK,SURF)) GO TO 60
      IF (KK.GE.NSP) GO TO 70
      KK = KK+1
      GO TO 50
   60 S= MSP(KK,SURF)-MSP(KK-1,SURF)
      EMKM1= EM(KK-1,SURF)
      EMK= EM(KK,SURF)
      MSPMM= MSP(KK,SURF)-M
      MMMSP= M-MSP(KK-1,SURF)
      THK= THSP(KK,SURF)/S
      THKM1= THSP(KK-1,SURF)/S
      THETA= EMKM1*MSPMM**3/6./S + EMK*MMMSP**3/6./S + (THK-EMK*S/6.)*
     1 MMMSP + (THKM1-EMKM1*S/6.)*MSPMM
      DTDM= -EMKM1*MSPMM**2/2./S + EMK*MMMSP**2/2./S + THK-THKM1-(EMK-
     1 EMKM1)*S/6.
      D2TDM2(IM,SURF) = EMKM1*MSPMM/S+EMK*MMMSP/S
      RETURN
C
C  AT TRAILING EDGE RADIUS
C
   70 CMM= CHORD(SURF)+MLE(SURF)-M
      IF (CMM.LT.-DMLR) GO TO 90
      CMM= AMAX1(0.,CMM)
      THETA= SQRT(CMM*(2.*RO(SURF)-CMM))*SIGN
      IF (THETA.EQ.0.) GO TO 80
```

```
      RMM= RC(SURF)-CMM
      DTDM =(-RMM/THETA/RMC(SURF))
      THETA = THETA/RMC(SURF)
      D2TDM2(IM,SURF) = (-THETA+RMM*DTDM)/(RMC(SURF)*THETA)**2
      THETA =(THETA+STGR(SURF)+THLE(SURF))
      RETURN
   80 INF= 1
      DTDM = -1.E10*SIGN
      THETA=(THLE(SURF)+STGR(SURF))
      D2TDM2(IM,SURF) = 0.
      RETURN
C
C   ERROR RETURN
C
   90 WRITE(6,1030) LER(2),M,SURF
      STOP
 1000 FORMAT (1H1,13X,33HBLADE DATA AT INPUT SPLINE POINTS)
 1010 FORMAT(1HL,17X,16HBLADE     SURFACE,I4)
 1020 FORMAT (7X ,1HM,10X,5HTHETA,10X,10HDERIVATIVE,5X,10H2ND DERIV. /
     1  (4G15.5) )
 1030 FORMAT (14HLBLCD CALL NO.,I3/33H M COORDINATE IS NOT WITHIN BLADE/
     14H M =,G14.6,10X,6HSURF =,G14.6)
 1050 FORMAT(1H1////10X,23H BLADE GEOMETRY ROTATED
     1 46H INTO COORDINATE SYSTEM WITH INLET BLADE ANGLE
     2 14H EQUAL TO KIC. )
      END



      SUBROUTINE INPUT
C
C   INPUT READS AND PRINTS ALL INPUT DATA CARDS AND CALCULATES HORIZONTAL
C   SPACING (MV ARRAY)
C
C
      COMMON/ROT/ KAPIN,KIC,RLED,XCTRN,YCTRN,R
      COMMON /ADD/ SFTOL
      COMMON SRW,ITER,IEND,LER(2),NER(2)
      COMMON /INP/GAM,AR,TIP,RHOIP,WTFL,OMEGA,ORF,BETAI,BETAO,REDFAC,
     1   DENTOL,MBI,MBO,MM,NBBI,NBL,NRSP,MR(10),RMSP(10),BESP(10),
     2   BLDAT,AANDK,ERSOR,STRFN,SLCRD,INTVL,SURVL
      COMMON /CALCON/ACTWT,ACTOMG,ACTLAM,MBIM1,MBIP1,MBOM1,MBOP1,MMM1,
     1   HM1,HT,DTLR,DMLR,PITCH,CP,EXPON,TWW,CPTIP,TGROG,TBI,TBO,LAMBDA,
     2   TWL,ITMIN,ITMAX,NIP,IMS(2),BV(2),MV(100),IV(101),ITV(100,2),
     3   TV(100,2),DTDMV(100,2),BETAV(100,2),MH(100,2),DTDMH(100,2),
     4   BETAH(100,2),RMH(100,2),BEH(100,2),RP(100),BE(100),DBDM(100),
     5   SAL(100),AAA(100)
      COMMON /GEOMIN/ CHORD(2),STGR(2),MLE(2),THLE(2),RMI(2),RMO(2),
     1   RI(2),RO(2),BETI(2),BETO(2),NSPI(2),MSP(50,2),THSP(100,2)
      INTEGER BLDAT,AANDK,ERSOR,STRFN,SLCRD,SURVL,AATEMP,SURF,FIRST,
     1   UPPER,S1,ST,SRW
      REAL KAPIN,KIC
      REAL K,KAK,LAMBDA,LMAX,MH,MLE,MR,MSL,MSP,MV,MVIM1
C
C   READ AND PRINT ALL INPUT DATA
C
      WRITE(6,1000)
      READ(5,1100)
      WRITE(6,1100)
      WRITE(6,1110)
```

```
      READ (5,1030) GAM,AK,TIP,RHOIP,WTFL,BLANK,OMEGA,ORF
      WRITE(6,1040) GAM,AK,TIP,RHOIP,WTFL,BLANK,OMEGA,ORF
      WRITE(6,1120)
      READ (5,1030)BETAI,BETAO,CHORD(1),STGR(1)
      WRITE(6,1040)BETAI,BETAO,CHORD(1),STGR(1)
      WRITE (6,1125)
      READ  (5,1030) REDFAC,DENTOL,SFTOL
      IF(DENTOL.LE.0.) DENTOL = .001
      IF (SFTOL.LE.0.) SFTOL=.000001
      WRITE (6,1040) REDFAC,DENTOL,SFTOL
      WRITE(6,1130)
      READ (5,1010) MBI,MBO,BLANK,BLANK,MM,NBBI,NBL,NRSP
      WRITE(6,1010) MBI,MBO,BLANK,BLANK,MM,NBBI,NBL,NRSP
      DO 10 J=1,2
      IF (J.EQ.1) WRITE(6,1140)
      IF (J.EQ.2) WRITE(6,1150)
      WRITE(6,1180) J,J,J,J,J
      READ (5,1030) RI(J),RO(J),BETI(J),BETO(J),SPLNO
      WRITE(6,1040) RI(J),RO(J),BETI(J),BETO(J),SPLNO
      NSPI(J)= SPLNO
      NSP = NSPI(J)
      WRITE(6,1190) J
      READ (5,1030) (MSP(I,J),I=1,NSP)
      WRITE(6,1040) (MSP(I,J),I=1,NSP)
      WRITE(6,1200) J
      READ (5,1030) (THSP(I,J),I=1,NSP)
   10 WRITE(6,1040) (THSP(I,J),I=1,NSP)
      WRITE(6,1210)
      READ (5,1030) (MR(I),I=1,NRSP)
      WRITE(6,1040) (MR(I),I=1,NRSP)
      WRITE(6,1220)
      READ (5,1030) (RMSP(I),I=1,NRSP)
      WRITE(6,1040) (RMSP(I),I=1,NRSP)
      WRITE(6,1230)
      READ (5,1030) (BESP(I),I=1,NRSP)
      WRITE(6,1040) (BESP(I),I=1,NRSP)
      WRITE(6,1240)
      READ (5,1010) BLDAT,AANDK,ERSOR,STRFN,SLCRD,INTVL,SURVL
      WRITE(6,1020) BLDAT,AANDK,ERSOR,STRFN,SLCRD,INTVL,SURVL
      READ(5,1280) KAPIN,KIC,RLED,XCTRN,YCTRN
      WRITE(6,1290) KAPIN,KIC,RLED,XCTRN,YCTRN
      R=RMSP(1)
      IF(XCTRN.EQ.0.) XCTRN=RLED
      IF (MM.LE.100.AND.NBBI.LE.50.AND.NRSP.LE.50.AND.NSPI(1).LE.50
     1    .AND.NSPI(2).LE.50) GO TO 20
      WRITE (6,1250)
      STOP
C
C  CALCULATE MV ARRAY
C
   20 HM1 = CHORD(1)/FLOAT(MBO-MBI)
      DO 30 IM=1,MM
   30 MV(IM) = FLOAT(IM-MBI)*HM1
      MV(MBO) = CHORD(1)
C
C  CALCULATE MISCELLANEOUS CONSTANTS
C
      NER(1)=0
      NER(2)=0
      PITCH = 2.*3.1415927/FLOAT(NBL)
      HT= PITCH/FLOAT(NBBI)
      DTLR= HT/1000.
```

```
      DMLR = HM1/1000.
      BV(1) = 0.
      BV(2) = 1.
      MBIM1= MBI-1
      MBIP1= MBI+1
      MBOM1= MBO-1
      MBOP1= MBO+1
      MMM1 = MM-1
      CP = AR/(GAM-1.)*GAM
      EXPON= 1./(GAM-1.)
      TWW= 2.*OMEGA/WTFL
      CPTIP= 2.*CP*TIP
      TGROG= 2.*GAM*AR/(GAM+1.)
      CALL SPLINT(MR,RMSP,NRSP,MV,MM,RM,SAL)
      CALL SPLINT(MR,BESP,NRSP,MV,MM,BE,DBDM)
C
C  CALCULATE GEOMETRICAL CONSTANTS
C
      CHORD(2) = CHORD(1)
      STGR(2) = STGR(1)
      XLE(1) = 0.
      XLE(2) = 0.
      THLE(1) = 0.
      THLE(2) = PITCH
      RMI(1) = RM(MBI)
      RMI(2) = RM(MBI)
      RMO(1) = RM(MBO)
      RMO(2) = RM(MBO)
      RETURN
 1000 FORMAT (1H1)
 1010 FORMAT (16I5)
 1020 FORMAT (1X,16I7)
 1030 FORMAT (8F10.5)
 1040 FORMAT (1X,8G16.7)
 1100 FORMAT (80H
     1                              )
 1110 FORMAT (7X,3HGAM,14X,2HAR,13X,3HTIP,12X,5HRHOIP,12X,4HWTFL,11X,6H
     1      ,10X,5HOMEGA,12X,3HORF)
 1120 FORMAT (6X,5HBETAI,10X,5HBETAO,11X,6HCHORDF,11X,5HSTGRF)
 1125 FORMAT (6X,6HREDFAC,10X,6HDENTOL,11X,5HSFTOL)
 1130 FORMAT (41H   MBI  MBO              MM  NBBI  NBL NRSP)
 1140 FORMAT (39HL     BLADE SURFACE 1  --  UPPER SURFACE)
 1150 FORMAT (39HL     BLADE SURFACE 2  --  LOWER SURFACE)
 1180 FORMAT (7X,2HRI,I1,12X,2HRO,I1,12X,4HBETI,I1,11X,4HBETO,I1,11X,5HS
     1PLNO,I1)
 1190 FORMAT (7X,3HMSP,I1,2X,5HARRAY)
 1200 FORMAT (7X,4HTHSP,I1,2X,5HARRAY)
 1210 FORMAT (16HL       MR  ARRAY)
 1220 FORMAT (7X,11HRMSP  ARRAY)
 1230 FORMAT (7X,11HBESP  ARRAY)
 1240 FORMAT (52HL     BLDAT  AANDK  ERSOR  STRFN  SLCRD  INTVL  SURVL)
 1250 FORMAT (41H1 MM,NBBI,NRSP,OR SOME SPLNO IS TOO LARGE)
 1260 FORMAT (//4X,6H INITI,4X,6H INITO,4X,6H IFILE,8X,2HIC,
     1 7X,3H IO,6X,4H TPI,6X,4H TPO,//(5I10,4X,A6,4X,A6))
 1270 FORMAT (5I5,2A6)
 1280 FORMAT (5F10.7)
 1290 FORMAT (//9X,6H KAPIN,6X,4H KIC,6X,4H RLE,4X,6H XCTRN,4X,6H YCTRN,
     1 //5X,2F10.3,3F10.7)
      END
```

```
      SUBROUTINE ROTATE(FMS,THTAS,DTDM,D2TDM2,NS,NF,ISURF,PITCH)
C
C   THIS PROGRAM ROTATES COORDINATES AND ANGLES OF A GIVEN
C   SURFACE THROUGH THE ANGLE (KAPIN - KIC).
C   THE CENTER OF ROTATION IS ON THE X-AXIS AT X=RI.
C
C
C   ANGL        ROTATION ANGLE, RADIANS.
C
C   CURV        CURVATURE.
C
C   DTDM(K)     FIRST DERIVATIVE OF THTAS(K) WITH RESPECT TO FMS(K).
C
C   D2TDM2      SECOND DERIVATIVE OF THTAS(K) WITH RESPECT TO FMS(K).
C
C   FMO         ROTATED MERIDONAL COORDINATE.
C
C   FMS(K)      MERIDIONAL COORDINATE.
C
C   ISURF       SUBSCRIPT DESIGNATING BLADE SURFACES-
C               1= SUCTION SURFACE
C               2= PRESSURE SURFACE
C
C   KAPIN       INLET BLADE ANGLE IN STAGGERED POSITION, DEG.
C
C   KIC         INLET BLADE ANGLE IN UNSTAGGERED POSITION, DEG.
C
C   NN          NUMBER OF FMS(K) VALUES INPUT.
C
C   PITCH       DISTANCE BETWEEN BLADES IN TANGENTIAL DIRECTION, RADIANS,
C               USE ZERO FOR SUCTION SURFACE.
C
C   R           RADIUS OF STREAM SURFACE.
C
C   RI          RADIUS OF LEADING EDGE CIRCLE.
C
C   TANANG      ROTATED TANGENT ANGLE AT POINT FMS(K).
C
C   THO         ROTATED TANGENTIAL COORDINATE IN UNITS OF LENGTH.
C
C   THTAS(K)    TANGENTIAL COORDINATE, RADIANS.
C
C   XCTRN       X-COORDINATE OF THE CENTER OF THE ARTIFICIALLY DEFINED
C               LEADING EDGE CIRCLE WHEN THE X-AXIS PASSES THROUGH
C               THE CENTERS OF THE ORIGINAL EDGE CIRCLES.  IN THE
C               USUAL CASE WHERE IT IS NOT NECESSARY TO DEFINE AN
C               ARTIFICIAL LEADING EDGE CIRCLE, XCTRN IS SET
C               EQUAL TO RI.
C   YCTRN       Y-COORDINATE OF THE CENTER OF THE ARTIFICIALLY
C               DEFINED LEADING EDGE CIRCLE WHEN THE X-AXIS PASSES
C               THROUGH THE CENTERS OF THE ORIGINAL EDGE CIRCLES.
C               WHEN XCTRN=RI, THEN SET YCTRN=0.
C
C
      COMMON/ROT/ KAPIN,KIC,RLED,XCTRN,YCTRN,R
      DIMENSION DTDM(1),D2TDM2(100,2),FMS(50,2),THTAS(100,2),
     1 TITLE(20)
      REAL KAPIN,KIC
C
C
      IO=6
      WRITE(IO,5050) KAPIN,KIC
```

```
C  ROTATE COORDINATES AND ANGLES.
C
      ANGL=(KAPIN-KIC)/57.295779
      WRITE(IO,5100)
      WRITE(IO,5200)
      DO 100 K=NS,NF
      CURV=R*D2TDM2(K,ISURF)/((1.+R*DTDM(K)*R*DTDM(K)
     1 )**1.5)
      FMO=(FMS(K,ISURF)-RLED)*COS(ANGL)+R*(THTAS(K,ISURF)-PITCH)*
     1 SIN(ANGL)+XCTRN
      THO=-(FMS(K,ISURF)-RLED)*SIN(ANGL)+R*(THTAS(K,ISURF)-PITCH)
     1 *COS(ANGL)+YCTRN
      TANANG=(ATAN(R*DTDM(K))-ANGL)*57.295779
  100 WRITE(IO,5300) K,FMO,THO,TANANG,CURV,FMS(K,ISURF),THTAS(K,ISURF),
     1 DTDM(K),D2TDM2(K,ISURF)
      RETURN
 5050 FORMAT(//,10X,7H KAPIN=,F10.7,3X,5H KIC=,F10.7///)
 5100 FORMAT (18X,19H REFERENCE POSITION, 33X,15H INPUT POSITION)
 5200 FORMAT (8X,2H K,10X,2H M,5X,7H RTHETA,3X,9H SURF ANG,7X,
     1 5H CURV,4X,8H INPUT M,12H INPUT THETA,1X,11H INPUT DTDM,
     2 1X,13H INPUT D2TDM2//)
 5300 FORMAT (I10,2F12.7,2F12.4,3F12.7,F14.3)
      END
```

```
      SUBROUTINE SPLINT (X,Y,N,Z,MAX,YINT,DYDX)
C
C  SPLINT CALCULATES INTERPOLATED POINTS AND DERIVATIVES
C  FOR A SPLINE CURVE
C   END CONDITION - SECOND DERIVATIVE AT EITHER END POINT IS ONE-HALF
C   THAT AT THE ADJACENT POINT
C
      COMMON SRW
      COMMON /BOX/ G(100),SB(100)
      DIMENSION X(N),Y(N),Z(MAX),YINT(MAX),DYDX(MAX)
      INTEGER SRW
      DIMENSION EM(100)
      EQUIVALENCE (SB,EM)
      IF(MAX.LE.0) RETURN
      III = SRW
      SB(1) = -.5
      G(1) = 0
      NC=N-1
      IF(NC.LT.2) GO TO 20
      DO 10 I=2,NC
      A = (X(I)-X(I-1))/6.
      C = (X(I+1)-X(I))/6.
      W = 2.*(A+C)-A*SB(I-1)
      SB(I) = C/W
      F = (Y(I+1)-Y(I))/(X(I+1)-X(I))-(Y(I)-Y(I-1))/(X(I)-X(I-1))
   10 G(I) = (F-A*G(I-1))/W
   20 EM(N) = G(N-1)/(2.+SB(N-1))
      DO 30 I=2,N
      K = N+1-I
   30 EM(K) = G(K)-SB(K)*EM(K+1)
      DO 140 I=1,MAX
      K=2
      IF(Z(I)-X(1)) 70,60,90
   60 YINT(I)=Y(1)
      SK = X(K)-X(K-1)
      GO TO 130
```

```
   70 IF(Z(I).GE.(1.1*X(1)-.1*X(2))) GO TO 120
      WRITE (6,1000) Z(I)
      SRW = 16
      GO TO 120
   80 K=N
      IF(Z(I).LE.(1.1*X(N)-.1*X(N-1))) GO TO 120
      WRITE (6,1000) Z(I)
      SRW = 16
      GO TO 120
   90 IF(Z(I)-X(K)) 120,100,110
  100 YINT(I)=Y(K)
      SK = X(K)-X(K-1)
      GO TO 130
  110 K=K+1
      IF(K-N) 90,90,80
  120 CONTINUE
      SK = X(K)-X(K-1)
      YINT(I) = EM(K-1)*(X(K)-Z(I))**3/6./SK  +EM(K)*(Z(I)-X(K-1))**3/6.
     1  /SK+(Y(K)/SK  -EM(K)*SK  /6.)*(Z(I)-X(K-1))+(Y(K-1)/SK  -EM(K-1)
     2  *SK/6.)*(X(K)-Z(I))
  130 DYDX(I)=-EM(K-1)*(X(K)-Z(I))**2/2.0/SK  +EM(K)*(X(K-1)-Z(I))**2/2.
     1   /SK+(Y(K)-Y(K-1))/SK  -(EM(K)-EM(K-1))*SK/6.
  140 CONTINUE
      MXA = MAXO(N,MAX)
      IF(SRW.EQ.16) WRITE(6,1010) N,MAX,(X(I),Y(I),Z(I),YINT(I),DYDX(I),
     1   I=1,MXA)
      SRW = III
      RETURN
 1000 FORMAT (54H SPLINT USED FOR EXTRAPOLATION.  EXTRAPOLATED VALUE = ,
     1G14.6)
 1010 FORMAT (2X,21HNO. OF POINTS GIVEN =,I3,30H, NO. OF INTERPOLATED PO
     1INTS =,I3/10X,1HX,19X,1HY,16X,11HX-INTERPOL.,9X,11HY-INTERPOL.,
     28X,14HDYDX-INTERPOL./(5E20.8))
      END



      SUBROUTINE SPLN22 (X,Y,Y1P,YNP,N,SLOPE,EM)
C
C  SPLN22 CALCULATES FIRST AND SECOND DERIVATIVES AT SPLINE POINTS
C  END CONDITION - DERIVATIVES SPECIFIED AT END POINTS
C
      COMMON SRW
      COMMON /BOX/ G(100),SB(100)
      DIMENSION X(N),Y(N),EM(N),SLOPE(N)
      INTEGER SRW
      SB(1) = .5
      F = (Y(2)-Y(1))/(X(2)-X(1))-Y1P
      G(1) = F*3./(X(2)-X(1))
      NC=N-1
      IF(NC.LT.2) GO TO 20
      DO 10 I=2,NC
      A = (X(I)-X(I-1))/6.
      C = (X(I+1)-X(I))/6.
      W = 2.*(A+C)-A*SB(I-1)
      SB(I) = C/W
      F = (Y(I+1)-Y(I))/(X(I+1)-X(I))-(Y(I)-Y(I-1))/(X(I)-X(I-1))
```

```
   10 G(I) = (F-A*G(I-1))/W
   20 F = YNP-(Y(N)-Y(N-1))/(X(N)-X(N-1))
      W = (X(N)-X(N-1))/6.*(2.-SB(N-1))
      EM(N) = (F-(X(N)-X(N-1))*G(N-1)/6.)/W
      DO 30 I=2,N
      K = N+1-I
   30 EM(K) = G(K)-SB(K)*EM(K+1)
      SLOPE(1) = (X(1)-X(2))/6.*(2.*EM(1)+EM(2))+(Y(2)-Y(1))/(X(2)-X(1))
      DO 40 I=2,N
   40 SLOPE(I) = (X(I)-X(I-1))/6.*(2.*EM(I)+EM(I-1))+(Y(I)-Y(I-1))/
     1    (X(I)-X(I-1))
      IF(SR.EQ.18) WRITE (6,1000) N,(X(I),Y(I),SLOPE(I),EM(I),I=1,N)
      RETURN
 1000 FORMAT (2X,15HNO. OF POINTS =,I3/10X,1HX,19X,1HY,19X,5HSLOPE,15X,
     12HEM/(4G20.8))
      END
```

APPENDIX D. STAGNATION POINT PROGRAM (STGPLS)

The purpose of the STGPLS program is to provide a consistent procedure for estimating the location of the stagnation point on the trailing edge circle of a blade section. Meridional and tangential coordinates of the stagnation streamline at vertical mesh lines downstream of the blade are available from MAGNFY output (appendix A). STGPLS approximates the stagnation streamline by a least-squares parabola using six coordinate points from MAGNFY output. The parabola is extrapolated to the trailing edge circle to approximately locate the stagnation point (fig. 53).

The procedure is valid for conical stream surfaces if the edge circle is assumed to be an undistorted circle on the $m - R\theta$ plane. The input data required are indicated in figure 54 and the variables are defined in figure 53 and on comment cards in the listing of STGPLS source cards at the end of this appendix.

The first page of output lists the input data and the coefficients of the least-square parabola. The second page gives intermediate results of the stagnation point location iteration and the final stagnation streamline position data. Headings are variable names which are defined in figure 53 and on comment cards in the source card which follows.

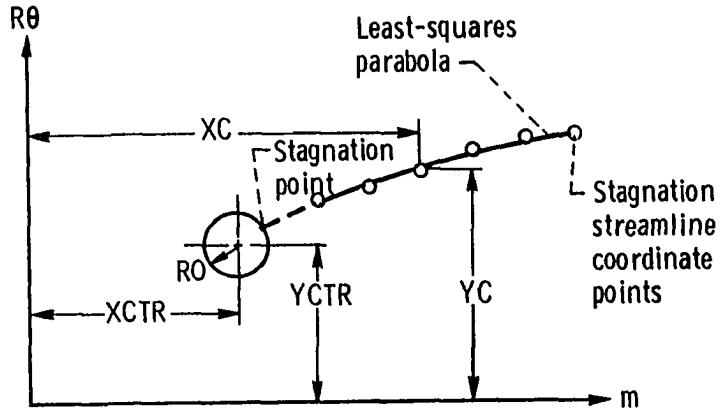

Figure 53. - STGPLS input and output parameters.

			TITLE			
XCTR	YCTR	RD				
ITMAX	TOLY					
NUMPTS						
XC(1)	XC(2)	XC(3)	XC(4)	XC(5)	XC(6)	
YC(1)	YC(2)	YC(3)	YC(4)	YC(5)	YC(6)	
NUMCOF						

Figure 54. - Input data required for STGPLS.

```
C  THIS PROGRAM DETERMINES THE LOCATION OF STAGNATION POINT
C  ON THE TRAILING EDGE CIRCLE.
C
C
C  ANGSP       ANGLE BETWEEN LINE CONNECTING CIRCLE CENTER
C              TO STAGNATION POINT AND THE ABSCISSA, DEG.
C
C  COEF(K)     THE DOUBLE PRECISION VECTOR CONTAINING COEFFIENTS
C              OF THE POLYNOMIAL LEAST SQUARE FIT.  COEF(K) IS THE
C              COEFFICIENT OF XC(I)**(K-1).
C
C  EPSY(L)     DIFFERENCE BETWEEN ORDINATES OF PARABOLA
C              AND CIRCLE AT GIVEN ABSCISSA VALUE.
C
C  ITMAX        LIMIT ON NUMBER OF ITERATIONS ALLOWED.
C
C  NUMCOF      THE DIMENSION OF COEF. AND IS ONE GREATER THAN THE
C              DEGREE OF THE POLYNOMIAL FIT.
C
C  NUMPTS      THE NUMBER OF XC,YC PAIRS INPUT, ALSO THEIR DIMENSION.
C
C  RO          RADIUS OF EDGE CIRCLE, METERS.
C
C  SIGN        +1. FOR ORDINATES GREATER THAN YCTR,
C              -1. FOR ORDINATES LESS THAN YCTR.
C
C  SUMSQR      THE SUM OF THE SQUARES OF THE RESIDUALS.
C
C  TOLY        TOLERANCE FOR INTERSECTION ITERATION
C
C  X           ESTIMATED MERIDIONAL COORDINATE OF STAGNATION POINT, METERS.
C
C  XC(I)       MERIDIONAL COORDINATE OF THE STAGNATION STREAMLINE, METERS
C
C  XCTR        MERIDIONAL COORDINATE OF THE EDGE CIRCLE CENTER, METERS.
C
C  XMAX        MAXIMUM ABSCISSA VALUE ON CIRCLE.
C
C  XMIN        MINIMUM ABSCISSA VALUE ON CIRCLE.
C
C  XNXT        NEXT BEST ESTIMATE FOR MERIDIONAL COORDINATE OF
C              STAGNATION POINT, METERS.
C
C  YC(I)       TANGENTIAL COORDINATE OF THE STAGNATION STREAMLINE, METERS
C
C  YCIR        ORDINATE OF CIRCLE AT ESTIMATED STAGNATION POINT, METERS.
C
C  YCTR        ORDINATE OF CENTER OF CIRCLE.
C
C  YPAR        ORDINATES ON PARABOLA, METERS.
C
C  YPR         ORDINATE OF PARABOLA AT ESTIMATED STAGNATION POINT, METERS.
C
      DIMENSION COEF(3),EPSY(2),X(2),XC(6),YC(6)
      DOUBLE PRECISION COEF
C
      II=5
      IO=6
C
C  READ AND WRITE INPUT
C
```

```
   50 WRITE(IO,995)
      READ(II,1000)
      WRITE(IO,1000)
      READ(II,1005) XCTR,YCTR,RO
      IF (RO.EQ.0.) GO TO 400
      WRITE(IO,1010) XCTR,YCTR,RO
      READ(II,1015) ITMAX,TOLY
      WRITE(IO,1016) ITMAX,TOLY
      READ (II,1020) NUMPTS
      WRITE(IO,1025) NUMPTS
      READ(II,1030) (XC(I),I=1,NUMPTS)
      READ(II,1030) (YC(I),I=1,NUMPTS)
      WRITE(IO,1040) (I,XC(I),YC(I),I=1,NUMPTS)
      READ (II,1020) NUMCOF
      WRITE(IO,1050) NUMCOF
C
C  CALCULATE STAGNATION STREAMLINE PARABOLA COEFFICIENTS
C
C
C  ORTLES IS A LOCAL ROUTINE WHICH FITS LEAST-SQUARES POLYNOMIALS
C  TO (XC,YC) ARRAYS.  THE USER MUST REPLACE ORTLES WITH HIS OWN LOCAL
C  ROUTINE.
C
      CALL ORTLES(NUMPTS,XC,YC,NUMCOF,COEF,SUMSQR)
      WRITE(IO,1060) (COEF(I),I=1,NUMCOF),SUMSQR
C
C  INITIALIZE VARIABLES AND ASSIGN VALUE TO SIGN
C
      X(1)= XCTR+.5*RO
      X(2)= XCTR+RO
      XMAX= X(2)
      XMIN= XCTR-RO
      SIGN=1.
      YPR=COEF(1)+COEF(2)*X(2)+COEF(3)*X(2)*X(2)
      IF(YPR.LT.YCTR) SIGN=-1.
C
C  BEGIN STAGNATION POINT LOCATION ITERATION
C
      WRITE (IO,1065)
      WRITE(IO,1070)
      DO 200 J=1,ITMAX
      FJ=J
      IF(X(1).EQ.X(2)) X(1)=(.98+FJ)*X(1)/(1.+FJ)
      IF(X(1).LT.XMIN) X(1)=X(2)*X(2)/X(1)
      WRITE(IO,1080)
      DO 100 L=1,2
      YPR=COEF(1)+COEF(2)*X(L)+COEF(3)*X(L)*X(L)
      YCIR=YCTR+SIGN*SQRT(RO*RO-(X(L)-XCTR)*(X(L)-XCTR))
      EPSY(L)=YPR-YCIR
      WRITE(IO,1090) J,L,X(L),EPSY(L),YPR,YCIR
      IF(ABS(EPSY(L)).LE.TOLY) GO TO 300
  100 CONTINUE
C
C  INTERPOLATE FOR X AT WHICH EPSY=0.
C
      CALL FITLIN(XNXT,0.,X,EPSY)
      IF (XNXT.LT.XMIN) XNXT=XMIN
      IF (XNXT.GT.XMAX) XNXT=XMAX
      X(1)=X(2)
  200 X(2)=XNXT
      L=1
C
```

```
C  PRINT ERROR MESSAGE
C
      WRITE(IO,1100) ITMAX
C
C  CALCULATE ANGULAR LOCATION OF STAGNATION POINT
C
  300 TOP=YCIR-YCTR
      BOT=X(L)-XCTR
      ANGSP=57.295779*ATAN2(TOP,BOT)
      WRITE (IO,1105)
      WRITE(IO,1110) ANGSP
      WRITE(IO,1200)
C
C  CALCULATE ORDINATES OF LEAST SQUARE PARABOLA AT INPUT XC VALUES
C  PLUS TWO MORE.
C
      DO 340  I=1,2
      FI= I
      XX=X(L)+FI*(XC(1)-X(L))/3.
      YPAR= COEF(1)+COEF(2)*XX+COEF(3)*XX*XX
  340 WRITE(IO,1210) XX,YPAR
      DO 380  I=1,NUMPTS
      YPAR= COEF(1)+COEF(2)*XC(I)+COEF(3)*XC(I)*XC(I)
  380 WRITE(IO,1220) I,XC(I),YC(I),YPAR
      GO TO 50
  400 STOP
  995 FORMAT(1H1/////)
 1000 FORMAT (    80H
     1                                        )
 1005 FORMAT (3F10.7)
 1010 FORMAT (1H0,6X,5H XCTR,5X,5H YCTR,7X,3H RC//2X,3F10.7)
 1015 FORMAT (I10,F10.7)
 1016 FORMAT (/// 5X,7H ITMAX=,I5,5X,6H TOLY=,F11.8)
 1020 FORMAT (I5)
 1025 FORMAT (///10X,7H NUMPTS,//10X,I7)
 1030 FORMAT (8F10.7)
 1040 FORMAT (///10X,2H I,6X,6H XC(I),6X,6H YC(I),//(I12,2F12.8))
 1050 FORMAT (///10X,7H NUMCOF,//10X,I7)
 1060 FORMAT(//3X,9H COEF(1)=,F12.8,3X,9H COEF(2)=,F12.8,
     1 3X,9H COEF(3)=,F12.8,4X,8H SUMSQR=,F12.8)
 1065 FORMAT(1H1//20X,27H STAGNATION POINT ITERATION )
 1070 FORMAT (//9X,2H J,8X,2H L,7X,5H X(L),4X,8H EPSY(L),
     1 7X,5H YPAR,7X,5H YCIR//)
 1080 FORMAT(/)
 1090 FORMAT (1X,2I10,4F12.8)
 1100 FORMAT (////10X,35H STAGNATION POINT ITERATION DID NOT,
     1 12H CONVERGE IN, I4,8H TRIALS.)
 1105 FORMAT(//10X,27H STAGNATION STREAMLINE DATA)
 1110 FORMAT(//10X,7H ANGSP=,F10.3)
 1200 FORMAT(//3X,2H I,6X,6H XC(I),6X,6H YC(I),7X,5H YPAR//)
 1210 FORMAT(5X,F12.8,12X,F12.8)
 1220 FORMAT(I5,3F12.8)
      END
```

```
      SUBROUTINE FITLIN (XA,YA,XB,YB)
C
C
C  THIS SUBROUTINE FITS A STRAIGHT LINE THROUGH TWO (XB,YB)
C  POINT PAIRS AND INTERPOLATES OR EXTAPOLATES TO FIND THE
C  XA VALUE CORRESPONDING TO A GIVEN YA VALUE.
C
C
      DIMENSION XB(1),YB(1)
C
C
      SLOPE=(XB(2)-XB(1))/(YB(2)-YB(1))
      XINTCP=XB(1)-SLOPE*YB(1)
      XA=SLOPE*YA+XINTCP
      RETURN
      END
```

REFERENCES

1. Miller, Max J. Deviation angle prediction methods - a review. Iowa State University, Engineering Research Institute Interim Report ERI-580. 1969.

2. Carter, A. D. S. and Hughes, Hazel P. A theoretical investigation into the effect of profile shape on the performance of aerofoils in cascade. Aeronautical Research Council Reports and Memoranda No. 2384. 1946.

3. Emery, James C., Herrig, L. Joseph, Erwin, John R., and Felix, A. Richard. Systematic two-dimensional cascade tests of NACA 65-series compressor blades at low speeds. U.S. National Advisory Committee for Aeronautics Report 1368. 1958.

4. Matsuki, Masakatsu and Takahara, Kitao. Cascade tests of high stagger compressor blades. Japan Society of Mechanical Engineers Bulletin 5: 277-291. 1962.

5. Taylor, W. E., Murrin, T. A., and Colombo, R. M. Systematic two-dimensional cascade tests. Volume 1: Double circular-arc hydrofoils. U.S. National Aeronautics and Space Administration Contractor Report 72498. 1969.

6. Taylor, W. E., Murrin, T. A., and Colombo, R. M. Systematic two-dimensional cascade tests. Volume 2: Multiple circular-arc hydrofoils. U.S. National Aeronautics and Space Administration Contractor Report 72499. 1970.

7. Colombo, R. M. and Murrin, T. A. Systematic two-dimensional cascade tests. Volume 3: Slotted double circular-arc hydrofoils. U.S.

National Aeronautics and Space Administration Contractor Report 72870. 1972.

8. Ikui, T., Inoue, M., and Keneko, K. Two-dimensional cascade performance of circular-arc blades. Tokyo Joint International Gas Turbine Conference and Products Show Proc. 1971: 57-64. 1971.

9. Roudebush, William H. Potential flow in two-dimensional cascades. In Johnsen, Irving A. and Bullock, Robert O., eds. Aerodynamic design of axial-flow compressors. U.S. National Aeronautics and Space Administration Special Publication 36: 101-149. 1965.

10. Scholz, N. A survey of the advances in the treatment of the flow in cascades. In Internal aerodynamics (turbomachinery). pp. 20-31. London, Institution of Mechanical Engineers. 1970.

11. Schilhansl, Max J. Survey of information on two-dimensional cascades. U.S. Air Force Wright Air Development Center Technical Report 54-322. 1955.

12. Landau, L. D. and Lifshitz, E. M. Fluid mechanics. Reading, Mass., Addison-Wesley Publishing Company, Inc. 1959.

13. Gostelow, J. P., Lewkowicz, A. K., and Shaalan, M. R. A. Viscosity effects on the two-dimensional flow in cascades. Aeronautical Research Council Current Papers No. 872. 1965.

14. Wilkinson, D. H. Discussion. Thermodynamics and fluid mechanics. Volume 2: Axial and radial turbomachinery. Institution of Mechanical Engineers Proc. 184, part 3G(II): 113-116. 1970.

15. Sanger, Nelson L. Analytical study of the effects of geometric changes on the flow characteristics of tandem-bladed compressor

stators. U.S. National Aeronautics and Space Administration Technical Note D-6264. 1971.

16. Schlichting, Hermann. Berechung der reibungslosen inkompressiblen Strömung für ein vorgegebenes ebenes Schaufelgitter. VDI Forschungsheft 447. 1955.

17. Martensen, E. The calculation of the pressure distribution on a cascade of thick airfoils by means of Fredholm integral equations of the second kind. U.S. National Aeronautics and Space Administration Technical Translation F-702. 1971.

18. Giesing, Joseph P. Extension of the Douglas Neumann program to problems of lifting, infinite cascades. McDonnell Douglas Report No. LB 31653. 1964.

19. Katsanis, Theodore. A computer program for calculating velocities and streamlines for two-dimensional, incompressible flow in axial blade rows. U.S. National Aeronautics and Space Administration Technical Note D-3762. 1967.

20. Imbach, H. E. Calculation of the compressible, frictionless subsonic flow through a plane blade cascade. Brown Boveri Review 51: 752-761. 1964.

21. Katsanis, Theodore. FORTRAN program for calculating transonic velocities on a blade-to-blade stream surface of a turbomachine. U.S. National Aeronautics and Space Administration Technical Note D-5427. 1969.

22. Smith, D. J. L. Computer solutions of Wu's equations for the compressible flow through turbomachines. In Laksminarayana, B.,

Britsch, W. R., and Gearhart, W. S., eds. Fluid mechanics and design of turbomachinery. U.S. National Aeronautics and Space Administration Special Publication 304: 60-114. 1973.

23. Katsanis, Theodore and McNally, William D. FORTRAN program for calculating velocities in a magnified region on a blade-to-blade stream surface of a turbomachine. U.S. National Aeronautics and Space Administration Technical Note D-5091. 1969.

24. Katsanis, Theodore and McNally, William D. Computer program for calculating velocities and streamlines on a blade-to-blade stream surface of a turbomachine. U.S. National Aeronautics and Space Administration Technical Note D-4525. 1968.

25. Vavra, M. H. Aero-thermodynamics and flow in turbomachines. New York, N.Y., John Wiley & Sons, Inc. c1960.

26. Varga, Richard S. Matrix iterative analysis. Englewood Cliffs, N.J., Prentice-Hall, Inc. c1962.

27. Howell, A. R. The present basis of axial flow compressor design. Part 1. Cascade theory and performance. Aeronautical Research Council Reports and Memoranda No. 2095. 1942.

28. McNally, William D. and Crouse, James E. FORTRAN program for computing coordinates of circular arc single and tandem turbomachinery blade sections on a plane. U.S. National Aeronautics and Space Administration Technical Note D-6020. 1970.

29. Ahlberg, J. H., Nilson, E. N., and Walsh, J. L. The theory of splines and their applications. New York, N.Y., Academic Press. 1967.

30. Kramer, James J. Theoretical analysis of incompressible flow through a radial-inlet centrifugal impeller at various weight flows. II:

Solution in leading-edge region by relaxation methods. U.S. National Advisory Committee for Aeronautics Technical Note 3449. 1955.

31. Weinig, Fritz. Die Strömung um die Schaufeln von Turbomaschinen. Leipzig, Johann Ambrosius Barth. 1935.

32. Felix, A. Richard and Emery, James C. Comparison of typical National Gas Turbine Establishment and NACA axial-flow compressor blade sections in cascade at low speeds. U.S. National Advisory Committee for Aeronautics Technical Note 3937. 1957.

33. Preston, J. H. The calculation of lift taking account of the boundary layer. Aeronautical Research Council Reports and Memoranda No. 2725. 1953.